

**PALACKÝ UNIVERSITY OLMOUC**

Faculty of Medicine and Dentistry



**Metabolomic tools in diagnosis of inborn errors  
of metabolism**

**Doctoral Thesis**

**Mgr. Lukáš Najdekr**

Supervisor: prof. RNDr. Tomáš Adam, Ph.D.

Consultant: RNDr. David Friedecký, Ph.D.

## **Acknowledgement**

I would like to express my gratitude to prof. RNDr. Tomáš Adam, Ph.D. and RNDr. David Friedecký, Ph.D. for their patience, guidance and valuable advices. I would also like to thank them for their professional supervision of my Ph.D. study and their trust. The big thanks is also going to my colleagues in the Laboratory for Inherited metabolic diseases (FNOL) and Laboratory of metabolomics (IMTM, LF UP) who provided beautiful working environment and for their patience. And the last, but not least, thanks going to Jaroslav Pól, Ph.D., Yingying Huang, Ph.D., Junhua Wang, Ph.D., Ralf Tautenhahn, Ph.D. and Tomáš Pluskal, Ph.D. for their help during my internships and general research.

Finally, I would like to express my gratitude to my family, especially my mother and sister, for the support and patience during my studies and thesis writing.

This study was supported by grants LF\_2012\_016, LF\_2013\_010, LF\_2014\_011, IGA\_LF\_2015\_015, IGA\_LF\_2016\_014 (Ministry of Education, Youth, and Sports of the Czech Republic) and Czech Science Foundation Grant 15-34613L. The infrastructural part of this project (Institute of Molecular and Translational Medicine) was supported from the Operational Programme Research and Development for Innovations (project CZ.1.05/2.1.00/01.0030) and NPU I (LO1304).

**Declaration**

I hereby declare that this thesis has been fully written by me under the expert guidance of my supervisor prof. RNDr. Tomáš Adam, Ph.D. All the used literature is cited in *Chapter 7*.

In Olomouc, .....

..... Mgr. Lukáš Najdekr

## Table of Contents

<b>1. INTRODUCTION</b>	<b>6</b>
1.1. INBORN ERRORS OF METABOLISM – HEREDITARY ENZYMOPATHIES	6
1.1.1. <i>Medium chain acyl-CoA dehydrogenase deficiency (MCADD)</i>	8
1.1.2. <i>Adenosine deaminase deficiency</i>	11
1.2. METABOLOMICS	13
1.2.1. <i>Targeted and Semi-Targeted Metabolomics</i>	15
1.2.2. <i>Untargeted metabolomics</i>	16
1.2.3. <i>Mass spectrometry in metabolomics</i>	16
1.2.4. <i>Mass spectrometry in detection of inborn errors of metabolism</i>	18
1.2.5. <i>Structural elucidation and metabolite identification</i>	19
1.2.6. <i>“Seven golden rules” of identification</i>	21
1.2.7. <i>Spectral trees</i>	22
1.2.8. <i>Influence of high resolution</i>	23
<b>2. AIMS OF THE WORK</b>	<b>25</b>
<b>3. MATERIALS AND METHODS</b>	<b>26</b>
3.1. CHEMICALS	26
3.2. SAMPLES	26
3.2.1. <i>Medium chain acyl-CoA dehydrogenase deficiency</i>	26
3.2.2. <i>Adenosine deaminase deficiency</i>	26
3.2.3. <i>Control samples</i>	27
3.3. SAMPLE PREPARATION AND PROCESSING METHODS	27
3.3.1. <i>Medium chain acyl-CoA dehydrogenase deficiency</i>	27
3.3.1.1. Untargeted metabolomics experiment	27
3.3.1.2. Targeted analysis – confirmation experiment	28
3.3.1.3. Data processing	29
3.3.1.4. Confirmation of important discriminatory metabolite features	30
3.3.2. <i>Adenosine deaminase deficiency</i>	30
3.3.2.1. LC-MS metabolite profiling of urine samples	30
3.3.2.2. MS <sup>n</sup> analyses of selected purine metabolites in human urine	31
3.3.3. <i>Influence of a mass spectrometry resolution on feature (metabolite) detection in LC-HRMS untargeted metabolomics</i>	31
3.3.3.1. Sample preparation and LC-HRMS method	31
3.3.3.2. <i>In silico</i> calculations	32
3.3.3.3. LC-MS data processing	33

3.3.3.4.	Peak detection algorithm settings .....	34
<b>4.</b>	<b>RESULTS &amp; DISCUSSIONS .....</b>	<b>35</b>
4.1.	NEW POTENTIAL BIOMARKERS OF OXIDATIVE STRESS IN PATIENTS SUFFERING FROM MCADD .....	35
4.2.	SPECTRAL TREES AS A USEFUL TOOL IN IDENTIFICATION OF SMALL MOLECULE IN METABOLOMICS ..	50
4.3.	INFLUENCE OF A MASS SPECTROMETRY RESOLUTION ON METABOLITE DETECTION IN LC-MS	
	UNTARGETED METABOLOMICS .....	65
4.3.1.	<i>In silico calculations</i> .....	65
4.3.2.	<i>LC-MS data</i> .....	69
<b>5.</b>	<b>CONCLUSION.....</b>	<b>79</b>
<b>6.</b>	<b>LIST OF ABBREVIATIONS.....</b>	<b>81</b>
<b>7.</b>	<b>REFERENCES.....</b>	<b>85</b>
<b>8.</b>	<b>LIST OF AUTHORS PUBLICATIONS .....</b>	<b>94</b>
8.1.	PUBLICATION ASSOCIATED WITH THE THESIS .....	94
8.1.1.	<i>Original research articles published in journals with IF</i> .....	94
8.1.2.	<i>Published abstracts</i> .....	94
8.1.3.	<i>Poster presentations</i> .....	94
8.1.4.	<i>Oral presentations</i> .....	96
8.2.	OTHER PUBLICATIONS .....	97
8.2.1.	<i>Original research articles published in journals with IF</i> .....	97

# 1. Introduction

## 1.1. Inborn errors of metabolism – hereditary enzymopathies

Enzymes are biological catalysts capable of substrate conversion into a product with high efficiency. The group is mainly consisted of proteins (exceptions are few catalytic RNA) and it is influencing a vast number of substrates (amino acids, sugars, organic acids, fatty acids, complex lipids, purines, porphyrins, etc.). In human genome there are over 5000 genes coding enzymes, therefore there are hundreds of human enzyme defects – enzymopathies.<sup>1</sup> Inborn errors of metabolism are inherited in monogenic or Mendelian form, due to the fact that one gene determinates the disease. Majority of the IEMs are of autosomal recessive inheritance (67%), autosomal dominant inheritance is 21%, 6% are X-linked and the rest 6% are associated with mitochondrial inheritance.<sup>2</sup> From pathological point of view inborn errors of metabolism (IEM) can be divided into three groups: IEM leading to intoxication, IEM of energetic metabolism and disorders of a complex molecules.

First group includes errors in metabolism of intermediates, which leads into an accumulation of (toxic) compounds ahead of the metabolic block leading into an acute or progressive intoxication. This includes errors in amino acid catabolism (phenylketonuria, tyrosinemia, maple syrup urine disease, etc.), almost all organic acidurias (propionic, methylmalonic, isovaleric aciduria, etc.), inborn errors of metabolism of urea cycle, saccharides intolerance (hereditary fructose intolerance, galactosemia), intoxication by metals (defects of transport proteins) (hereditary hemochromatosis, Wilson's disease, Menkes syndrome) and porphyria. All diseases in this first group have common marks: they are not influencing embryonal or fetal development and after an asymptomatic period, those diseases manifest by clinical symptoms of the "intoxication" which may be acute (nausea, vomiting, thromboembolic complications, acute liver failure, etc.) and/or chronic (late thrive, ectopia lentis, cardiomyopathy, etc.). Clinical manifestations have often late start and they are intermittent.<sup>3</sup> Diagnostics is based on direct evaluation of amino acids in urine and plasma, organic acids in urine, acylcarnitines in plasma and saccharides (and/or their alcohol or phosphate derivates) in urine. Diseases involved in the metabolism of metals (e.g. Wilson's disease, hemochromatosis) are estimated upon the levels of relevant

protein carriers (e.g. ceruloplasmin) or the concentration of the metals itself.<sup>3,4</sup> Most of these disease are treatable and require removal of the toxins. This may be achieved by special diets and/or by special medications (e.g. carnitine, penicillin-amine, etc.). The errors in synthesis and degradation of neurotransmitters (e.g. monoamines, GABA and glycine) and amino acids can be also included into this group, although the pathophysiology is different. These diseases have much in common: they are both inherited errors of intermediate metabolism, their diagnostics is based on examination of urine, plasma and cerebrospinal fluid and some of them are treatable.

The second group includes inborn errors of intermediate metabolism with symptoms which are caused by production or consumption of energy in liver, myocardia, brain, muscle or other tissue. One part of the diseases are mitochondrial disorders, which may be most severe (the exception may be long-chain acyl-CoA dehydrogenase deficiency and very long-chain acyl-CoA dehydrogenase deficiency). Inherited lactic acidemia (deficit of pyruvate carboxylase, pyruvate dehydrogenase and enzymes of Krebs cycle, pyruvate carrier defects), defects of the respiratory cycle,  $\beta$ -oxidation defects and creation/degradation of ketones belong into this second group. Less severe are disorders of energy metabolism located in the cytoplasm (defects of glycolysis, gluconeogenesis and metabolism of glycogen, hyperinsulinism, creatinine metabolism and pentose-phosphate metabolism). Usual symptoms are hypoglycemia, hyperlactacidemia, hypotonia (a.k.a. floppy baby syndrome), hepatomegaly, cardiomyopathy, myopathy, sudden infant death syndrome (SIDS), heart failure and brain defects. Some of pentose-phosphate metabolism and mitochondrial defects may interfere with embryonal and fetal development causing malformations, dysplasia and dysmorphia.<sup>5</sup> Diagnosis is complicated, based on several examinations including biopsies and molecular diagnostics tools.

The third group of disorders influences cellular organelles and synthesis or catabolism of complex molecules. Symptoms are progressive, long-term and independent on diet or intercurrent diseases. All lysosomal and peroxisomal disorders, disorders of intracellular transport and processes (e.g.  $\alpha_1$ -antitrypsin, disorders of glycosylation, and inherited errors of cholesterol synthesis) are belonging into this group. Almost none of them are treatable, so far. For some lysosomal storage disease, the enzymatic replacement therapies are available.<sup>3</sup> In this thesis, for further work of

developing and testing new metabolomics tools, two well-known IEM's - medium chain acyl-CoA dehydrogenase deficiency (MCADD) and adenosine deaminase deficiency (ADA) were chosen.

#### **1.1.1. Medium chain acyl-CoA dehydrogenase deficiency (MCADD)**

The group of mitochondrial fatty acid oxidation disorders (FAODs) is known since 1970s and its combine incidence is 1:9300 (data processed in 2010 based on new born screening (NBS) programs in Australia, Germany and USA).<sup>6</sup> Today there is at least 15 disorders associated with fatty acid metabolism.<sup>7</sup> One of the most common fatty acid oxidation defect is medium chain acyl-CoA dehydrogenase deficiency (MCAD OMIM #201450) which is inherited by autosomal recessive trait. The disease was described and published for the first time by Gregersen et al. in 1976.<sup>8</sup> There are 9 members of ACAD family. First five are responsible for beta-oxidations: short, medium, long and very-long chain acyl-CoA dehydrogenase (SCAD, MCAD, LCAD, VLCAD, respectively) and ACAD-9 (VLCAD-2). Other four members are involved in amino acid oxidation pathways: iso(3)valeryl-CoA dehydrogenase (i3VD) for leucine, iso(2)valeryl-CoA dehydrogenase (i2VD or short/branched chain acyl-CoA dehydrogenase or 2-methylbutyryl-CoA dehydrogenase) for isoleucine, tryptophan isobutyryl-CoA dehydrogenase (iBD) for valine and glutaryl-CoA dehydrogenase (GD) for lysine. Except VLCAD and VLCAD-2 all other enzymes are water soluble homotetramers, which each subunit has approximate mass of 43 kDa and containing a FAD<sup>9</sup>. The VLCAD1 is homodimer with a 70 kDa subunits and one FAD molecule. The native state has a mass of 154 kDa.<sup>10</sup>

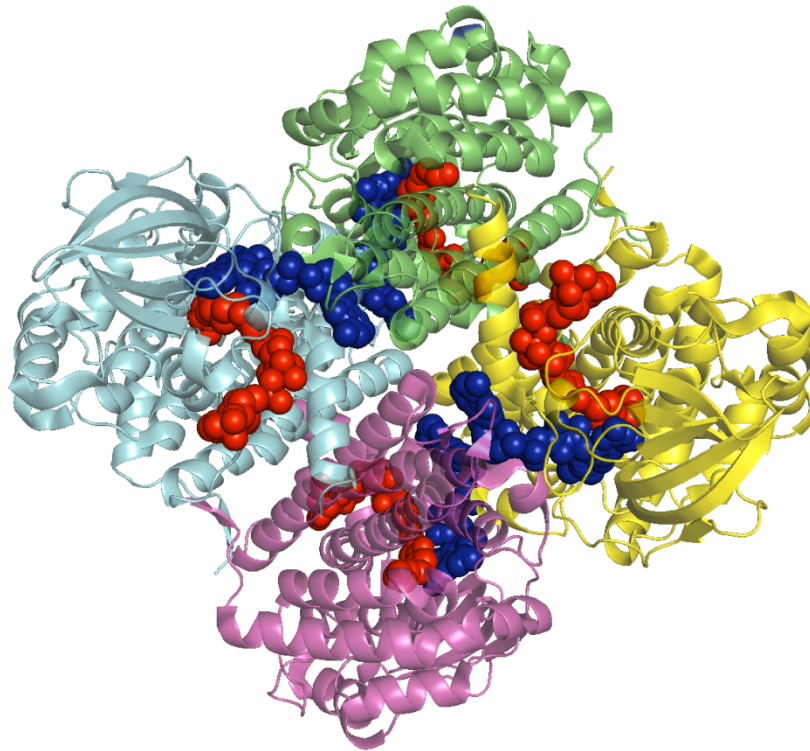


**Figure 1:** A ribbon diagram of a tetramer MCAD. Green ribbons are representing protein structure in tetrahedral conformation, red dots represent enzyme substrate - octanoyl carnitine and blue dots location of the FAD. (Picture was created in PyMOL<sup>11</sup> based on *1udy* PDB structure<sup>12</sup>)

The monomer structure is composed of 3 main domains which N-terminal and C-terminal domain consists mainly from  $\alpha$ -helices. The middle domain is created by two orthogonal  $\beta$ -sheets which lies at the surface of the enzyme (Figure 1). The cavity for the substrate is laying between the helices structure and it can accommodate substrate of length up to 12 carbons. Its C2-C3 portion is stacked between the carboxyl group of Glu376 and isoalloxazine ring of FAD, in a position for the  $\alpha$ - $\beta$ -dehydrogenation reaction.<sup>9</sup>

Substrates for the medium chain acyl-CoA dehydrogenase (MCAD) enzyme (EC.1.3.99.3) are acyl carnitines with medium size carbon moiety (length from 4 -12). The enzyme starts the  $\beta$ -oxidation pathway, which is localized in mitochondria, by introduction of double bond into a  $\beta$ -position of acyl-Coenzyme A (acyl-CoA).

Clinical picture can be highly variable, but generally with trigger mechanisms like metabolic stress (fever, fasting) or other illness can lead to hypo-ketotic hypoglycemia with lethargy, resulting into a coma and death. At the other side of the clinical spectrum are asymptomatic patients, with no symptoms for years, identified retrospectively by newborn screening. Up to 70 mutations were found in *ACADM* (gene is located at 1p31.1) gene so far, the prevalent mutation is c.985A>G (K329E).<sup>13</sup> The incidence varies differently through the world with high number of cases in north Europe and no case in Japan: Denmark 1:8954,<sup>13</sup> England 1:10 000,<sup>14</sup> Netherlands 1:30 000,<sup>15</sup> Germany 1:133 000, overall incidence in USA 1:15 000,<sup>16</sup> Greece 1:16 000,<sup>17</sup> and general incidence in south Europe with exception of Greece 1:300 000.<sup>18</sup> The most common presentation of MCADD is between 3 and 15 months. However, the symptoms may appear at any age from newborn to the adult. If untreated symptoms may cover fasting intolerance, hypoglycemia, hyperammonemia, acute encephalopathy commonly initiated by regular infectious diseases or fasting.<sup>19</sup> These conditions can be avoided by preventing the hypoglycemia. Patients are exhibiting high levels of adipic, suberic and sebamic acids in urine. As well as 5-OH-hexanoic acid and hexanoylglycine were excreted in excessive amounts. Contrary, 7-OH-octanoic acid, 9-OH-decanoic acid, octanoylglycine and decanoylglycine were excreted in limited amounts.<sup>20</sup> Several glycine conjugates are occurring as well (n-hexanoylglycine, 3-phenylpropionylglycine and suberylglycine).<sup>21</sup> Above mentioned biochemical picture depends on clinical status and can vanish during the period of normalcy.

Many diseases, including MCADD, are screened in the majority of the developed world. The tandem mass spectrometry has become a routine tool in the diagnosing of inherited metabolic diseases and plays a key role in the newborn screening. A typical FIA-TMS analysis takes less than minute per sample. Dozens of diagnostically relevant molecules are analyzed with very high specificity and sensitivity.<sup>22</sup> Main biomarker is octanoylcarnitine (C8) and secondary markers are hexanoylcarnitine (C6), decanoylcarnitine (C10) and decenoylcarnitine (C10:1), respectively. Determination of elevated acylcarnitines and their ratios with other acylcarnitines (e.g. acetylcarnitine (C2), dodecanoylcarnitine (C12) – C8/C2; C8/C12; C8/C6) is used for determination of MCADD in dried blood spots, taken within 1-3 days after birth.<sup>23</sup>

### 1.1.2. Adenosine deaminase deficiency

Deficiency of adenosine deaminase (ADA) (OMIM #102700, chromosome 20q13.11) belongs to the broad group of inborn errors of purine metabolism. Its incidence is between 1:200000 and 1:1000000. Most defects of purine metabolism are autosomal recessively inherited, only exceptions are: hypoxanthine-guanine phosphoribosyl transferase deficiency (HPRT) and phosphoribosyl-pyrophosphate synthetase superactivity (PRPS) which are X-linked inherited and familial juvenile hyperuricaemic nephropathy (FJHN) and IMP dehydrogenase 1 (IMPDH1) retinitis pigmentosa which are autosomal dominantly inherited.<sup>24</sup> Adenosine deaminase (E.C.3.5.4.4.) is responsible for transformation of adenosine and 2'-deoxyadenosine into inosine and 2'-deoxyinosine and it is highly expressed in lymphoid cells. There are two isoforms of ADA: ADA1 which is monomeric (41 kDa) and predominantly intracellular (Figure 2) and ADA2 is a homodimer largely expressed in the plasma.

For Educational Use Only

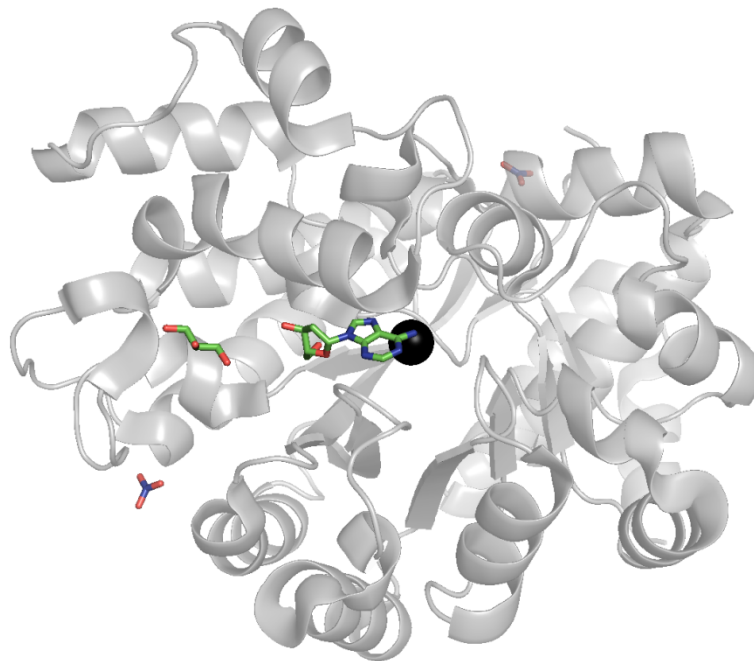


**Figure 2:** A ribbon diagram of a monomeric ADA1 with adenosine substrate. Grey ribbons represent protein structure and black sphere in the middle is a central atom of Ni. Blue group of nitrogen can be seen close to the Ni atom. (Picture was created in PyMOL<sup>11</sup> based on *3iar* PDB structure)

In patients with heritable deficiency of ADA the actions of its metabolites and related products impair with lymphocyte differentiation, function and viability (deoxyadenosinetriphosphate (deoxyATP) appears to be highly toxic for bone marrow). If untreated, it can result in fatal ADA-SCID with lymphopenia, impaired differentiations and function of T-lymphocytes, B-lymphocytes and “natural killers” (NK) cells, auditory defects, cognitive impairment and other systemic malfunctions.<sup>25</sup> First reports are by Giblett et al. who reported two unrelated girls with impaired cellular immunity and almost no ADA activity in red cells. First child had recurrent respiratory infections, candidiasis, and marked lymphopenia from birth. Second child as without symptoms up to second year of life. At the age of 24 months mild upper respiratory infections began and at the age of 30 months severe pulmonary insufficiency and hepatosplenomegaly had progressed.<sup>26</sup>

As mentioned above ADA genes are located on chromosome 20q13.11. There is over 60 gene mutations of ADA located in patients with immune deficiency. Several others were found in a small group of patients with so called partial ADA deficiency, who were clinically unaffected due to significant ADA activity in nucleated cells despite their absence of ADA activity in red blood cells.

The most effective treatment of ADA deficiency is a transplantation of bone marrow from a human leukocyte antigen (HLA)-identical donor which leads mostly to full immune system recovery. Investigate study report that 6.5-year survival rate is 86% and 83% from matched sibling/matched donor and 67% from MUD (HLA-matched unrelated donor). Other option is transplantation form a HLA-haploidentical donor which has been also successful, but with higher morbidity and mortality (43%). The survival rate for mismatched unrelated donor is 29%. Alternative sources of stem cells require a conditioning regimen and posttreatment immunosuppression to prevent graft-versus-host disease (GVHD).<sup>25,27</sup> Recovery of humoral immunity is also less effective. The alternative to the transplantation is an enzyme replacement therapy (ERT) where bovine ADA attached to the polyethylene-glycol (PEG-ADA) is injected into muscle once or twice weekly. The high levels of plasma PEG-ADA can effectively degrade 2'-deoxyadenosine (dAdo) and reverse intracellular pool of deoxyATP. Survival may be high as 78% over twenty years. However, this treatment is expensive and not available in all countries. It was also proven that this therapy decrease number and functionality of

lymphocytes over the time, leaving patients vulnerable to infection, autoimmunity and malignancy.<sup>28,29</sup> Autologous transplant of hematopoietic stem cells corrected by gene transfer has been examined as a potential treatment. So far few dozens of patients were treated like that.<sup>25</sup> In year 1990, a first clinical trial was set using retroviral-mediated transfer of the adenosine deaminase gene into the T cells of two children, after 2 years the treatment ended, but the integrated vector persisted. First successful use of gene therapy treatment in history.<sup>30</sup>

## **1.2. Metabolomics**

The field of metabolomics is highly evolving branch of the „omics“ research. Its main goal is high throughput identification and quantification of small molecule (less than 1500 Da).<sup>31</sup> The set of low molecular weight compounds is called metabolome. In recent years, the metabolome grows rapidly by including not only compounds produced by organism metabolism (e.g. human metabolome), but also by microbes present within the organism (microbiome), compounds related to the diet and drugs or other environmental compounds and their metabolites. All these molecules together are creating highly diverse metabolome which is a subject of study for metabolomics. Metabolites can be divided into several groups by their physicochemical properties (hydrophobicity/hydrophilicity, acidity/basicity and boiling point). Volatility of the compounds can vary from low molecular volatile compounds such as isoprene or carbon dioxide present in the breath up to high molecular weight compounds (e.g. lipids, gangliosides, small peptides).

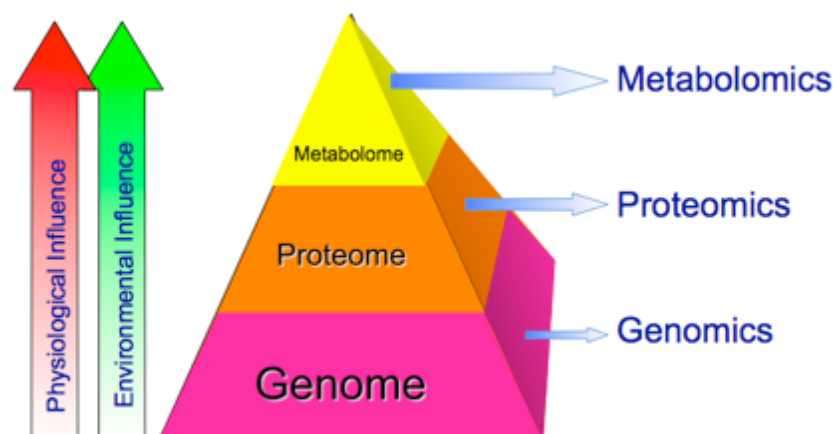


**Figure 3:** Intensity of physiological and environmental influence genome, proteome and metabolome.

Hydrophobicity/hydrophilicity has wide range from highly polar amino acids up to non-polar lipids.<sup>32</sup> Physiological state and influence of the environment are the most influencing factors of metabolome (Figure 3). Today metabolomics studying microbial, plant environmental and mammalian systems.<sup>33</sup> In 2005 Metabolomic Standard Initiative (MSI) was assembled to set standards for data exchange, communicate results and bring general consensus around proposed standards. The aim is to provide a common mechanism for describing the work so that the data can be made available to others for evaluation. Also to suggest an extension or repeat of previously published work, if necessary.<sup>34</sup> Within last five years the number of publications published per year almost tripled in the field of metabolomics (Figure 4).

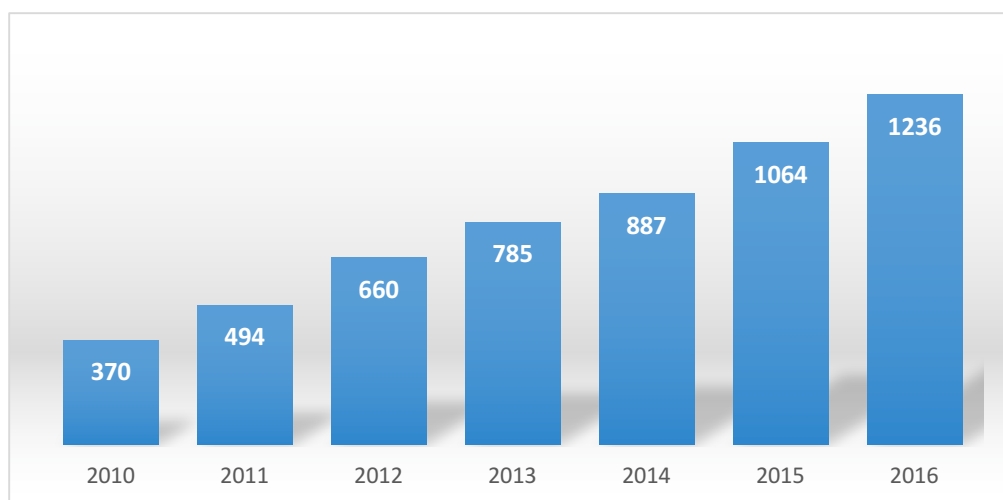


**Figure 4:** Number of publications in mass spectrometry metabolomics since 2010. The data were obtained from Web of Science 10.1.2017 using key words “metabolomics” and “mass spectrometry”.

### 1.2.1. Targeted and Semi-Targeted Metabolomics

Nowadays, three different methodological approaches can be distinguished in the field of metabolomics. First two, targeted and semi-targeted approach can be characterized as a quantification of small group (several dozens in case of semi-targeted approach) of (related) metabolites using mass spectrometers based on triple quadrupoles (QqQ) coupled with ultra-high performance liquid chromatography (UHPLC) or capillary electrophoresis (CE). The acquisition is usually based on multiple-reaction-monitoring (MRM) principle on triple quadrupoles. The first quadrupole is used as for selection of a parent ion of interest (metabolite), in the second quadrupole the fragmentation of that ion occurs and in the third quadrupole the most abundant fragment is selected for the detection, in order to achieve highest sensitivity. When multiple metabolites are being analysed, this process is repeated for each of them creating a cycle (MRM). Each metabolite takes time for analysis (cycle or dwell time) thus analytes are monitored intermittently.<sup>35</sup> Metabolite identity is already known; thus, no further identification is required. Development of related analytical methods is based on isotopically labelled internal standards (analogues of metabolites) which provides high selectivity and precision. The result is absolute quantification of detected metabolites.<sup>33,36</sup>

### 1.2.2. Untargeted metabolomics

The third option, untargeted metabolomics, is the most suitable one for the new biomarker and metabolite discoveries. Analyses are designed to obtain as much information as possible about the sample without any prior knowledge. Instrumentation is based on mass spectrometers capable of data acquisition with high resolving power together with high mass accuracy (e.g. Orbitrap, TOF and Q-TOF instruments, FTICR) and nuclear magnetic resonance (NMR).<sup>32</sup> The key bottleneck in untargeted metabolomics is identification. This is caused by several factors: the diversity of small molecule structures is huge (e.g. PubChem contains almost 90 million compounds, tested compounds - 2 millions); different variety of physicochemical properties (variability is bigger than in proteomics); the number of tools for semi-automated process of metabolite identification developed and tested on the experimental conditions are limited. Nowadays, mass spectrometry and the nuclear magnetic resonance are the most frequent methods used for structure elucidation and metabolite identification.<sup>37</sup> Another important part of untargeted metabolomics is a sample preparation, since it is highly influencing the number of potentially detectable compounds. In order to sustain high metabolite coverage, the non-selective sample pre-treatment methods such as protein-solvent precipitation and dilution are commonly used. The comprehensive metabolomics and lipidomics covers compounds with ~40 orders of magnitude on scale of octanol/water coefficient scale, thus extraction efficiency should be optimized.<sup>38</sup> It is worth mentioning that there is no single method or platform possibly covering all of metabolome. Hence, there is a necessity for development of more robust methods and strategies using as few analytical platforms as possible.

### 1.2.3. Mass spectrometry in metabolomics

The roots of mass spectrometry (MS) are more than one hundred years old when pioneer of the mass spectrometry J.J. Thomson was able to sort constituents of the beams into positive ray parabolas each with defined mass-charge-ratio.<sup>39</sup> In general, mass spectrometers are operating by formation of negatively or positively charged species (ions), their separation is done by mass-to-charge ratio ( $m/z$ ). To reduce ion-ion

and ion-molecules interactions the instruments are working under high vacuum. For formation of ions (ionization) many techniques were developed. Ionization techniques can be divided by energy applied - “soft” and “hard” ionization techniques and by the place where ionization occurs - in vacuum (“matrix assisted laser desorption/ionization” - MALDI, “electron impact” - EI) and those which occurs at atmospheric pressure (APCI, ESI, etc). Great milestone was publication of Electrospray Ionization (ESI) by John Fenn<sup>40</sup> which is now one the most used ionization technique in metabolomics. Majority of the molecules are usually singularly charged due to their low molecular weight which is capable of carrying only one charge. Unlike the proteomics where peptides/proteins are carrying multiple charge. Mass spectrometers are capable of scanning mass range of interest (metabolomics 20 – 2000  $m/z$ , some instruments up to 6000  $m/z$ ) with acquisition time of several spectra per second. Many information about the sample can be acquired due to measuring “full-scan” and  $MS^n$  spectra operating in data independent acquisition (DIA)<sup>41</sup> or data dependent acquisition (DDA).<sup>42</sup> Such approach might be very helpful in metabolite identification and structure elucidation. The advances in electronics and precise manufacturing provided scientist with a broad range of platforms capable precise measurements – time of flight (TOF), quadrupole, Fourier transform and hybrid instruments (quadrupole-TOF (QTOF), ion trap-Orbitrap, triple quadrupoles (QQQ)).

Previous liquid chromatography (LC) instrumentation has not provided sufficient chromatographic resolution as gas chromatography (GC) and thus the LC was not frequently used. The introduction of ultra(-high) performance liquid chromatography on the market by Waters Inc. in 2004 allowed LC to become major separation technique in metabolomics. Nowadays the most comprehensive platforms for metabolomics are combining capillary electrophoresis, gas chromatography (or two dimensional GC) and liquid chromatography (UHPLC) as a separation techniques coupled with mass spectrometers as detectors. In order to find most discriminating features statistical methods based on data clustering, dimension reduction and multiple hypothesis testing are applied.<sup>43</sup>

#### 1.2.4. Mass spectrometry in detection of inborn errors of metabolism

Before 1980, the gas chromatography analysis was usually required for the diagnosis of organic acid and fatty acid metabolism errors. The identification was based just on the retention times. In late 1970' the introduction of mass spectrometry greatly improved the analysis of organic acids – GC/MS became a gold standard for identification of metabolic disorders from urine.<sup>44</sup> It is almost three decades since the tandem mass spectrometry (MS/MS) entered this field. It has a positive impact on the number of screened diseases, development of multi-disease screening tests and on number of newborn screening (NBS) programs around the world. Great excitement was especially about the detection of acylcarnitine profile which was difficult to analyse because the molecules polarity, zwitterionic nature, concentration levels and the lack of a chromophore.<sup>45</sup>

The newborn screening was established in order to detect diseases in their pre-clinical state. Thus, the disease can be diagnosed and treated before it can develop clinical symptoms and be dangerous to the children. In a broader way NBS may include medical examination by doctors (ophthalmologist, orthopaedist, paediatrician). Here the NBS is meant in more narrow way as a laboratory analysis of a biological material, where levels of diagnostically important metabolites are measured. Since the 1<sup>st</sup> June 2016 – 18 disorders are routinely screened in Czech Republic. Among screened disorders belong: congenital hypothyroidism (CH), congenital adrenal hyperplasia (CAH), cystic fibrosis (CF), inborn errors in metabolism of amino acids (*phenylketonuria (PKU)*, *hyperphenylalaninemia (HPA)*, *argininemia (ARG)*, *citrulinemia type I. (CIT)*, *maple syrup urine disease (MSUD)*, *classical homocystinuria - cystathionine beta synthase deficiency (CBS, pyridoxine non-responsive form)*, *homocystinuria based on deficiency of methylene tetrahydrofolate reductase (MTHFR)*, *glutaric aciduria type I (GA I)* and *isovaleric aciduria (IVA)*), inborn errors in metabolism of fatty acids (*medium chain acyl-CoA-dehydrogenase deficiency (MCADD)*, *long chain acyl-CoA-dehydrogenase deficiency (LCADD)*, *very-long chain acyl-CoA-dehydrogenase deficiency (VLCADD)*, *carnitine palmitoyltransferase I deficiency (CPT I)*, *carnitine palmitoyltransferase II deficiency (CPT II)*, *carnitine acyl-carnitine translocase deficiency (CACT)*) and biotinidase deficiency (BTD). ([www.novorezeneckyscreening.cz](http://www.novorezeneckyscreening.cz)) As a screening material a single 3.2-mm dried blood

spot (equivalent to 3.1  $\mu\text{L}$  of blood) is mostly used together with plasma and urine samples. It seems that the best time for sample collection for a large number of disorders lies between 48 – 72 hours.<sup>45,46</sup>

For the NBS purpose is probably most effective the use of flow injection analysis coupled with tandem mass spectrometry (FIA-TMS) with heated electrospray ionization. Although, mass spectrometer without purification or chromatography is not really selective, the tandem mass spectrometry in MRM mode (as described in Chapter 1.2.1) can overcome this issue. It is worth mentioning that relatively short time of analysis (approx. 2 min) provides a high throughput and selective screening at very cost-effective rates.<sup>44</sup>

As an extension of NBS the “selective screening” was introduced, depending on laboratory several diseases can be screened. The analysis usually involves separation technique such as gas chromatography,<sup>47</sup> capillary chromatography<sup>48</sup> and liquid chromatography<sup>49</sup>. Initial approach in LC separation was a reversed-phase chromatography based C18 with acidic mobile phase. Nevertheless, many compounds like ATP did not elute as a defined peaks and many polar compounds did not retain and were eluted in the void volume. More efficient method is hydrophobic interaction chromatography (HILIC) on an amino propyl columns capable of separating broad range of metabolites including amino acids, sugar phosphates, coenzyme A derivatives, nucleosides, nucleotides and carboxylic acids using both positive and negative ionization mode.<sup>35</sup>

### **1.2.5. Structural elucidation and metabolite identification**

As mentioned previously in the text structural elucidation and metabolite identification are key bottlenecks in the field metabolomics. Since the confident assignment is sometimes almost impossible to achieve, the Metabolomic Standard Initiative established four levels of identification (Table 1).<sup>50</sup>

**Table 1:** Level of confidence in metabolite identification set by Metabolomic Standard Initiative.<sup>50</sup>

<i>Level</i>	<i>Confidence of identity</i>	<i>Description</i>
1	Identified compounds	A minimum of two independent and orthogonal data relative to an authentic compound are necessary (e.g. retention time and mass spectrum, retention time and NMR spectrum, accurate and tandem MS, accurate mass and isotope pattern)
2	Putatively annotated compounds	No chemical standard available, based on physicochemical properties and/or structural similarity with public/commercial spectral library (or other laboratories published results)
3	Putatively characterized compound classes	Based upon physicochemical properties and spectral similarity with known compounds of chemical class
4	Unknown compounds	Although unidentified and unclassified, these metabolites can still be differentiated and quantified based upon spectral data

Definitive identification (Level 1) requires at least two orthogonal properties (e.g. retention time/index,  $m/z$ , fragmentation spectra) of a chemical standard analysed under identical analytical conditions. However, even at this level of identification is almost impossible to distinguish some isomers, especially stereoisomers. In that case, the development of an unambiguous separation method is required. Putative annotation (Level 2 or 3) is mainly based on comparison of data acquired in other laboratories by different analytical methods instead of direct data analysis acquired from an authentic standard. In GC-MS, fragmentation spectral libraries can be used for putative annotation because the electron impact (EI) fragmentation patterns are easily

matched between different platforms. In case of UHPLC-MS the accurate  $m/z$  is obtained as a first property for identification, combined with RT and fragmentation spectra are used for comparison with experimental and/or computationally derived databases (e.g. Metlin, HMDB, Foodb.ca, mzCloud, MoNA, LipidMaps, etc.).<sup>33</sup> At the Level 4 confidence of identity, two different kind of compounds can be distinguished – “known unknowns” and “unknown unknowns”. Identification of “known unknowns” is based on examination of acquired mass spectra with those present in the database, thus the metabolite is known and was already described. The real challenge is identification of “unknown unknowns” because those metabolites were never described before and they are truly novel to the scientists (to the best of our knowledge). Due to high sensitivity of analytical techniques (LC-MS) unknown compounds may appear even in the well-studied organisms.<sup>51</sup>

#### **1.2.6. “Seven golden rules” of identification**

In 2007 Tobias Kind and Oliver Fiehn published “Seven golden rules” as basic suggestion for metabolite identification that is currently accepted by the metabolomic community.<sup>52</sup>

By application of the first rule the number of elements for computing the summary formula is restricted (e.g. molecule of 1000 Da containing only carbon will have 83 carbons at maximum).

Second rule are LEWIS and SENIOR check. In order to determine correct chemical formula, the ion species must be set to the neutral state (uncharged). Then calculation of the formula is done by using all combinations of all set elements (e.g. C, H, N, O, P, S, Cl, Br). LEWIS rule demands that all atoms (especially carbon, oxygen, nitrogen) share electrons that meet the “octane rule” (all  $s$  and  $p$  valences shell are filled).<sup>53</sup> SENIOR theorem requires three different rules:<sup>54</sup>

- i) The sum of valences or the total number of atoms having odd valences is even;
- ii) The sum of valences is greater than or equal to twice the maximum valence;
- iii) The sum of valences is greater than or equal to twice the number of atoms minus 1.

The third rule applying isotopic pattern filter based on relative isotopic abundances (RIA). Molecules synthesized in nature contains isotopes according to the average nature abundance and are listed for each element.<sup>55</sup> Hydrogen/Carbon ratio check is applied as a fourth rule. Most abundant ratios are between  $2.0 > H/C > 0.5$ . Fifth and sixth rule are used to check ratios and probability of heteroatoms and other elements by heuristic rules. Seventh rule is applicable for gas chromatography analyses where derivatization of sample is necessary. MSTFA (N-Methyltrimethylsilyltrifluoroacetamide; CAS: 24589-78-4) is common compound involved in the sample preparation step. Trimethylsilyl (TMS –  $C_3H_8Si$ ) groups have to be subtracted for calculated underivatized molecule.

### **1.2.7. Spectral trees**

Each compound produces different mass spectra if exposed to diverse fragmentation techniques and various collisional energies. Spectral tree is an intuitively organized multistage tandem mass spectra acquired at different collision energies, and techniques (Figure 5). If you picture a spectral tree in the three dimensional space than on the X axis are plotted fragments of precursor ion(s). Y axis represents level of fragmentation ( $MS^n$ ). The depth of each column (Z axis) represents spectra of each individual fragment acquired at different collisional energies and by various fragmentation techniques. Curated database based on the spectral trees can highly increasing chance for positive match in a “spectrum search” findings and thus metabolite identification.

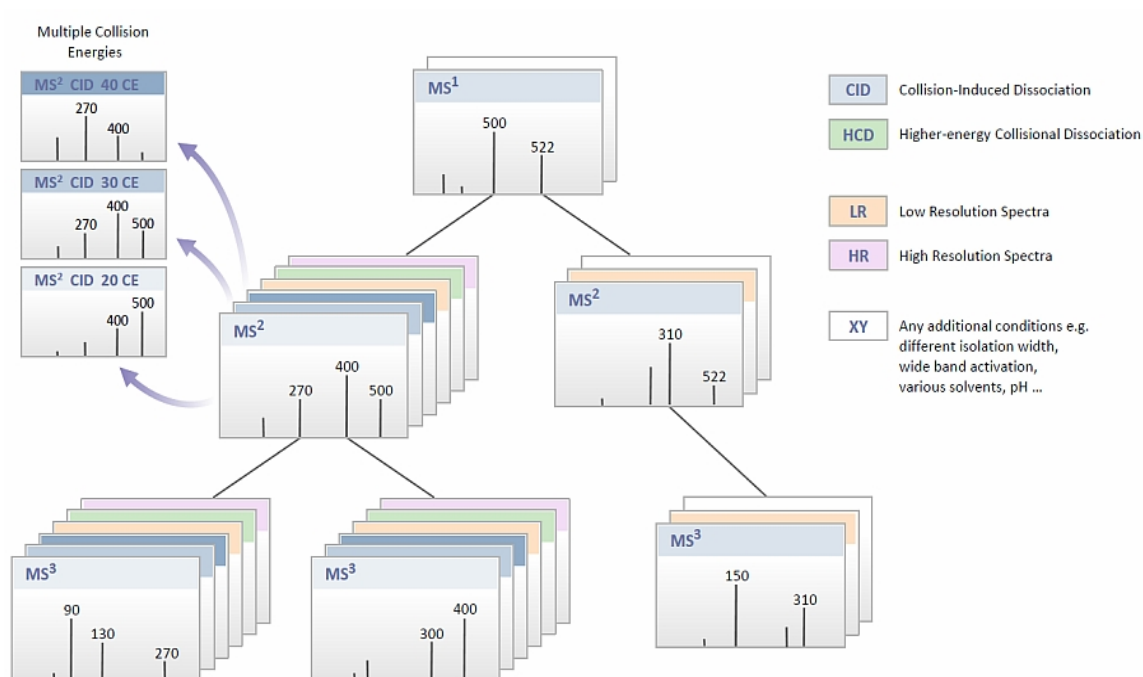


Figure 5: Spectral tree. On the X axis are plotted fragments of precursor ion. Y axis represents level of fragmentation ( $MS^n$ ). The depth of each column (Z axis) represents spectra of each individual fragment acquired at different collisional energies and by various fragmentation techniques. ([www.mzcloud.org](http://www.mzcloud.org) 4.8.2016)

### 1.2.8. Influence of high resolution

Electrospray ionization is preferable ionization technique because of its capability to produce “whole” molecular ions that aids initial metabolite identification. On contrary, EI ionization creates fragmentation patterns which provide unique information for database search (e.g. GC data against commercial NIST database).

Analysis of complex samples by modern separation techniques in conjunction with high resolution exact mass spectrometry can bring huge number of features, characterized by exact mass and chromatographic behaviour. High resolution mass spectrometry analysers are usually based on the FTICR, the double focused magnetic sectors, reflectron time-of-flight mass analysers or ion trap. The last two techniques are mostly used in the analysis of biological samples. Resolution of several tens of thousands of FWHM (full-width-at-half-maximum) with the acquisition of high-speed data transfer of up to 100 Hz can be achieved with the current time-of-flight instruments (TOF) for which scan speed is independent of resolution. In contrast, mass spectrometers based

on orbital ion trap using Fast Fourier Transform (FFT) allow resolution of up to 500,000 FWHM (at 200  $m/z$ ) at the expense of lower scan rates. For this reason, their greater mass resolution generally requires a longer scanning and, consequently, fewer data points are obtained over the studied peak. This could cause problems for the detection functions, deconvolution and quantification. Mass spectrometry measurements accurate to four decimal places are very important in prediction of the molecular formula. With increasing resolution, the number of compounds with apparently same  $m/z$ , decreases due to lower interference of the isobaric matrix. In many analyses of highly complex samples (e.g. metabolomics, proteomics), the balance between mass spectral acquisition speed and mass resolution is a problem.<sup>56</sup>

Chromatographic separation of complex biological samples is still a big challenge. Serum metabolome in human, is chemically highly variable and consists of many classes of metabolites, including amino acids, purines, lipids (e.g., glycerolipids, phospholipids), hydroxycarboxylic acids, etc. The analysis of these complex matrices is usually difficult and requires a number of different separation techniques (liquid chromatography, gas chromatography, capillary electrophoresis).<sup>31,57</sup> In addition, the concentration levels of metabolites may change over six orders of magnitude.

Metabolomics and high resolution mass spectrometry itself have brought a fresh perspective into a clinical diagnostic. Within the last few years many innovative and precise analytical methods have been developed creating a low-cost highly efficient medical care.

## 2. Aims of the work

- Investigate of pathophysiological/pathobiochemical changes connected with medium chain acyl-CoA dehydrogenase deficiency (MCADD) by means of untargeted metabolomics
- Study a “spectral trees” as a tool of metabolite identification in patients suffering from adenosine deaminase deficiency (ADA)
- Describe the influence of a mass spectrometry resolution on feature (metabolite) detection in LC-HRMS untargeted metabolomics by theoretical simulations and experimental measurements

### **3. Materials and methods**

#### **3.1. Chemicals**

Solvents acetonitrile, methanol and water (all LC-MS quality) and acetone (HPLC quality) as well as formic acid, acetic acid and ammonium hydroxide were purchased from Sigma-Aldrich (St. Louis, USA). Standards of PGPC (1-O-hexadecanoyl-2-O-(9-carboxybutanoyl)-*sn*-glyceryl-3-phosphocholine) and PAzPC (1-O-hexadecanoyl-2-O-(9-carboxyoctanoyl)-*sn*-glyceryl-3-phosphocholine) were purchased from Avanti Polar Lipids, Inc. (Alabaster, AL).

#### **3.2. Samples**

##### **3.2.1. Medium chain acyl-CoA dehydrogenase deficiency**

Two sets of patient samples were chosen for the experiment. First dataset consists of dry blood spots from healthy newborns (control group,  $n=25$ ) and patients suffering from MCADD (8 patients,  $n=25$ ; from subsequent sampling). Four patients were compound heterozygotes and four were homozygous with mutation c.985A>G. In order to confirm the results and validate the chemical species (metabolites) identified in untargeted metabolomics experiment a second set of samples from 250 newborns was used for targeted metabolite analysis. All samples were obtained from Laboratory for inherited metabolic disorders (University Hospital Olomouc, CZ) within the pilot project of Czech newborn screening program. Written informed consent according to the Declaration of Helsinki by the World Medical Association (WMA) was obtained from the volunteers for all samples used in the analyses.

##### **3.2.2. Adenosine deaminase deficiency**

For metabolite profiling of urine 4 samples of patients suffering from adenosine deaminase deficiency (ADA) and 4 control samples were chosen. All samples were obtained from Laboratory for inherited metabolic diseases in University Hospital Olomouc, CZ within the Czech newborn screening program. Written informed consent according to the Declaration of Helsinki by the World Medical Association was obtained

from the volunteers for all samples used in the analyses. Creatinine concentration was measured at the Department of Clinical biochemistry of University Hospital in Olomouc.

### **3.2.3. Control samples**

Plasma samples from healthy volunteers were collected at the University Hospital Olomouc (Czech Republic). The samples were pooled and then stored at -80°C until analysis. Written informed consent according to the Declaration of Helsinki by the World Medical Association (WMA) was obtained from the volunteers for all samples used in the analyses.

## **3.3. Sample preparation and processing methods**

### **3.3.1. Medium chain acyl-CoA dehydrogenase deficiency**

#### **3.3.1.1. Untargeted metabolomics experiment**

Two discs (3.2 mm) were dissected from dry blood spot and extracted in pure methanol (100 µL) and incubated in shaker (30 min, 25°C). Afterwards the samples were centrifuged (24 400 x *g*, 15 min, 4°C). Supernatant (50 µL) was mixed with water (50 µL) and analysed by LC-MS untargeted metabolomics method adopted from Bajad et al.<sup>49</sup>

The stationary phase employed an aqueous normal phase separation system using amino-propyl stationary Luna NH<sub>2</sub> 3 µm 100 Å, 150 x 2 mm (Phenomenex, Torrance, USA). An Dionex UltiMate 3000 Rapid Separation LC system (Thermo Fisher Scientific, MA, USA) was used for liquid chromatography and binary gradient elution consisted of 20 mM ammonium acetate in water, pH 9.45 (mobile phase A) and acetonitrile (mobile phase B). The gradient elution with flow rate of 0.3 mL/min was: t=0.0, 95% B; t=15.0, 30% B; t=17.0, 5% B; t=23.0, 5% B; t=23.1, 95% B; t=28.0 min 95% B. The injection volume was 10 µL.

An Orbitrap Elite (Thermo Fisher Scientific, MA, USA) was used for untargeted metabolomics experiments. The polarity was set to positive for full scan mode (120 000 FWHM) within range of 70 - 1200 *m/z*. Settings of the electrospray ionization were as follows: Heater temperature of 300°C; Sheath Gas of 35 arb. units; Auxiliary gas of 10 arb. units; Capillary temperature of 350°C and source voltage was +3.0 kV. A Thermo

Tune Plus 2.7.0.1103 SP1 was used as instrument control software and data were acquired in profile mode and processed in Thermo Excalibur 2.2 SP1.48 software (Thermo Fisher Scientific, MA, USA).

Quality control (QC) samples were prepared by pooling all patient and control samples together (10  $\mu$ L). Blank sample was prepared by the same procedure without discs from dry blood spot. All samples in the batch were randomized. QC samples were analysed and used as previously published.<sup>58</sup> Fragmentation spectra  $MS^n$  were acquired on an Orbitrap Elite using CID (collision-induced dissociation) and HCD (higher-energy collisional dissociation) fragmentation method with detection via FTMS (resolution 60 000 FWHM) in both positive and negative mode as required. Settings for  $MS^2$  and  $MS^3$  experiments were: act.Q. of 0.25, act. time of 10 ms (for  $MS^3$  20 ms) and normalized collision energy of 35 NCE (Normalized collisional energy). HCD fragmentation settings were: act.Q. of 0.10 and normalized collision energy of 40 NCE.

#### **3.3.1.2. Targeted analysis – confirmation experiment**

In order to confirm new metabolic findings, the samples from additional MCADD patients ( $n=25$ ) and healthy controls ( $n=250$ ) were measured by FIA-TMS method routinely used for metabolite target analysis (MassChrom<sup>®</sup> Amino Acids and Acylcarnitines/Non Derivatised, Chromsystems, DE) with addition of specific transitions for the selected phospholipids (Table 2). A liquid chromatography system Dionex UltiMate 3000 Rapid Separation LC system (Thermo Fisher Scientific, MA, USA) coupled with a triple quadrupole mass spectrometer API 4000 (AB Sciex, CA, USA) operating in MRM mode was used for metabolite targeted analysis.

**Table 2:** Table of phosphatidylcholines MRM transition added to the metabolite target analysis.

Q1 ( <i>m/z</i> )	Q3 ( <i>m/z</i> )	Compound
666.4	184.1	PAzPC - PC(16:0;9:0(COOH))
625.5	184.1	lipid (PC)
638.4	184.1	PC(18:0;5:0(COOH))
652.4	184.1	PC(16:0;8:0(COOH))
639.4	184.1	lipid (PC)
838.6	184.1	lipid (PC)
840.6	184.1	lipid (PC)
623.5	184.1	lipid (PC)

### 3.3.1.3. Data processing

Data from untargeted metabolomics experiment were processed in R software<sup>59</sup> with XCMS,<sup>60-62</sup> CAMERA<sup>63</sup> and muma<sup>64</sup> packages. Peak finding was performed by XCMS package using “matchedFilter” method and 1900 features were identified. Isotopes and adducts across the list of features were grouped by CAMERA package. First zero imputation was done by function of XCMS “fillpeaks” which integrates a noise in the same retention time of missing peak. Features containing more than 30% of zeros, isotopes and adducts were excluded from further processing.

Quality control-based robust LOESS (LOcal regrESSion) signal correction method was applied.<sup>58,65</sup> The curve was fitted through the QC points (based on LOESS) and smoothing factors were calculated for each feature. Smoothing factors with ratio of the maximum and the minimum of smoothing values higher than 10 were deleted from the data set. The feature values were divided by smoothing factors and used for further processing. Coefficients of variation were calculated and all features with a value higher than 30% were rejected from further processing, reducing the number of features to 273. Zero imputation was applied on the dataset. Zero values were replaced by two thirds of minimal value per features within each sample group. Data were transformed by centered logratio (clr) transformation and mean centered, respectively.<sup>66</sup>

For statistical evaluation both unsupervised (principal component analysis (PCA)) and supervised methods (orthogonal partial least squares discriminant analysis (OPLS-DA)) were applied. S-plot from OPLS-DA was used to elucidate features important for discrimination. This function was calculated using the muma package in R.

Spectra acquired in metabolite target analysis were evaluated in MultiQuant™ 2.1.1 (AB Sciex, CA, USA) and statistically processed in R. Data were referenced to the D3-octanoylcarnitine as an internal standard. Finally, the data were visualised by boxplots and scatter plots. Statistical significance (p-value) was calculated by non-parametric Wilcoxon Rank Sum test.

#### **3.3.1.4. Confirmation of important discriminatory metabolite features**

In order to identify features from the above process (S-plots from OPLS) four levels of identification reliability were applied as described in Chapter 1.2.4. Instead of simple fragmentation spectra approach “spectral trees” were applied (these are sets of MS<sup>n</sup> data using different fragmentation techniques and collision energies ([www.mzcloud.org](http://www.mzcloud.org))). The determination of lipid acyls and the level of their saturation were elucidated in negative mode using CID fragmentation up to MS<sup>3</sup>. PAzPC and PGPC standards were used for determination of general lipid retention time at this separation conditions. For drawing and annotating structures ACD/ChemSketch (ON, CA) software was used.

### **3.3.2. Adenosine deaminase deficiency**

#### **3.3.2.1. LC-MS metabolite profiling of urine samples**

Ultra-high performance liquid chromatography Dionex UltiMate 3000 Rapid Separation LC system (Thermo Fisher Scientific, MA, USA) coupled with hybrid mass spectrometer Orbitrap Elite (Thermo Fisher Scientific, MA, USA) was used for the analyses. Aqueous normal phase system containing amino-propyl column Luna (3 µm NH<sub>2</sub> 100 Å, 100 x 2 mm (Phenomenex, Torrance, USA)) was used for the separation with mobile phase A consists of ammonium acetate (20 mmol/L, pH 9.75) and B of acetonitrile. Gradient elution with flow of 300 µl/min was t=0.0, B 95%; t=1.0 95% B; t=7.0 5% B; t=13.0 5% B; t=13.1 95% B; t=17.0 95% B. Column was tempered to 35°C and injection volume was 2

µl. Hybrid mass spectrometer Orbitrap Elite operated in positive ionization mode with electrospray ionization settings as follows: Ion source: 250°C; Capillary temperature 350°C; Ion source voltage +3kV; Sheath gas 35 Arb; Auxiliary gas 15 Arb. All data were acquired in centroid mode in mass range 70 – 1200  $m/z$  with resolution of 120 000 FWHM. MS<sup>n</sup> fragmentation spectra were acquired with resolution of 60 000 FWHM.

### **3.3.2.2. MS<sup>n</sup> analyses of selected purine metabolites in human urine**

Four patient samples suffering from adenosine deaminase deficiency was used for analyses. All samples were diluted to creatinine concentration of 1 mmol/L. Metabolite profiling was performed by UHPLC with detection on Orbitrap Elite. LTQ Tune Plus 2.7.0.1103 SP1 was used for acquiring data in data-dependent mode (DDA) where the most intense fragments ( $n=5$ ) from MS<sup>2</sup> were selected for further MS<sup>n</sup> fragmentation. Spectra were detected by FTMS with resolution 60 000 FWHM. Settings for CID fragmentations were: act.Q. 0.25; act. time 20 ms; normalized collision energy 35. Settings for HCD were: activation time 0.10 ms; normalized collision energy 50. Isolation window was set to 2 Da. All acquired spectra were assembled into a respective spectral trees.

Data were processed in Compound Discoverer 1.0.0.692 (Thermo Fisher Scientific, USA). For fragment annotation software Mass Frontier 7.0.5.9 SP3 (HighChem, SK) and mzCloud database ([www.mzcloud.org](http://www.mzcloud.org), HighChem, SK) were used.

### **3.3.3. Influence of a mass spectrometry resolution on feature (metabolite) detection in LC-HRMS untargeted metabolomics**

#### **3.3.3.1. Sample preparation and LC-HRMS method**

Samples were prepared using a method modified from Yuan et al.<sup>67</sup> Pooled human plasma sample (500 µL) was solvent-precipitated by mixture of acetonitrile, acetone and methanol (v/v 1:1:1, 1500 µL, -80°C) and incubated overnight at -80°C. Samples were centrifuged (24 400  $\times g$ , 15 min, 4°C), freeze-dried and re-suspended in 1 mL of 10% methanol:90% water. The LC method followed that of Wang, J. et al.<sup>68</sup> using a Dionex UltiMate 3000 Rapid Separation LC system (Thermo Fisher Scientific, MA, USA). Samples were analysed on an Acquity UPLC BEH C18, 2.1  $\times$  100 mm, 1.7 µm column

(Waters, MA, USA). The mobile phase consisted of water with 0.1% formic acid (mobile phase A) and methanol with 0.1% formic acid (mobile phase B). A flow rate of 0.350 mL/min was used with the following elution gradient: t=0.0, 0.5% B; t=4.0, 70% B; t=4.5, 98% B; t=10.4, 98% B; t=10.6, 0.5% B; t=15.0 min, 0.5% B. The column temperature was set at 40°C and the injection volume was 2 µL. Peaks in the retention window from 1 – 15 minute were chosen for data processing.

An Orbitrap Elite hybrid mass spectrometer (Thermo Fisher Scientific, MA, USA) was operated in either positive or negative mode at 30 000, 60 000, 120 000, 240 000 and 480 000 FWHM at 400 *m/z* over the ranges 70–500 *m/z* and 300–2000 *m/z* (acquisition at 480 000 FWHM was possible by using a Tune Plus Developer's Kit, kindly provided by Thermo Fisher Scientific, MA, USA). Two regions were chosen in order to increase sensitivity and ensure one scan per spectrum (according to Mathieu equation). To eliminate variances due to sample injection, separation and detection, analyses of plasma samples were performed in sextuplicate for each mass spectrometry resolution. Settings of the electrospray ionization were as follows: heater temperature 250°C; sheath gas 35 arbitrary units; auxiliary gas 15 arbitrary units; capillary temperature 300°C and source voltage +3.0 kV. A Thermo Tune Plus 2.7.0.1103 SP1 was used as instrument control software and data were acquired in centroid mode using Thermo Excalibur 2.2 SP1.48 software (Thermo Fisher Scientific, MA, USA).

### 3.3.3.2. *In silico* calculations

In order to simulate effect of the mass spectrometry resolving power on the compound detection/identification in a metabolite rich biofluid the *in silico* calculations were performed. A comprehensive list of compounds known to constitute the human metabolome was established. A list of positively ionizable metabolites from the HMDB ([www.hmdb.ca](http://www.hmdb.ca)), LipidMaps ([www.lipidmaps.org](http://www.lipidmaps.org)) and KEGG (<http://www.genome.jp/kegg/>) databases was compiled (41 474 metabolites in total after removing duplicates). All calculations were performed using R software<sup>59</sup> in conjunction with the package Rdisop.<sup>69–72</sup> For each metabolite, the isotopic pattern based on the chemical formula was generated. From the database generated list, adducts for M, M+1 and M+2 isotopes ([M+H]<sup>+</sup>, [M+NH<sub>4</sub>]<sup>+</sup>, [M+Na]<sup>+</sup>, [M+K]<sup>+</sup>, [M+ACN+H]<sup>+</sup>) were calculated (622 110 features). Mass distribution graphs for 15 000,

30 000, 60 000, 120 000, 240 000, 480 000, 960 000, 1 920 000 and 3 840 000 FWHM at  $m/z$  400 were then plotted. By removing isobars from the metabolite list (41 474) based on  $m/z$ , a list of unique  $m/z$  was generated (15 722). For each unique  $m/z$  in the list, the theoretical mass spectrometry peak width [ $m/z - x$ ;  $m/z + x$ ] was calculated, where  $x = m/z \text{ mass}/(\text{resolving power} * ((400/(m/z \text{ mass}))^{(1/2)}))$ . Consequently, the entire final list of 622 110 features was searched against the interval defining the number of features not detectable due to isobaric matrix interferences within the calculated range of each unique  $m/z$  (15 722).

The influence of resolution on the number of detected peaks was calculated for  $m/z$  up to 2000. The list of generated in silico features (622 110) was filtered to give unique  $m/z$  values (227 060). The first value from the list of unique  $m/z$  was taken and the peak width based on resolution and its  $m/z$  were calculated. All  $m/z$  values lying within the peak width were grouped and removed from the list. The final number of groups was considered to be the number of peaks detectable in the mass spectrum for the given resolution and mass range.

### 3.3.3.3. LC-MS data processing

The acquired dataset from the plasma samples was processed using the three most frequently used software based on different feature detection algorithms, i.e., XCMS 1.44 (in R software environment), Compound Discoverer 2.0.0.303 and MZmine 2.13.1 centWave algorithm in XCMS, to detect regions of interest (ROI) within the particular  $m/z$  value. The Continuous Wavelet Transform (CWT) was applied to the intensity values of the ROI and local maxima in the CWT coefficients for each scale were determined.<sup>61</sup> Peak detection algorithms are mainly influenced by the parameters ppm mass error (ppm) and signal-to-noise ratio (snthresh). Various values of these parameters were tested (ppm = 2, 4, 6, 8, 10, 12, 14, 16, 18, 20; snthresh = 10, 12, 14, 16, 18, 20, 22, 24, 26, 28, 30) and after detailed study of the results, “ppm= 8” and “snthresh=20” were chosen as the best settings.

Retention time correction in each software was performed for individual sextuplicates. The processed lists of features for the ranges 70–500  $m/z$  and 300–2000  $m/z$  for each resolving power were merged at 400  $m/z$  in order to obtain the final number of features in the spectra per resolving power. Coefficient of variance (CV) was

calculated based on detected areas across six replicate injections. Peaks with CV > 30% were considered as noise and removed from further calculations.

#### 3.3.3.4. Peak detection algorithm settings

For XCMS the component detection parameters were set as follows: `xset <- xcmsSet(files=cdf_files, method = 'centWave', ppm = 8, snthresh = 20, prefilter = c(4, 10000), integrate = 1, mzdif = -0.001, verbose.columns = F, fitgauss = TRUE, peakwidth=c(3,10), nSlaves=6)`. Nodes in Compound Discoverer 2.0.0.303 were used as follows: *Select Spectra* (Lower RT Limit = 1; rest were left default); *Detect Unknown Compounds* (Mass tolerance = 8 ppm; S/N threshold = 3; Min. Peak Intensity = 10000; Ions = [M+H]<sup>+</sup>, [M+H-H<sub>2</sub>O]<sup>+</sup>, [M+H-NH<sub>3</sub>]<sup>+</sup>, [M+K]<sup>+</sup>, [M+Na]<sup>+</sup>, [M+NH<sub>4</sub>]<sup>+</sup>; Min. # Scans per peak = 4; Min. # Isotopes = 1; rest were left default); *Group Unknown Compounds* (Mass tolerance = 8 ppm; RT tolerance [min] = 0.05; rest were left default). In MZmine *Centroid Mass Detector* at threshold 5000 was used than *Chromatogram Builder* with *Minimum height 10000*. As chromatogram deconvolution method *Local minimum search* was used with parameters as follows: *Chrom. Threshold = 85%*, *Minimum RT range (min) = 0.2*, *Minimum relative height = 1%*, *Minimum absolute height = 10000*, *Min ration of peak top/edge = 2*, *Peak duration range (min) = 0 – 10*.

## 4. Results & Discussions

### 4.1. New potential biomarkers of oxidative stress in patients suffering from MCADD

Principal component analysis (PCA) used for data evaluation showed separation between group of patients and control group (Figure 6). Statistical unsupervised methods (e.g. PCA) more likely reflects true relationship between samples according to their metabolic state than supervised methods (e.g. linear discriminant analysis). Supervised methods have given sample groups in advance and based on this grouping are detecting distinguishing variables. On the contrary the unsupervised methods have no such information and thus more likely reflect the reality. In order to extract most differentiating features orthogonal-partial least square discriminant analysis (OPLS-DA) was used (Figure 7). Based on the derived S-plot (Figure 8) which is representing a visualization of covariance and correlation between features and the selected groups of samples. Parameters for selecting most discriminant features were as follows:  $p1 \geq \pm 10$  and  $p1(\text{corr}) \geq \pm 0.5$ .

PCA – Controls vs. MCADD

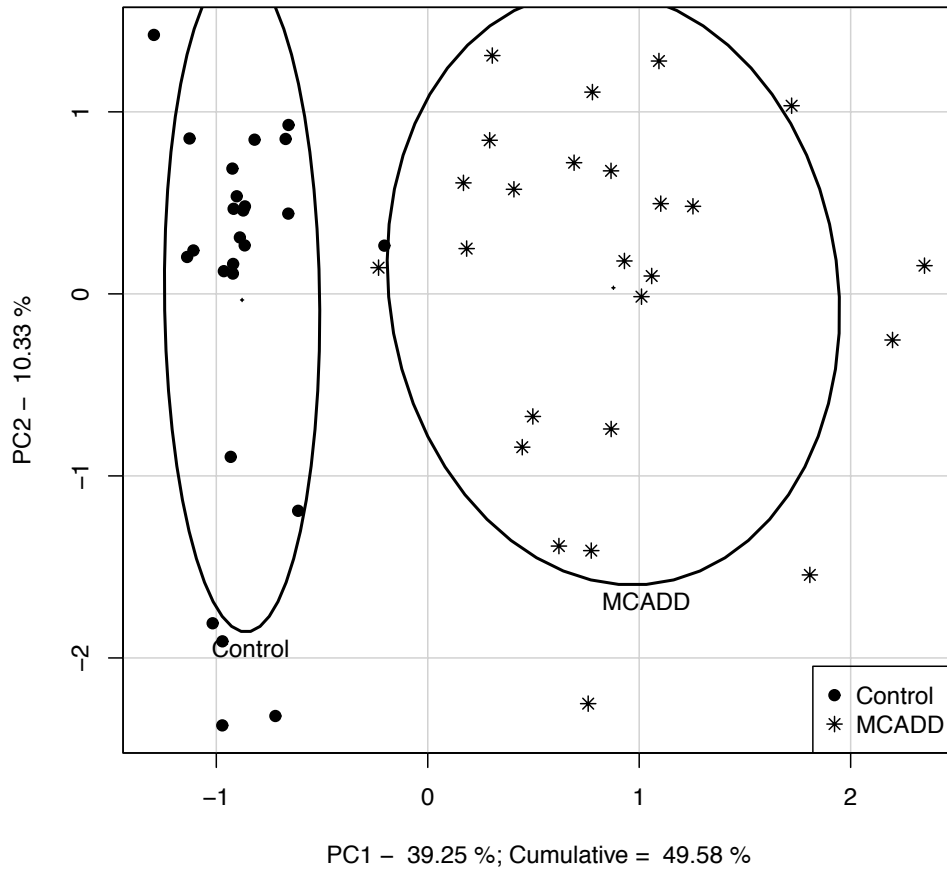
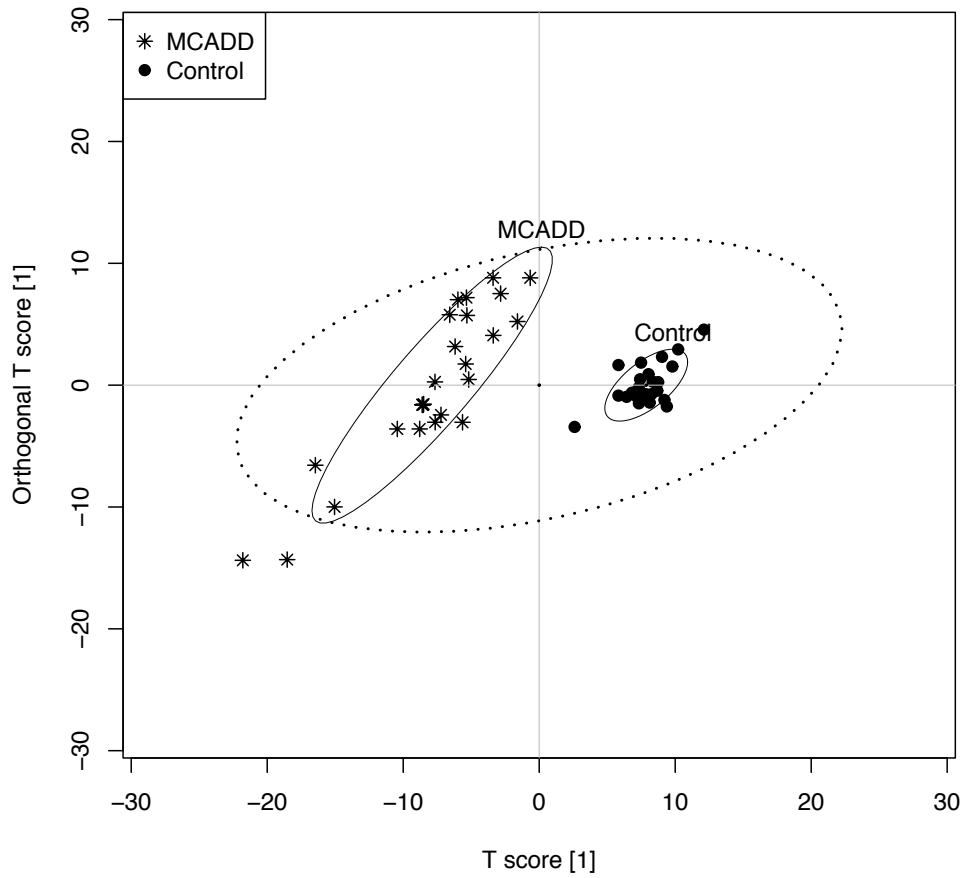
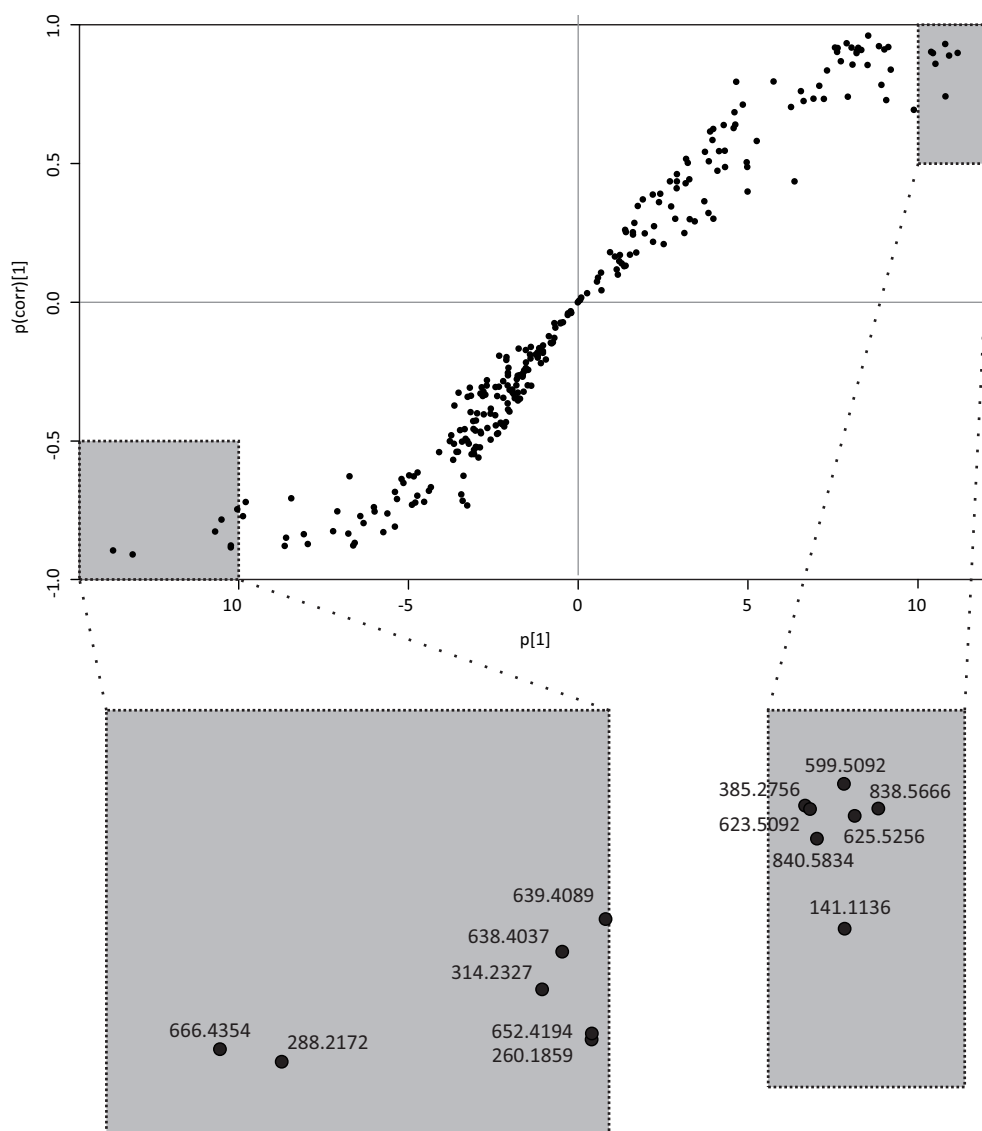


Figure 6: Principal component analysis of dried blood spots of patients suffering from MCADD and healthy controls.

### OPLS-DA score scatter plot



**Figure 7:** Orthogonal partial least square discriminant analysis (OPSL-DA) of dried blood spots of patients suffering from MCADD and healthy controls.



**Figure 8:** OPLS-DA derived S-plot of the most discriminating features.

Features which meet the selection criteria ( $n=14$ ) are shown in Table 3. Already known biomarkers octanoylcarnitine (C8), hexanoylcarnitine (C6) and decenoylcarnitine (C10:1) were found as well as new compound 1-O-hexadecanoyl-2-O-(9-carboxyoctanoyl)-*sn*-glyceryl-3-phosphocholine (PAzPC) – all MSI Level 1 identification. As putatively annotated compounds (MSI Level 2) another phosphocholines 1-O-octadecanoyl-2-O-(5-carboxybutanoyl)-*sn*-glyceryl-3-phosphocholine PC(18:0;5:0(COOH)) and 1-O-hexadecanoyl-2-O-(8-carboxyheptanoyl)-*sn*-glyceryl-3-phosphocholine, PC(16:0;8:0(COOH)) were identified based upon fragmentation similarity with PAzPC and phospholipids alike presented in the databases. In most  $MS^n$

spectra acquired in negative ionization mode we have identified palmitic acid moiety (255.2330  $m/z$ ) (Figure 9-11; 14-16) and 3-(hexadecanoyloxy)-2-hydroxypropyl 2-(dimethylaminoethyl) phosphate of  $m/z$  value 480.3096 (Figure 9 and 14). Likewise, stearic acid moiety (283.2643  $m/z$ ) and 3-(octadecanoyloxy)-2-hydroxypropyl 2-(dimethylaminoethyl) phosphate (508.3398  $m/z$ ) in case of PC(18:0;5:0(COOH)) were detected (Figure 12, 13). In positive ionization mode phosphocholine moiety was detected (184.0733  $m/z$ ) in all phosphatidylcholines presented in Table 3. The phosphocholine moiety confirmation was done by subsequent MS<sup>3</sup> fragmentation in positive ionization mode. Compounds labelled MSI Level 3 in Table 3 were identified as phosphatidylcholines (PC) regarding to the presence of phosphocholine in fragmentation spectra in positive ionization mode. No sufficient negative fragmentation spectra were acquired due to low abundance of the metabolites. Rest of the compounds listed in the Table 3 was labelled as “unknowns” (MSI Level 4).

**Table 3.** List of the most significant features identified by the S-plot. Restriction parameters ( $p_1 = +/-10$  and  $p_1(\text{corr}) = +/-0.5$ ); Levels of identification – see text for explanation; PC = phosphatidylcholine

abs(p1) S-Plot	Positive ( $m/z$ )	Error (ppm)	Chemical formula	RT (sec)	Name	Level of identification
+ 13.68	666.4354	2.0167	C33H65O10NP	514.1	PC(16:0;9:0(COOH)) - PAzPC	1
+ 13.1	288.2172	1.0201	C15H30O4N	407.6	Octanoylcarnitine (C8)	1
- 11.18	838.5666	1.7339	C39H85O15NP	511.1	lipid (PC)	3
- 10.93	625.5256	0.7066	C30H76O9NP	426.2	lipid (PC)	3
- 10.84	141.1136			411.8	unknown	
- 10.81	599.5092			427.2	unknown	
+ 10.68	314.2327	0.2864	C17H32O4N	401.2	Decenoylcarnitine (C10:1)	1
- 10.53	840.5834	3.7607	C39H87O15NP	510.9	lipid (PC)	3
+ 10.48	638.4037	1.3941	C31H61O10NP	510.0	PC(18:0;5:0(COOH))	2
- 10.46	623.5091	-0.7329	C30H74O9NP	426.1	lipid (PC)	3
- 10.4	385.2756			425.0	unknown	
+ 10.21	260.1859	0.9685	C13H26O4N	417.4	Hexanoylcarnitine (C6)	1
+ 10.21	652.4194	1.5374	C32H63O10NP	515.2	PC(16:0;8:0(COOH))	2
+ 10.01	639.4089	6.5858	C38H58O5NP	510.3	lipid (PC)	3

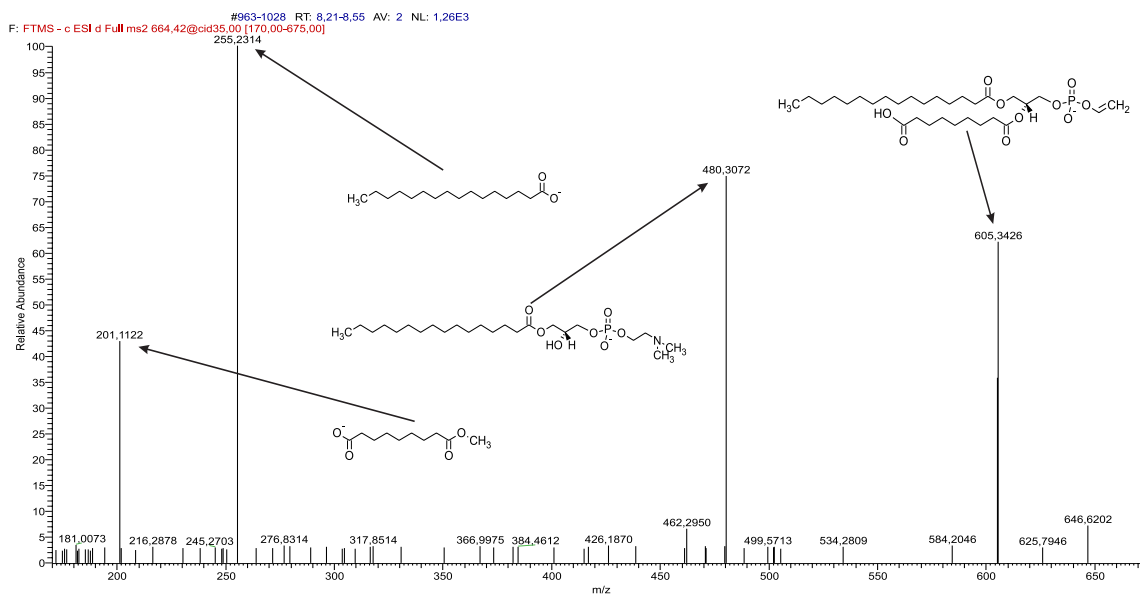


**Figure 9:** MS<sup>2</sup> fragmentation spectra of 1-O-hexadecanoyl-2-O-(9-carboxyoctanoyl)-*sn*-glyceryl-3-phosphocholine (PAzPC).

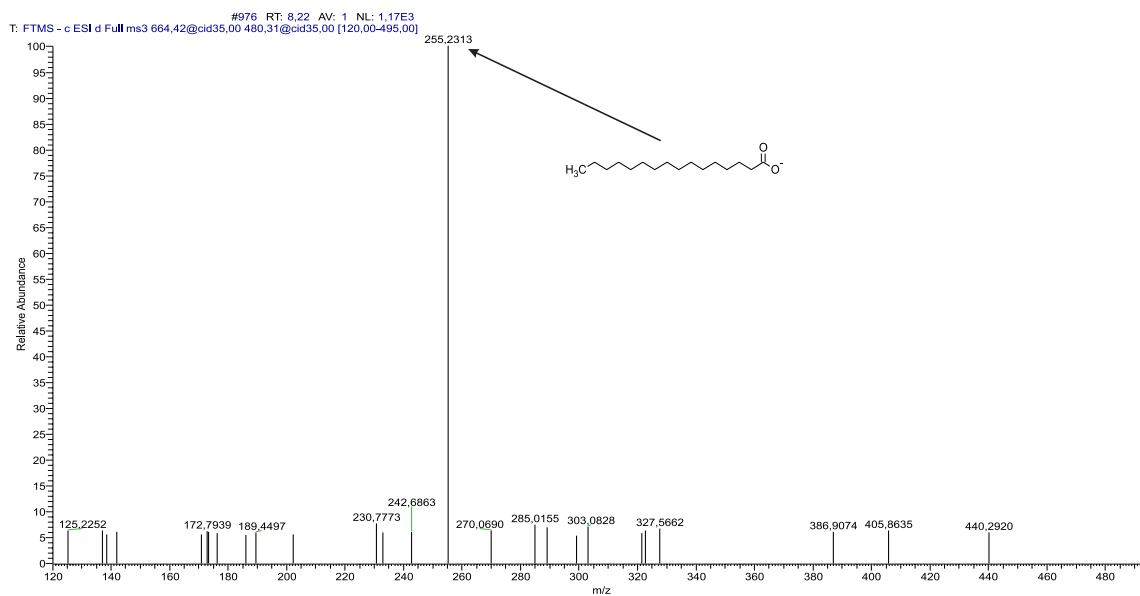


**Figure 10:** MS<sup>3</sup> fragmentation spectra of 1-O-hexadecanoyl-2-O-(9-carboxyoctanoyl)-*sn*-glyceryl-3-phosphocholine (PAzPC) and its fragment 480.3096 *m/z*.

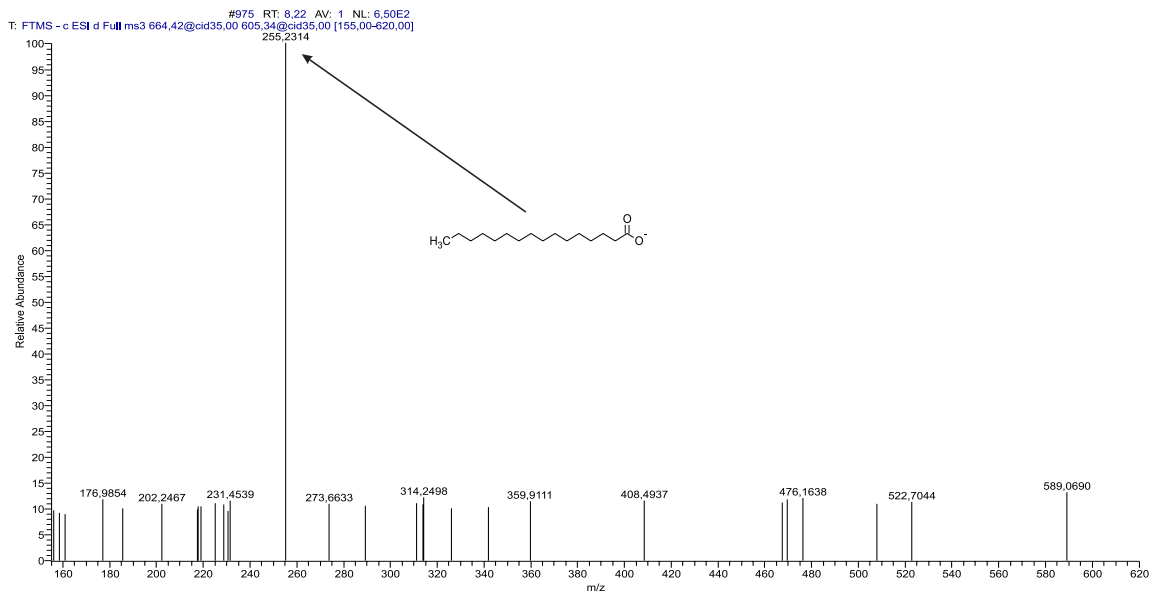


**Figure 11:** MS<sup>3</sup> fragmentation spectra of 1-O-hexadecanoyl-2-O-(9-carboxyoctanoyl)-*sn*-glyceryl-3-phosphocholine (PAzPC) and its fragment 605.3426 *m/z*. Palmitic acid moiety can be observed.

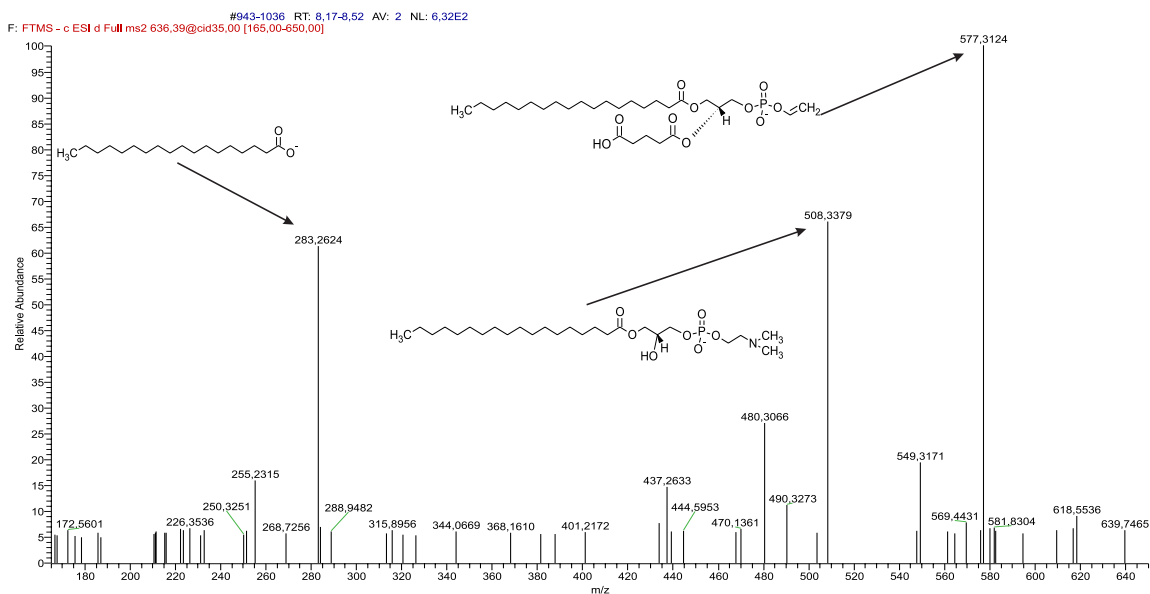


**Figure 12:** MS<sup>2</sup> fragmentation spectra of 1-O-octadecanoyl-2-O-(5-carboxybutanoyl)-*sn*-glyceryl-3-phosphocholine PC(18:0;5:0(COOH)).

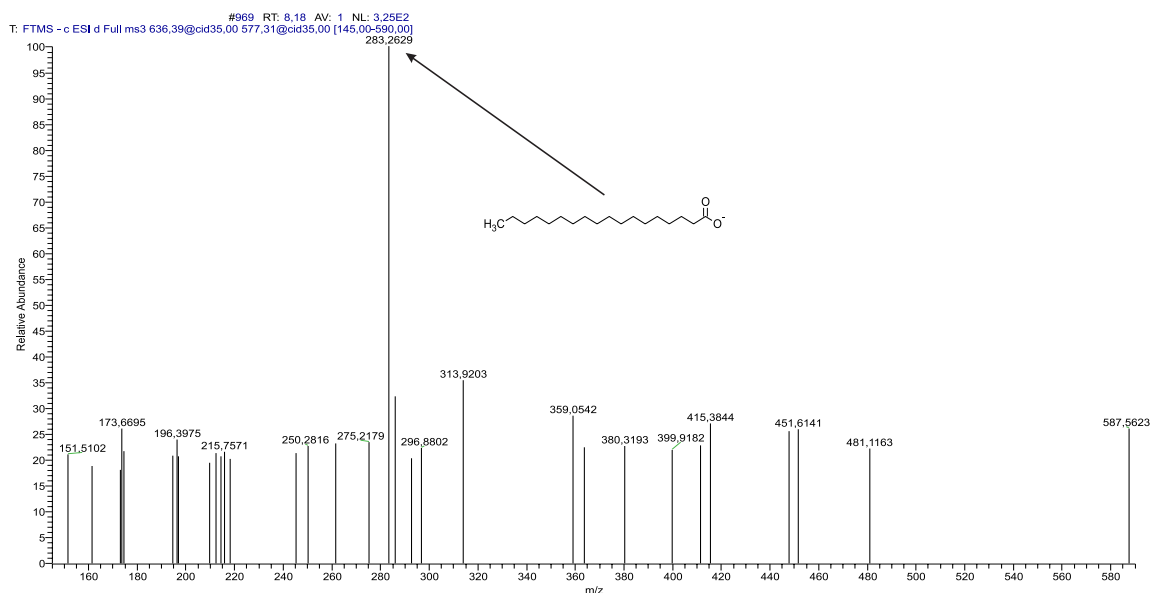


**Figure 13:** MS<sup>3</sup> fragmentation spectra of 1-O-octadecanoyl-2-O-(5-carboxybutanoyl)-*sn*-glyceryl-3-phosphocholine PC(18:0;5:0(COOH)) and its fragment 577.3124 *m/z*. Stearic acid moiety can be observed.

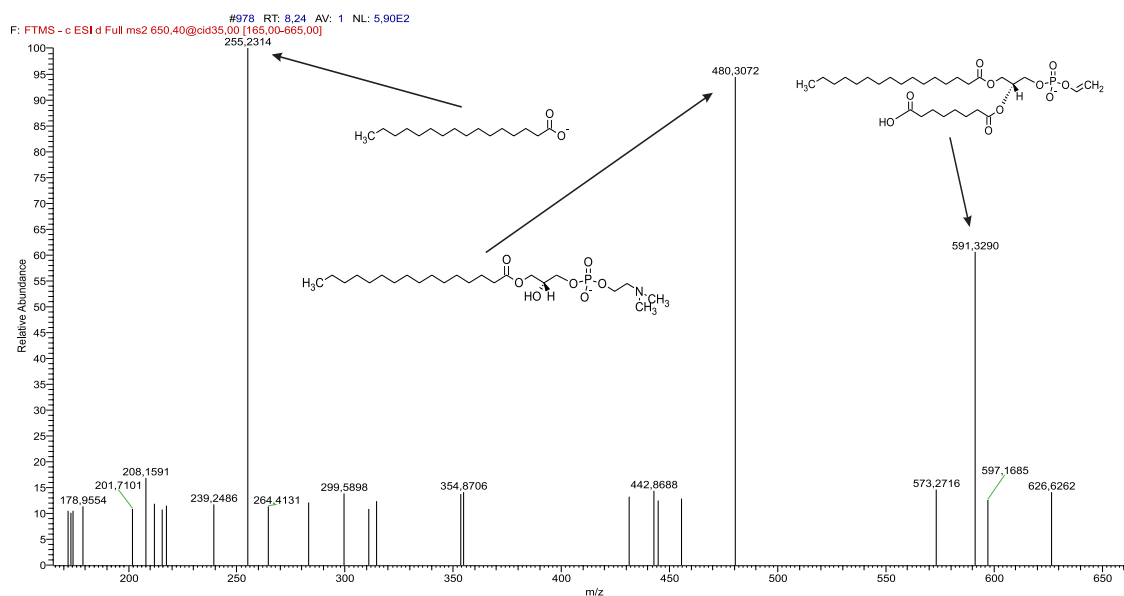


**Figure 14:** MS<sup>2</sup> fragmentation spectra of 1-O-hexadecanoyl-2-O-(8-carboxyheptanoyl)-*sn*-glyceryl-3-phosphocholine, PC(16:0;8:0(COOH)).

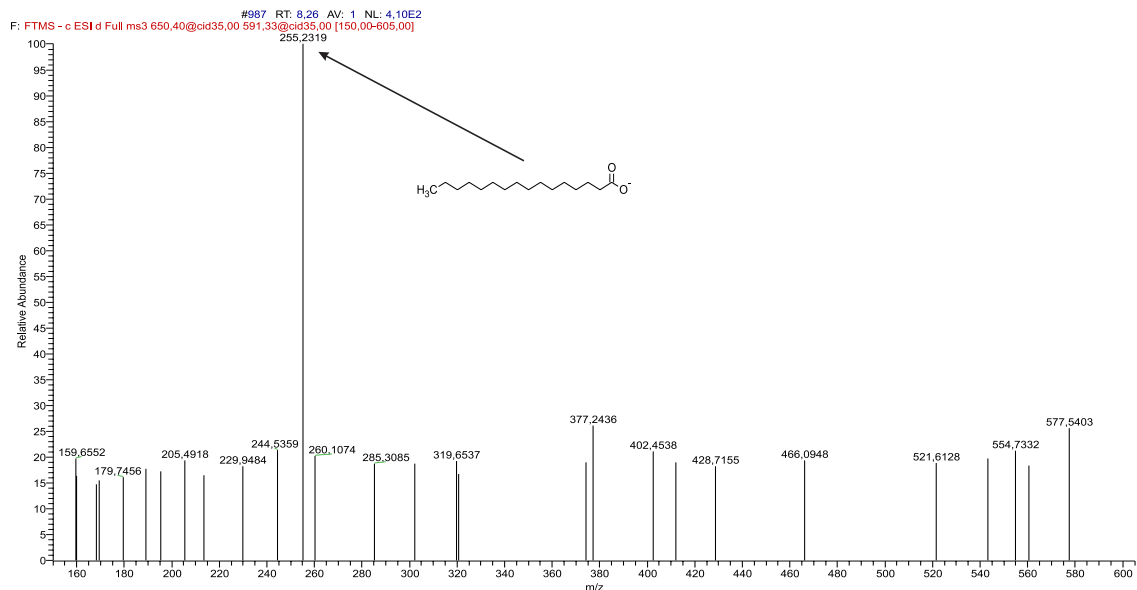


**Figure 15:** MS<sup>3</sup> fragmentation spectra of 1-O-hexadecanoyl-2-O-(8-carboxyheptanoyl)-*sn*-glycerol-3-phosphocholine, PC(16:0;8:0(COOH)) and its fragment 591.3290 *m/z*.

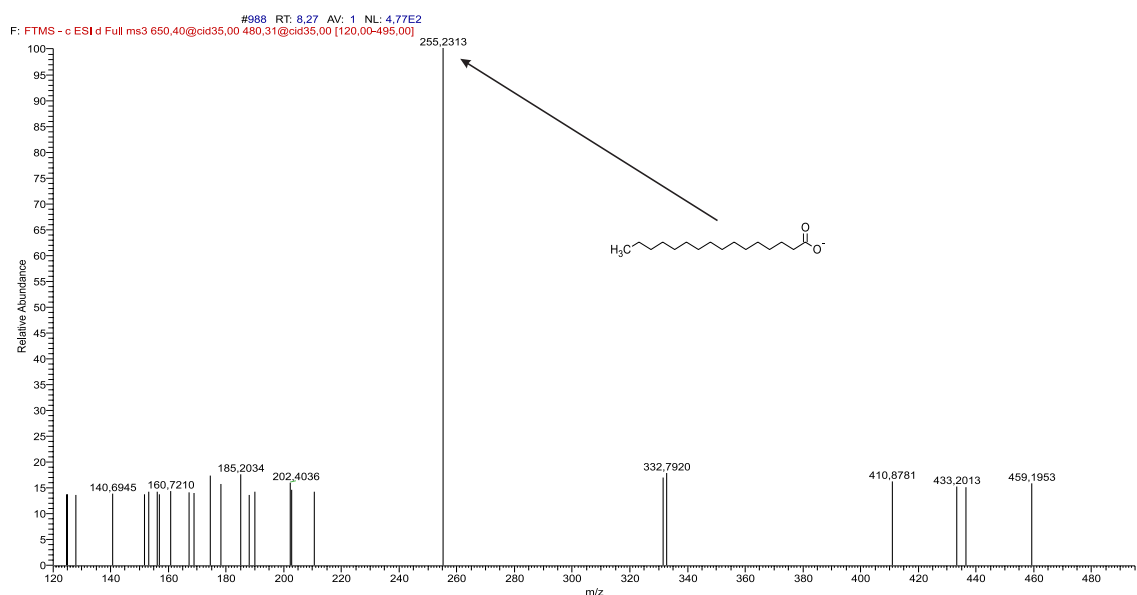


**Figure 16:** MS<sup>3</sup> fragmentation spectra of 1-O-hexadecanoyl-2-O-(8-carboxyheptanoyl)-*sn*-glycerol-3-phosphocholine, PC(16:0;8:0(COOH)) and its fragment 480.3072 *m/z*.

The oxidative stress is a damage potentially resulting from misbalance between oxidants and antioxidants in the way of oxidants. Truncated polyunsaturated fatty acids indicate the presence of oxidative stress in patients suffering from MCADD. Free radicals (superoxide  $O_2^-$ ; hydroxyl  $OH\cdot$ ; alkoxyl  $RO\cdot$  nad peroxy  $RO_2$ ) and also non-radical species (hydrogen peroxide  $H_2O_2$ ; peroxyxynitrite  $ONOO^-$ ) are products as common product of aerobic metabolism and also as a product of pathophysiological state.<sup>73,74</sup> Reactive

oxygen species (ROS) are interacting with polyunsaturated fatty acids and it is initiated by formation of carbon-centred radicals and/or hydroperoxides of polyunsaturated fatty acids (PUFAs) (peroxidation of PUFAs). It is one of the well understood process generation of oxidative stress.<sup>75</sup> The result of this interactions are lipids which contains carboxyl or carbonyl group in the end of the short carbon chain of their *sn2* position. Several oxidized lipids were found to be stable for analysis (PAzPC, PoxnoPC (1-O-hexadecanoyl-2-O-(9-oxononanoyl)-*sn*-glyceryl-3-phosphocholine)).<sup>76</sup> According the literature PAzPC is associated with oxidative stress.<sup>75,77</sup> As published previously ROS decrease mitochondrial membrane potential and increase in the ratio of Bax/Bcl2 leading to mitochondria mediated pathway involved in apoptosis.<sup>78</sup> Mitochondrial dysfunction may result in deterioration of the function of adipocytes in the way of upkeep of glucose homeostasis over fading insulin signalling, downregulation of Glut4 expression, and decrease in adiponectin secretion.<sup>79</sup> As previously published accumulation of C10:1 and C8 in mitochondria can result in increase of lipid peroxidation and decrease of non-enzymatic antioxidant defense.<sup>80,81</sup> Many bioactive lipids may contain oxidation products of PUFAs. By oxidation of 1- palmitoyl-2-arachidonoyl-*sn*-glycero-3-phosphorylcholine (PAPC) many oxidized species may be obtained including PGPC and PC(16:0;8:0(COOH)). Whereas origin of the PC(18:0,5:0(COOH)) can be considered as a result of the common oxidation mechanism on related lipids bearing unsaturated fatty acid at *sn-2* position.<sup>82</sup> This observation is supported by decreased levels of PAPC in patients (Figure 17). PAzPC is thus considered as a result linoleic acid moiety oxidation as reported previously.<sup>83</sup>

Relatively strong correlation between PAzPC and PC(16:0,8:0(COOH)) and PC(18:0,5:0(COOH)) were found 0.8929 and 0.8096, respectively (Figure 18-19). On the other hand, the observed correlation between C8 was low (less than 0.54) (Figure 20-22). These findings suggest common formation mechanism in patients. As mentioned above PAzPC is associated with oxidative stress and correlation findings support hypothesis that PC(16:0,8:0(COOH)) and PC(18:0,5:0(COOH)) may be associated with oxidation stress. Consequent study should be done in order of confirmation of this study.<sup>84</sup>

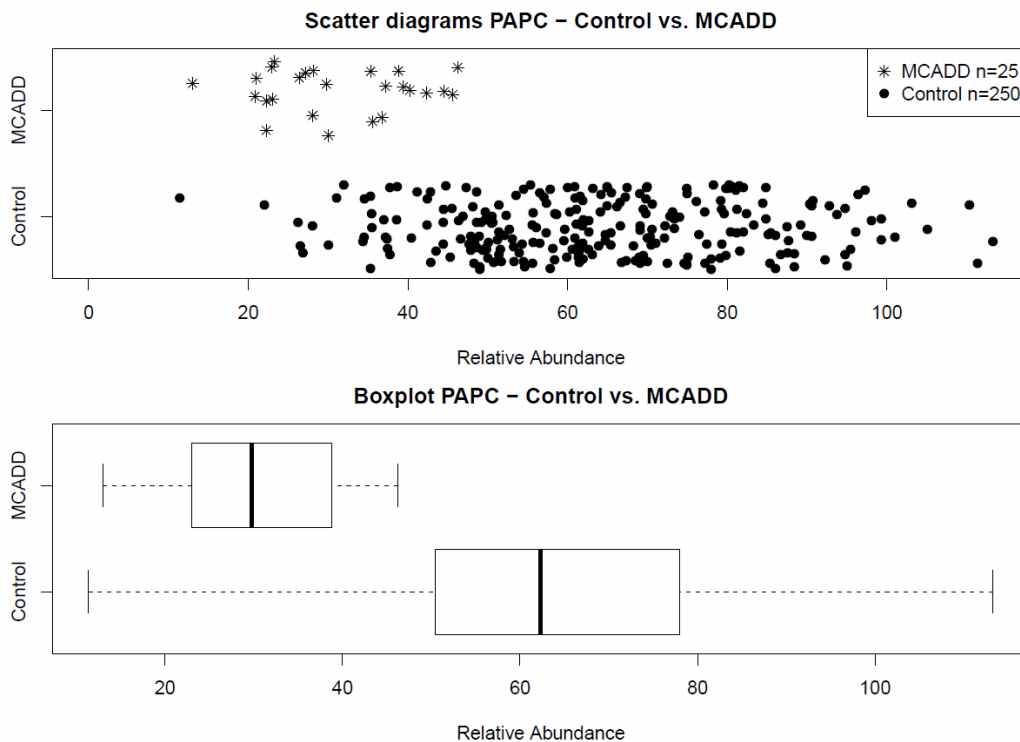


**Figure 17:** Boxplot and Scatter diagrams of 1- palmitoyl-2-arachidonoyl-sn-glycero-3-phosphorylcholine containing samples (n=25) and controls (n=250); data from FIA-TMS).

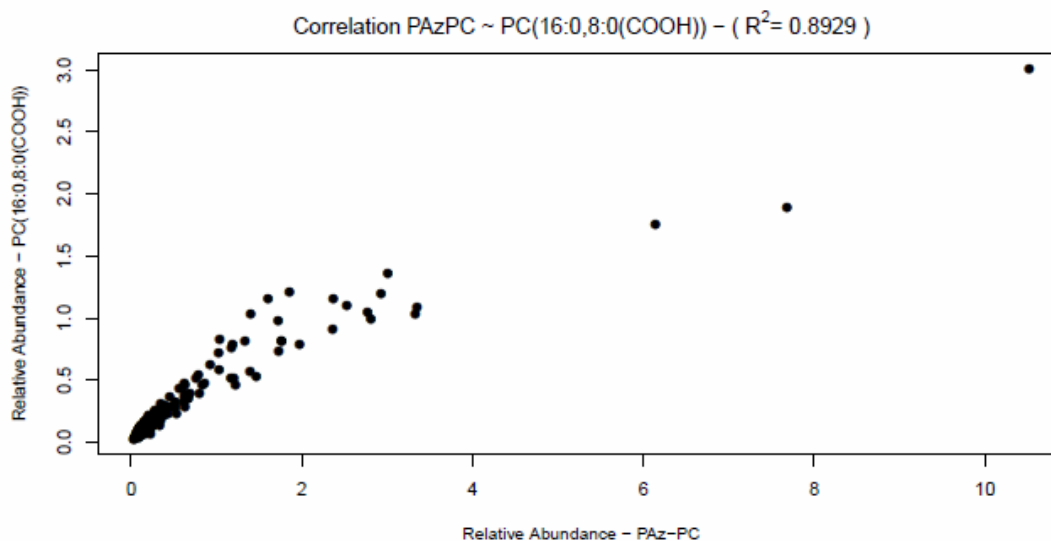


**Figure 18:** Correlation graph between PAzPC and PC(16:0,8:0(COOH)).

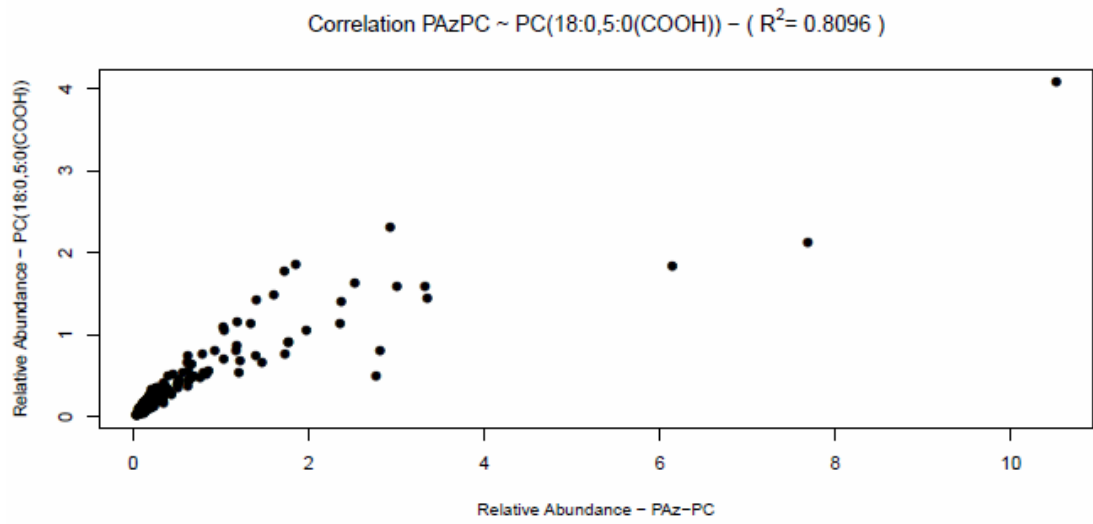


**Figure 19:** Correlation graph between PAzPC and PC(18:0,5:0(COOH)).

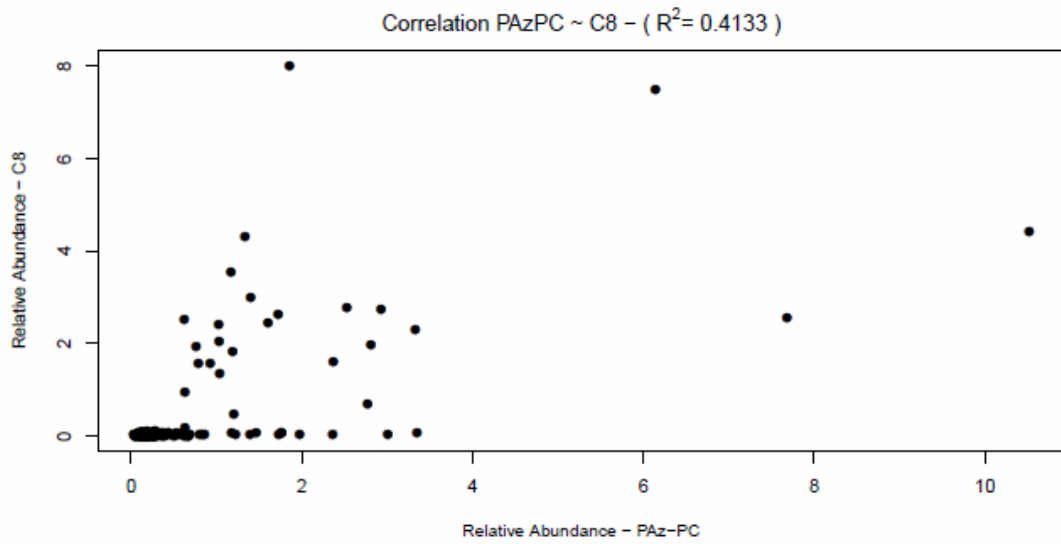


**Figure 20:** Correlation graph between PAzPC and octanoylcarnitine.

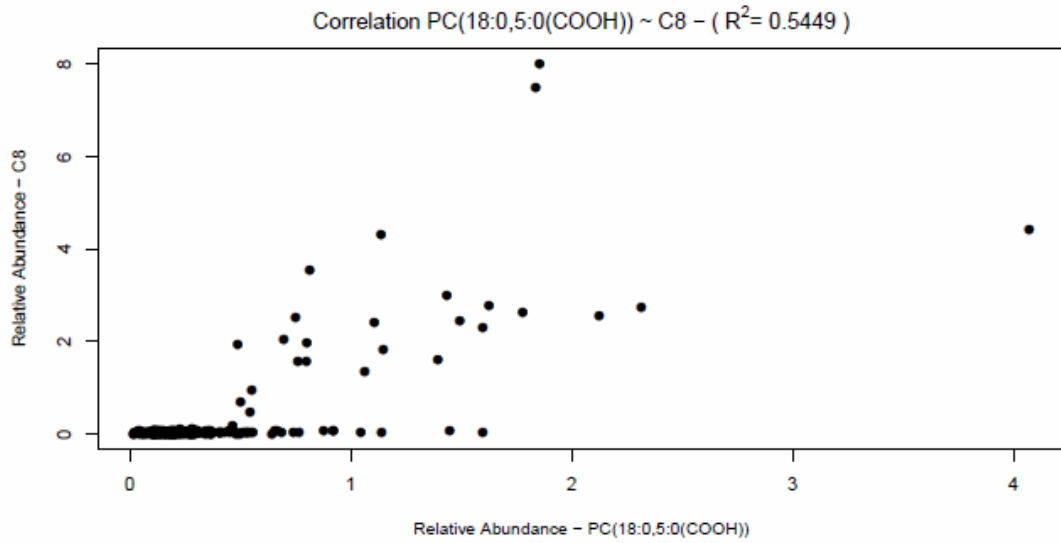


**Figure 21:** Correlation between PC(18:0,5:0(COOH)) and octanoylcarnitine.

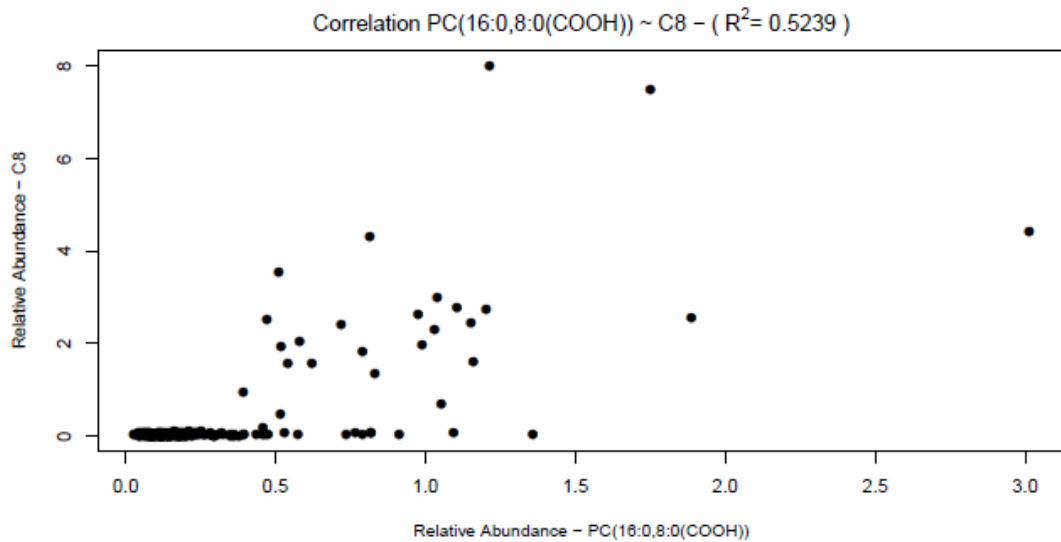


**Figure 22:** Correlation between PC(16:0,8:0(COOH)) and octanoylcarnitine.

In order to confirm our findings comparison experiment on the second cohort was performed. Control samples (n=250) and MCADD patients (n=25) were analysed by FIA-TMS operating in MRM mode with specific transitions of most differentiating phospholipids (Table 2). Calculated p-values for PAzPC was  $1.927 \times 10^{-14}$ , for PC(16:0,8:0(COOH))  $3.354 \times 10^{-15}$  and for PC(18:0,5:0(COOH)) was  $2.391 \times 10^{-15}$ .

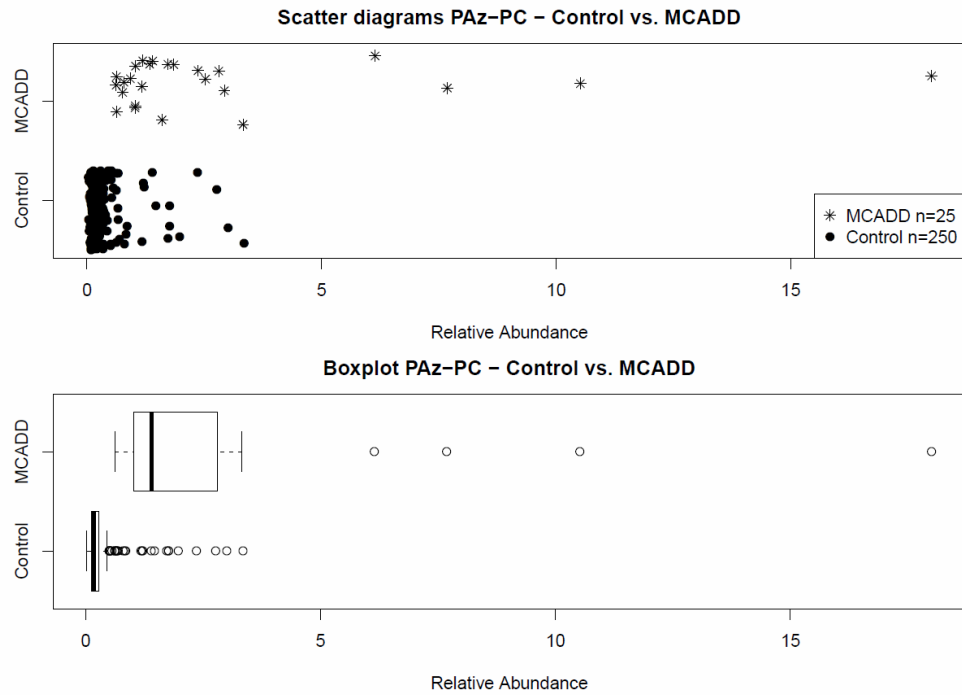


**Figure 23:** Boxplot and Scatter diagrams of PAzPC containing samples (n=25) and controls (n=250); data from FIA-TMS).

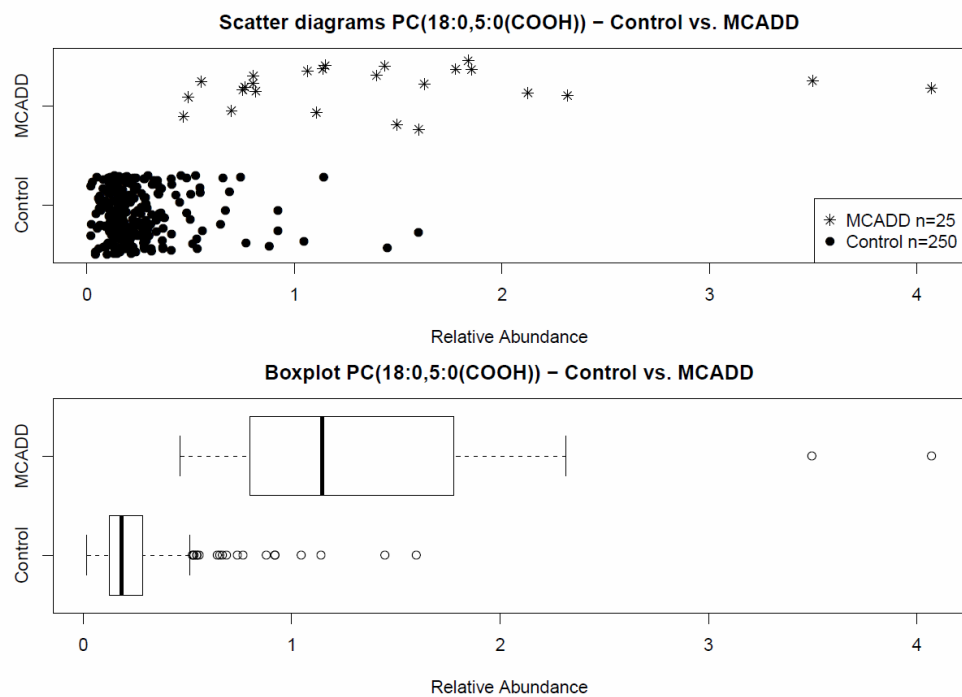


**Figure 24:** Boxplot and Scatter diagrams of PC(18:0,5:0(COOH)) containing samples (n=25) and controls (n=250); data from FIA-TMS).

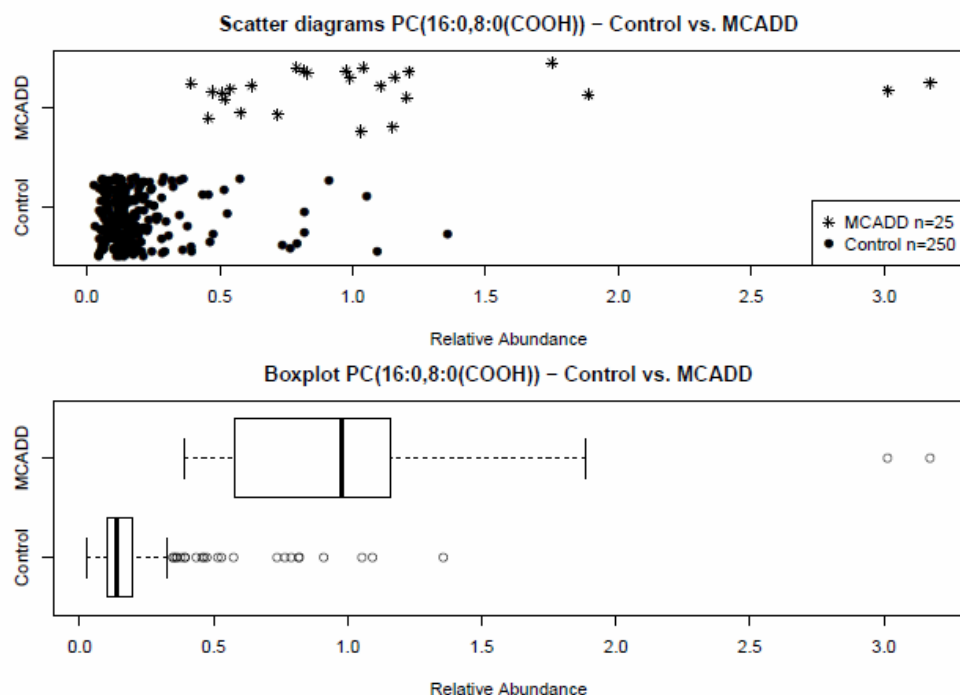


**Figure 25:** Boxplot and Scatter diagrams of PC(16:0,8:0(COOH)) containing samples (n=25) and controls (n=250); data from FIA-TMS).

Results from FIA-TMS validate findings from untargeted experiment and underline the significance of these three markers (Figure 23-25).<sup>84</sup>

#### 4.2. Spectral trees as a useful tool in identification of small molecule in metabolomics

In order to detect potentially new metabolites associated with ADA and metabolic degradation of the accumulated substrates the acquired LC-MS data were processed by different software. Based on the biochemical transformations by phase I and phase II metabolisation, 31 metabolites of adenosine and deoxyadenosine were suggested and detected in the raw data by Compound Discoverer 1.0.0.692 (Table 4). Most frequent metabolic transformations were methylation, oxidative deamination, dehydration and desaturation. By means of “spectral tree” approach several metabolites were confirmed and also false positive hits from Compound Discoverer

were removed. The combination of CID and HCD fragmentation techniques gives useful information necessary for elimination of MS and FT artefacts.

**Table 4:** Metabolites of adenosine and deoxyadenosine suggested and detected in the raw data by Compound Discoverer 1.0.0.692

Parent Compound	Suggested Formula	Molecular Weight	Transformations	Composition Change
Adenosine	C11 H15 N5 O4	281.1124	Methylation	"+(C H2)"
Adenosine	C10 H14 N4 O6	286.0913	Hydration, Oxidative Deamination to Alcohol	"-(N) +(H O2)"
Adenosine	C15 H21 N7 O6	395.1553	Glutamine Conjugation	"+(C5 H8 N2 O2)"
Adenosine	C11 H14 N4 O5	282.0964	Oxidative Deamination to Alcohol, Methylation	"-(N) +(C H O)"
Adenosine	C10 H13 N5 O3	251.1018	Dehydration, Reduction	"-(O)"
Adenosine	C12 H12 N4 O6	308.0757	Oxidative Deamination to Ketone, Acetylation	"-(H N) +(C2 O2)"
Adenosine	C11 H15 N5 O3	265.1175	Dehydration, Reduction, Methylation	"-(O) +(C H2)"
Adenosine	C10 H6 N4 O4	246.0384	Dehydration, Desaturation, Oxidative Deamination to Ketone	"-(H7 N)"
Adenosine	C15 H20 N6 O5	364.1495	Dehydration, Oxidative Deamination to Alcohol, Ornithine Conjugation	"+(C5 H7 N O)"
Adenosine	C12 H17 N5 O5	311.1230	Reduction, Acetylation	"+(C2 H4 O)"
Adenosine	C11 H15 N5 O5	297.1073	Oxidation, Methylation	"+(C H2 O)"
Adenosine	C14 H20 N6 O6	368.1444	Demethylation, Oxidative Deamination to Alcohol, Ornithine Conjugation	"+(C4 H7 N O2)"
Adenosine	C10 H13 N5 O4	267.0968		"none"
Adenosine	C10 H11 N5 O3	249.0862	Dehydration	"-(H2 O)"
Adenosine	C11 H16 N4 O6	300.1070	Hydration, Oxidative Deamination to Alcohol, Methylation	"-(N) +(C H3 O2)"

**Table 4:** Metabolites of adenosine and deoxyadenosine suggested and detected in the raw data by Compound Discoverer 1.0.0.692

Parent Compound	Suggested Formula	Molecular Weight	Transformations	Composition Change
Deoxyadenosine	C11 H15 N5 O4	281.1124	Oxidation, Methylation	"+(C H2 O)"
Deoxyadenosine	C10 H14 N4 O6	286.0913	Hydration, Oxidation, Oxidative Deamination to Alcohol	"-(N) +(H O3)"
Deoxyadenosine	C15 H21 N7 O6	395.1553	Oxidation, Glutamine Conjugation	"+(C5 H8 N2 O3)"
Deoxyadenosine	C11 H14 N4 O5	282.0964	Hydration, Oxidative Deamination to Ketone, Methylation	"-(N) +(C H O2)"
Deoxyadenosine	C10 H13 N5 O3	251.1018		"none"
Deoxyadenosine	C12 H12 N4 O6	308.0757	Oxidation, Oxidative Deamination to Ketone, Acetylation	"-(H N) +(C2 O3)"
Deoxyadenosine	C11 H15 N5 O3	265.1175	Methylation	"+(C H2)"
Deoxyadenosine	C10 H6 N4 O4	246.0389	Desaturation, Desaturation, Oxidative Deamination to Ketone	"-(H7 N) +(O)"
Deoxyadenosine	C15 H20 N6 O5	364.1495	Oxidative Deamination to Ketone, Ornithine Conjugation	"+(C5 H7 N O2)"
Deoxyadenosine	C12 H17 N5 O5	311.1230	Hydration, Acetylation	"+(C2 H4 O2)"
Deoxyadenosine	C11 H15 N5 O5	297.1073	Oxidation, Oxidation, Methylation	"+(C H2 O2)"
Deoxyadenosine	C11 H18 N6 O5 S	346.1059	Demethylation, Reduction, Taurine Conjugation	"+(C H5 N O2 S)"
Deoxyadenosine	C10 H13 N5 O4	267.0968	Oxidation	"+(O)"
Deoxyadenosine	C10 H11 N5 O3	249.0862	Desaturation	"-(H2)"
Deoxyadenosine	C12 H17 N5 O4	295.1281	Reduction, Acetylation	"+(C2 H4 O)"
Deoxyadenosine	C9 H11 N5 O2	221.0913	Dehydration, Demethylation, Reduction	"-(C H2 O)"

Main metabolites accumulated in adenosine deaminase deficiency – adenosine (Figure 26) and deoxyadenosine (Figure 27), were detected and identified. Figure 28 shows the structure of the adenosine acquired spectral tree as can be visualized in Mass Frontier 7.0.5.9. SR3. In case of adenosine the spectral tree is relatively simple. Small molecules usually not fragment further than MS<sup>3</sup> level since consequential fragments are very small (less than 50 *m/z*) and thus are beyond the point of detection in some mass spectrometers. On contrary some spectral trees can be pretty extensive, which can be seen on case of Acetyl-CoA (<https://www.mzcloud.org/DataViewer#Reference4596>; downloaded 6.9.2016) where fragmentation goes to level MS<sup>6</sup> with many precursors for CID and HCD fragmentation spectra.

Characteristic substructures of adenosine can be clearly seen in Figure 29 and Figure 30. Figure 31 shows complementary structural information acquired from HCD fragmentation where also fragments of ribose moiety can be seen. By comparison of acquired data with available databases and commercial standard, the MSI Level 1 identification can be assign.

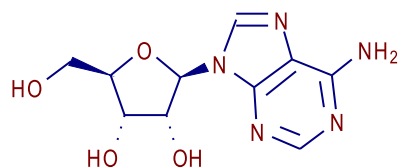


**Figure 26:** Structure of the adenosine (MSI Level 1)

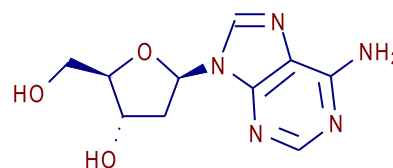


**Figure 27:** Structure of the 2'-deoxyadenosine (MSI Level 1)

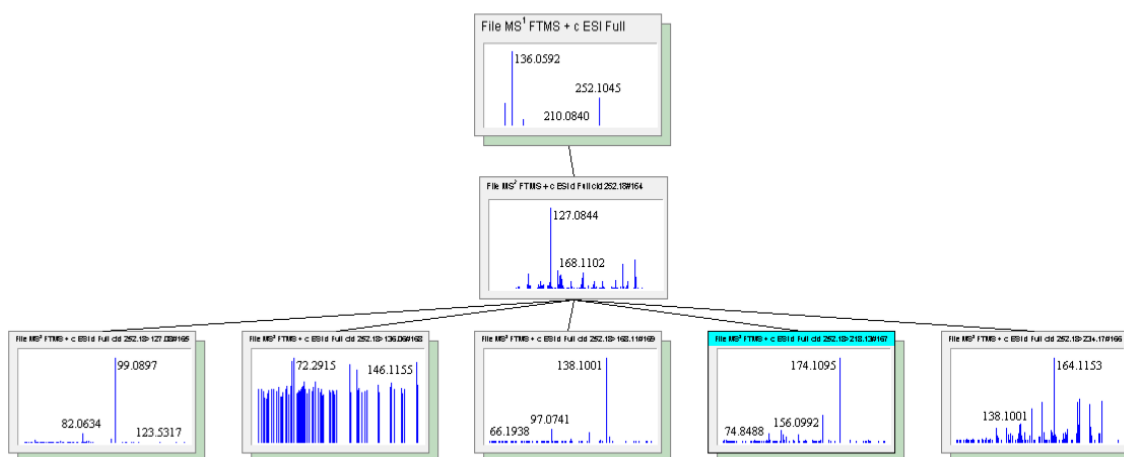


**Figure 28:** Spectral tree structure of the adenosine (Visualized in Mass Frontier 7.0.5.9. SR3)

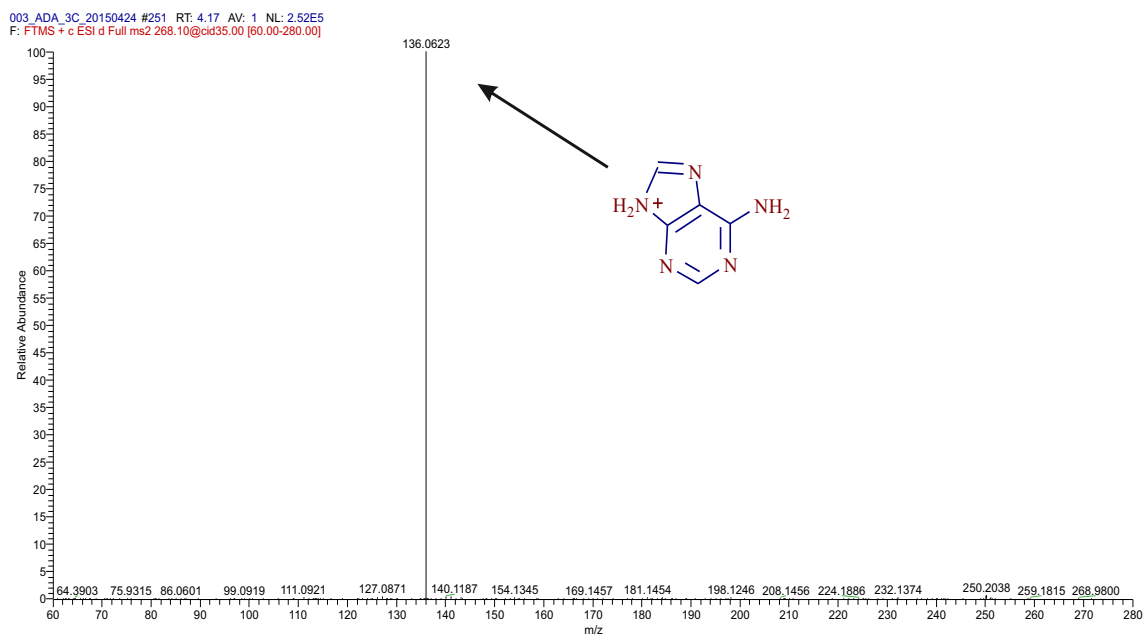


**Figure 29:** MS<sup>2</sup> fragmentation spectrum of adenosine (exp. 268.1052 *m/z*; CID; NCE 35).

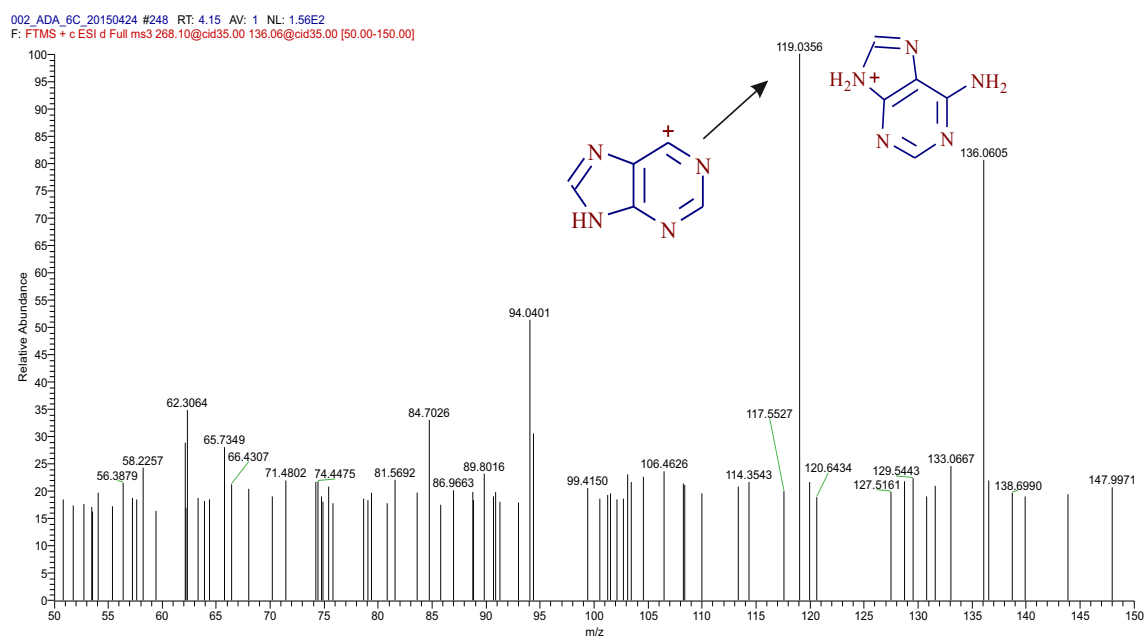


**Figure 30:** MS<sup>3</sup> fragmentation spectrum of adenosine. Selected precursor ion: adenine (exp. 136.0623 *m/z*; CID; 35 NCE).

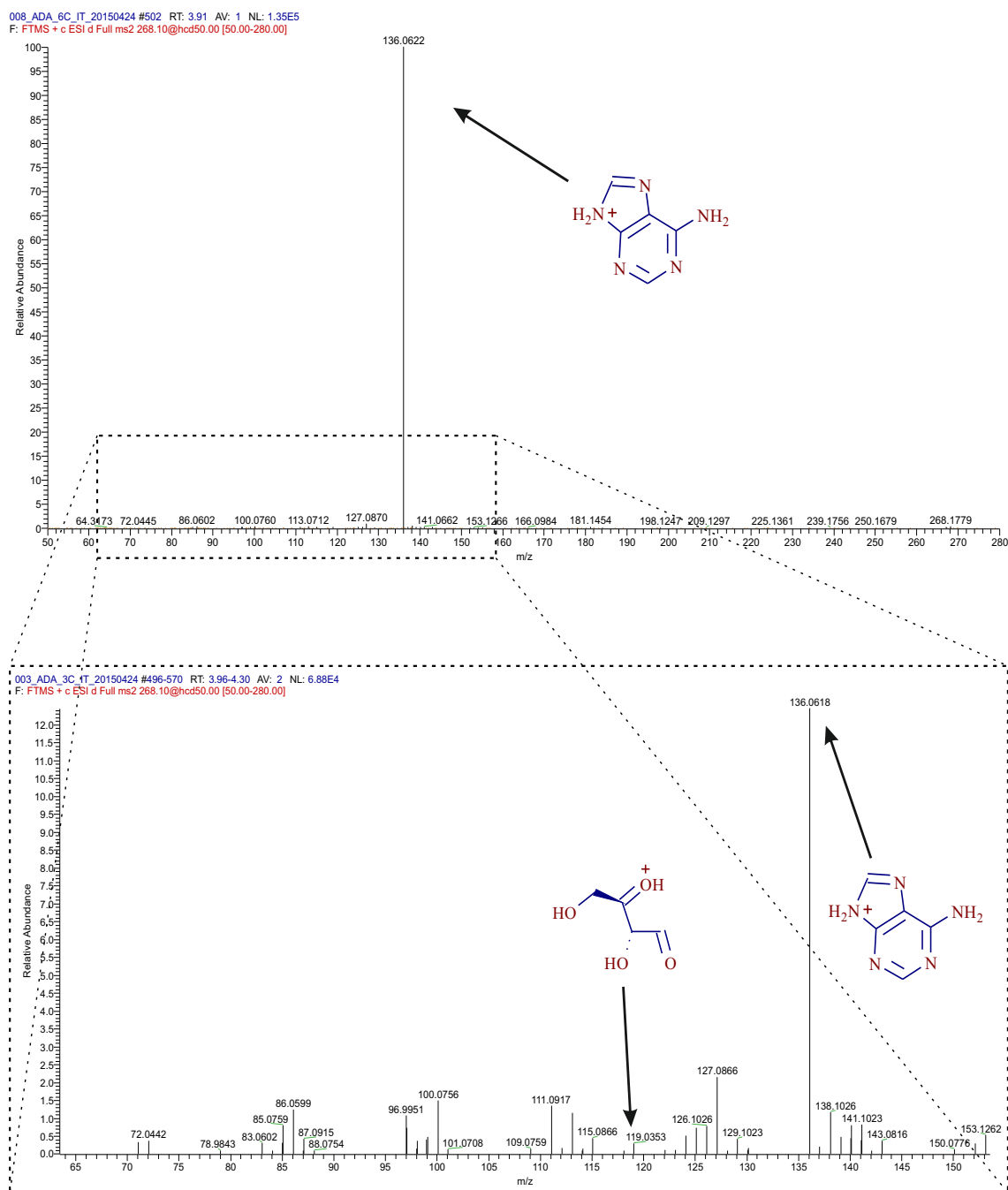


**Figure 31:** MS<sup>2</sup> fragmentation spectrum of adenosine (exp. 268.1052 *m/z*; HCD; NCE 50).

Spectral trees of 2'-deoxyadenosine in (Figure x28) and adenosine (Figure x32) looks similar due to almost identical structure. Fragmentation spectra are also similar (Figure x33, x34). Difference can be seen in HCD spectrum in Figure x35, where compare to the adenosine (Figure x31) 2'-deoxyadenosine contains more fragments from ribose moiety. By comparison of acquired data with available databases and commercial standard, the MSI Level 1 identification can be assign.

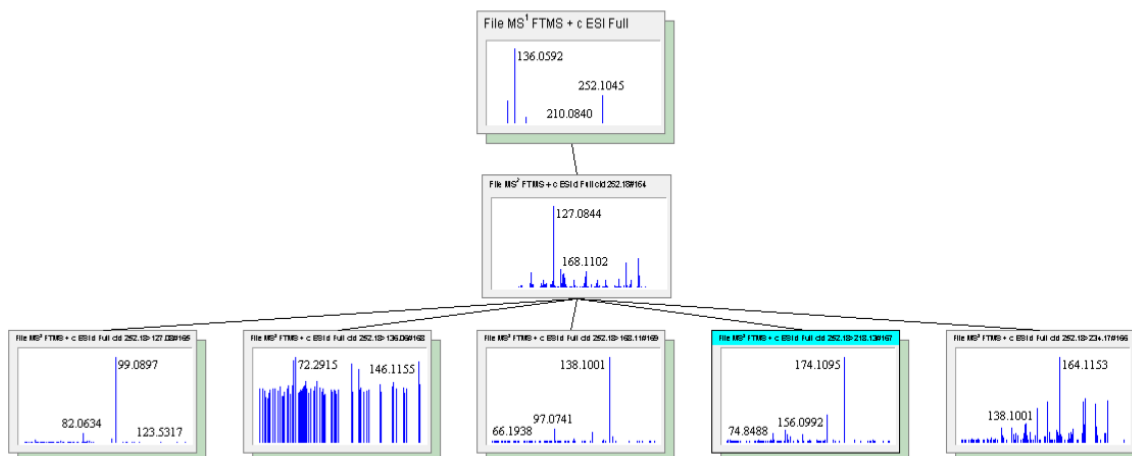


**Figure 32:** Spectral tree structure of the 2'-deoxyadenosine (Visualized in Mass Frontier 7.0.5.9. SR3).

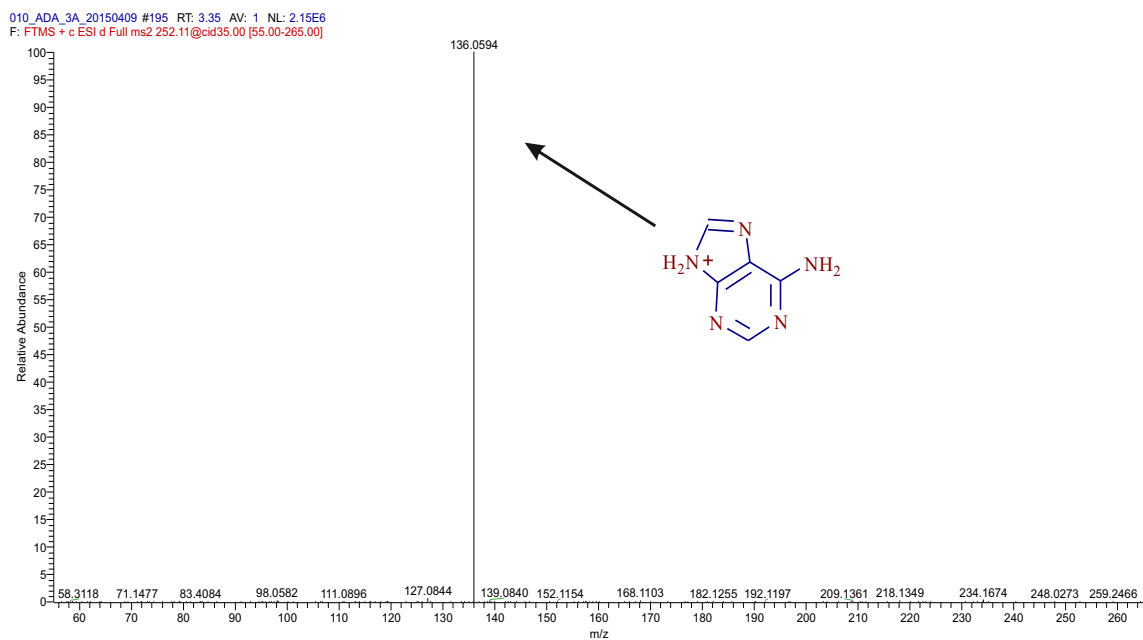


**Figure 33:** MS<sup>2</sup> fragmentation spectrum of 2'-deoxyadenosine (exp. 252.1096 m/z; CID; NCE 35).

014\_ADA\_12A\_20150409 #177 RT: 3.11 AV: 1 NL: 1.77E2  
F: FTMS + c ESI d Full ms3 252.11@cid35.00 136.06@cid35.00 [50.00-150.00]

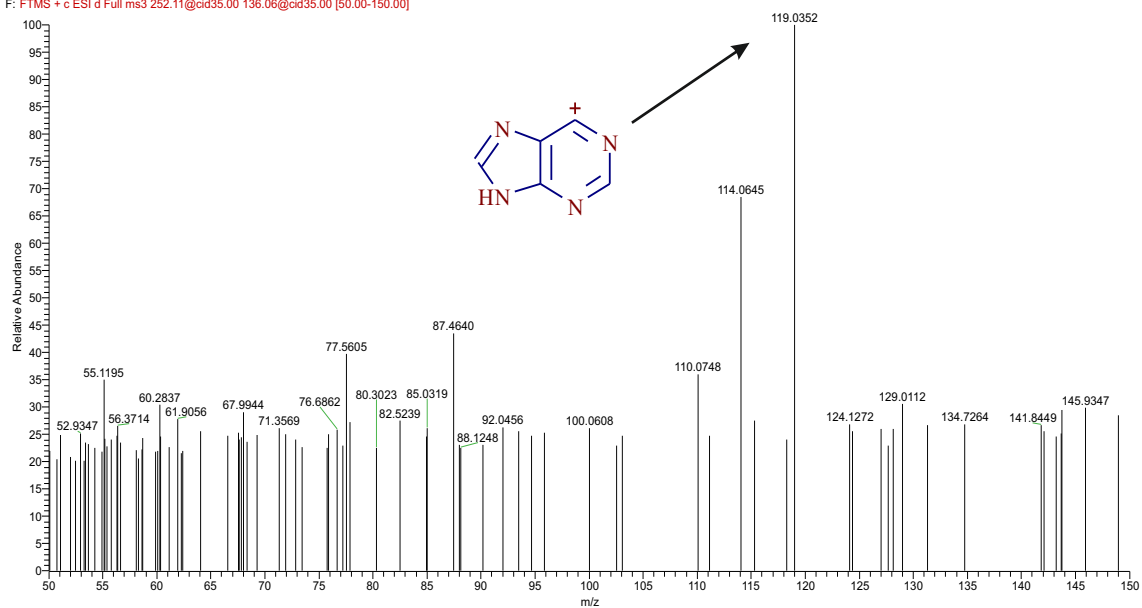


**Figure 34:** MS<sup>3</sup> fragmentation spectrum of 2'-deoxyadenosine. Selected precursor ion: adenine (exp. 136.0594 *m/z*; CID; 35 NCE).

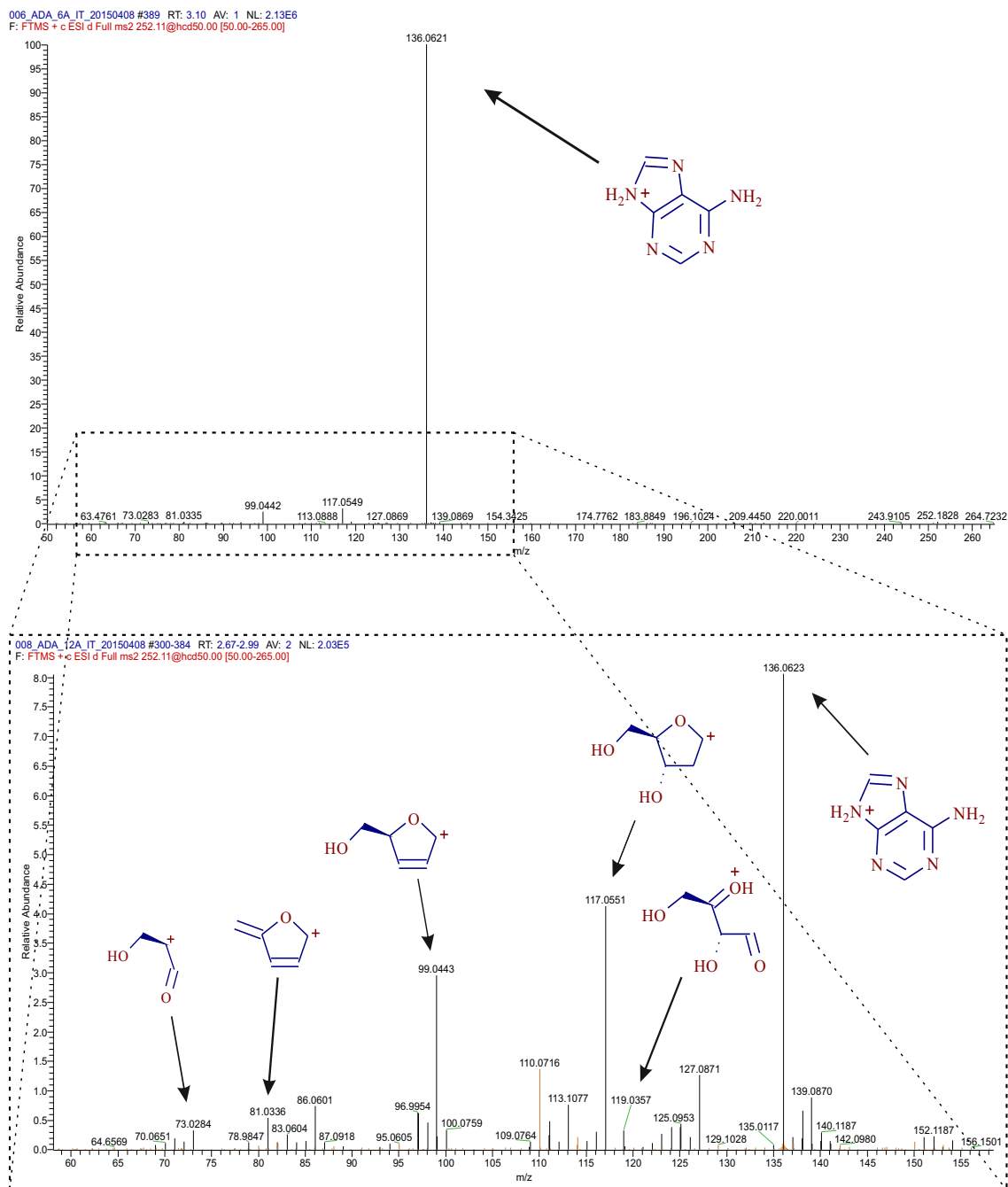


**Figure 35:** MS<sup>2</sup> fragmentation spectrum of adenosine (exp. 252.1096 *m/z*; HCD; NCE 50).

Slightly more complicated situation appears in case of 1-methyl adenosine, although the structure fragmentation is almost the same (Figure 36) as for adenosine and 2'-deoxyadenosine (Figure 28 and Figure 32, respectively). Fragmentation spectrum from CID at MS<sup>2</sup> level shows addition of methyl group on the adenine moiety (Figure 37), however from this spectrum we are not able to determine its exact position. By means of spectral tree, the data acquired at MS<sup>3</sup> shows methyl moiety at position one

on adenine (Figure 38). Complementary data acquired by HCD fragmentation are seen at Figure 39. By comparison of acquired data with available databases and commercial standard, the MSI Level 1 identification can be assigned.

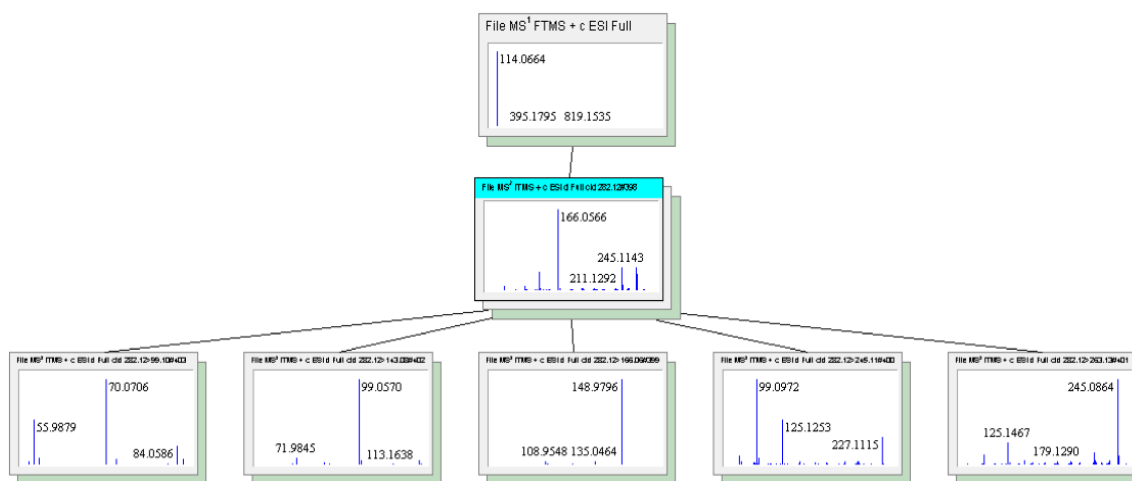


**Figure 36:** Spectral tree structure of the 1-methyladenosine (Visualized in Mass Frontier 7.0.5.9. SR3).

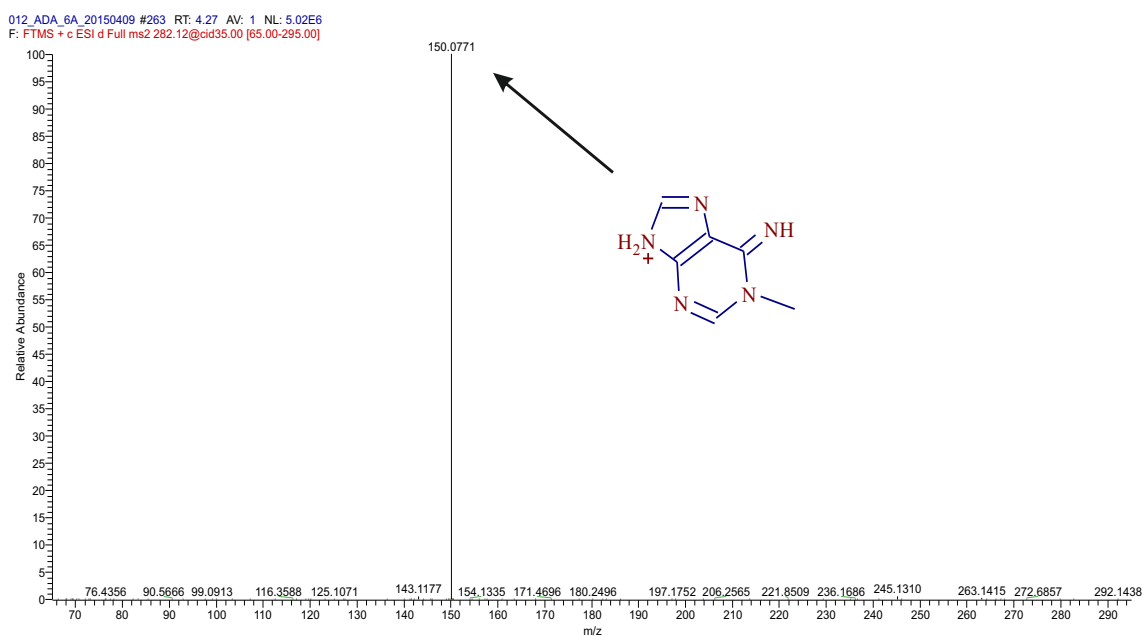


**Figure 37:** MS<sup>2</sup> fragmentation spectrum of 1-methyladenosine (exp. 282.1188 *m/z*; CID; NCE 35).

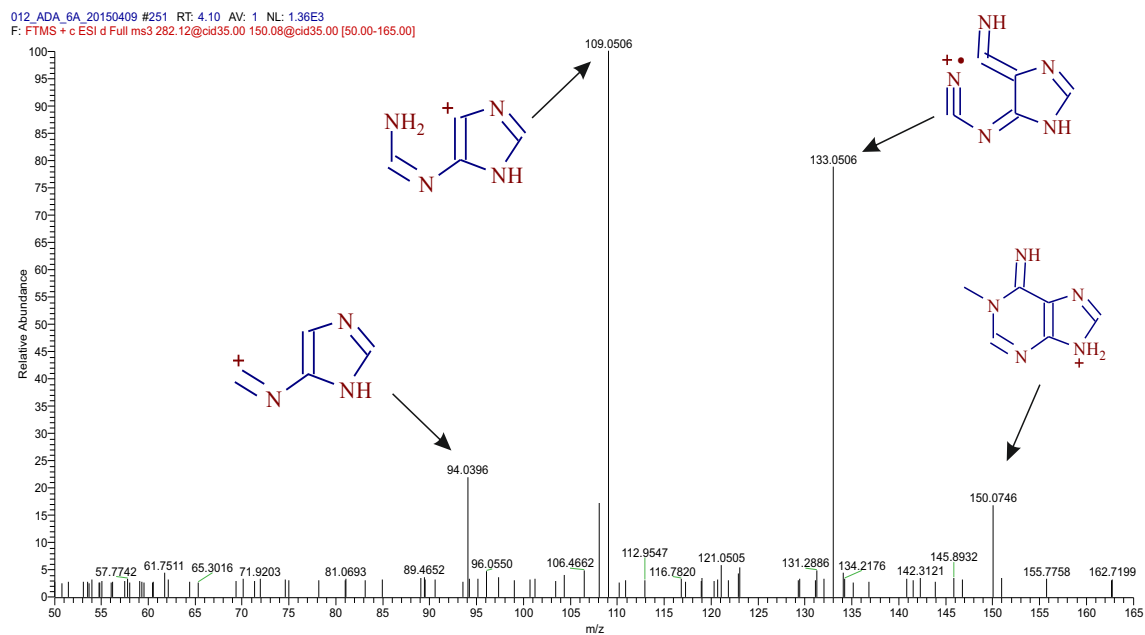


**Figure 38:** MS<sup>3</sup> fragmentation spectrum of 1-methyladenosine. Selected precursor ion: 1-methyladenine (exp. 150.0771 *m/z*; CID; 35 NCE).

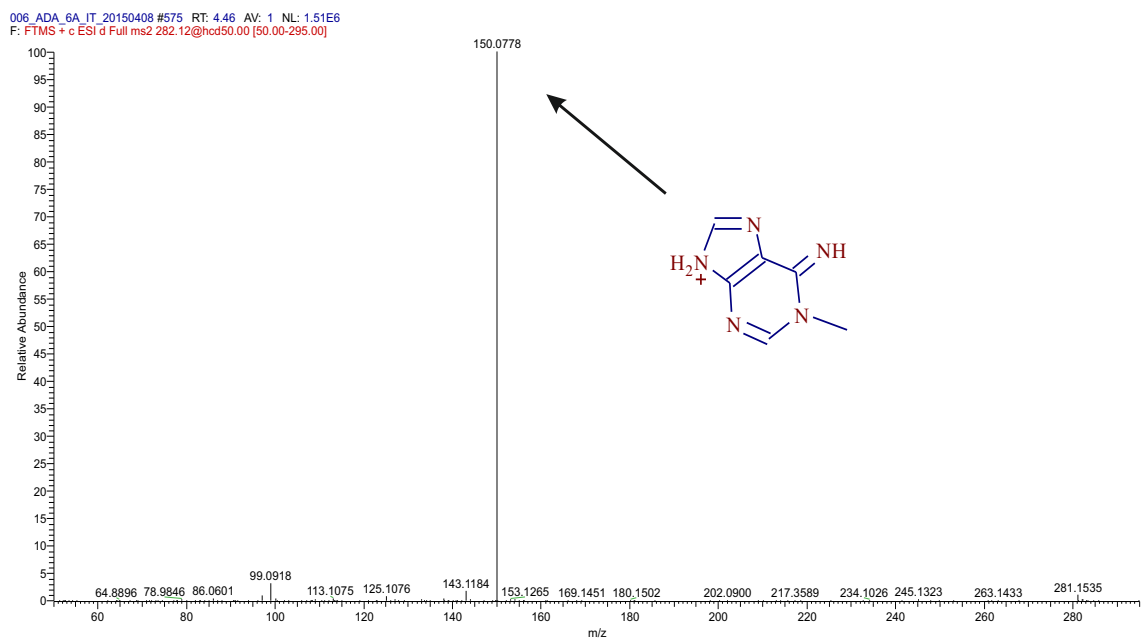


**Figure 39:** MS<sup>2</sup> fragmentation spectrum of 1-methyladenosine (exp. 282.1188 *m/z*; HCD; NCE 50).

Another interesting molecule which was identified in this experiment was 1-methyl-5-oxoadenosine. Strong structure similarity between previously described compounds results in the same scheme of the spectral tree. Fragmentation at MS<sup>2</sup> level

reveals two modifications of adenine – addition of oxygen and methyl group (Figure 40). Based on structural similarity with 1-methyladenine the exact position of methyl group was determined. The exact position of oxygen was resolved by mass spectra at MS<sup>3</sup> level fragmentation (Figure 41) and by complementary information from HCD fragmentation spectra (Figure 42). By comparison of acquired data with available databases and structurally similar compounds, the MSI Level 2 identification was assigned.

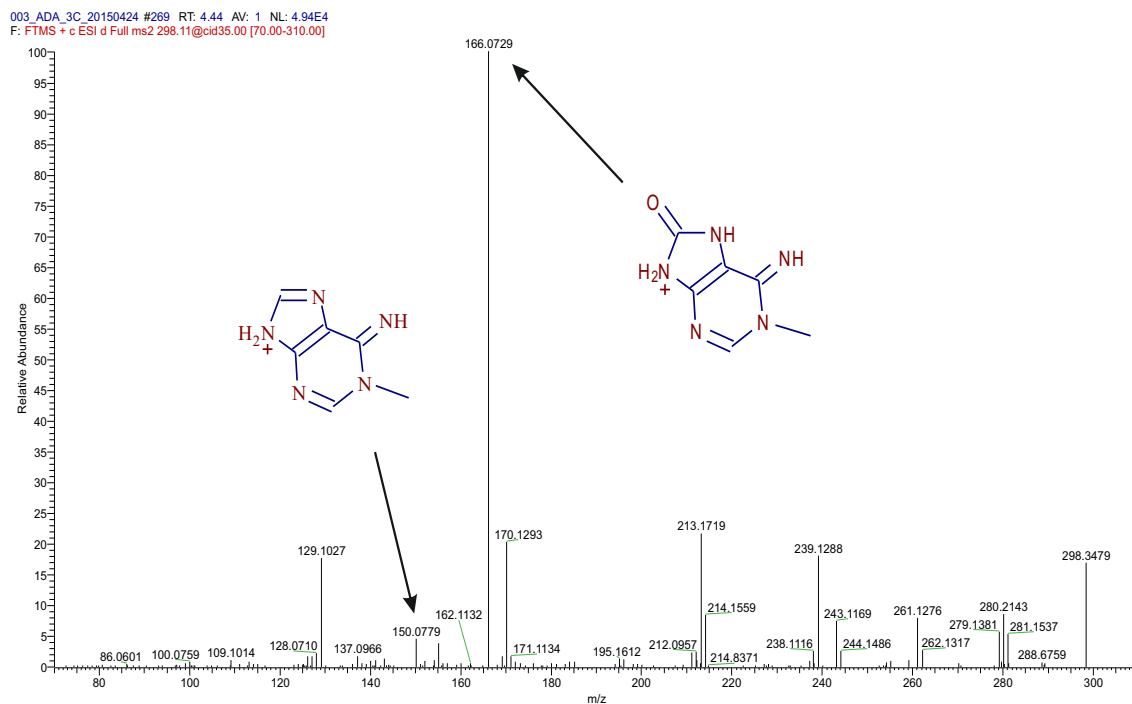


**Figure 40:** MS<sup>2</sup> fragmentation spectrum of 1-methyl-5-oxoadenosine (exp. 298.1151 *m/z*; CID; NCE 35).

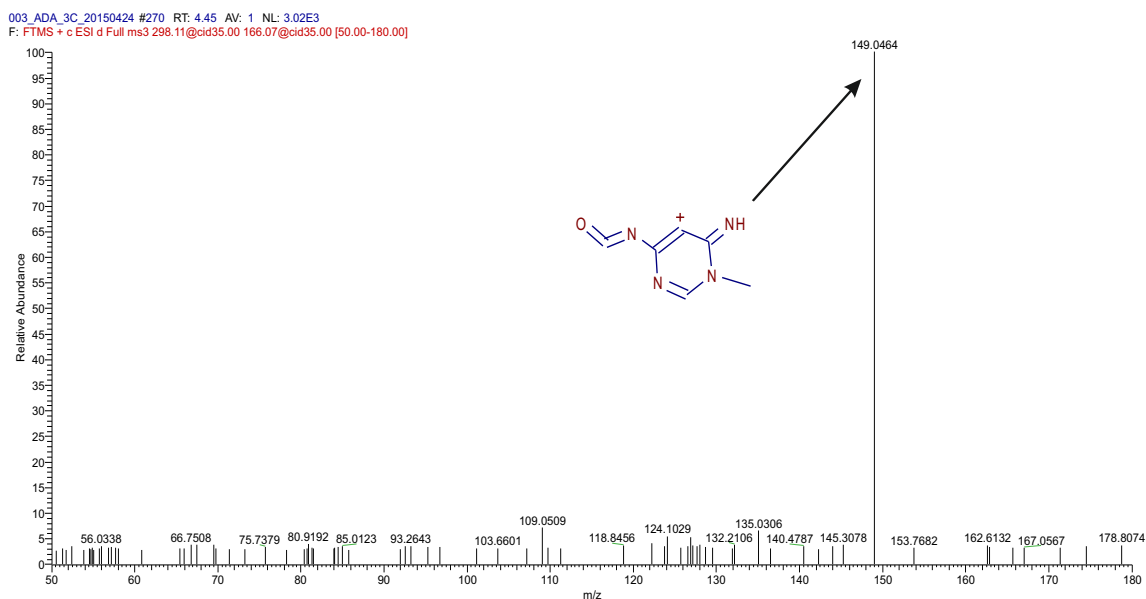


**Figure 41:** MS<sup>3</sup> fragmentation spectrum of 1-methyl-5-oxoadenosine. Selected precursor ion: 1-methyl-5-oxadenine (exp. 166.0729 *m/z*; CID; 35 NCE).

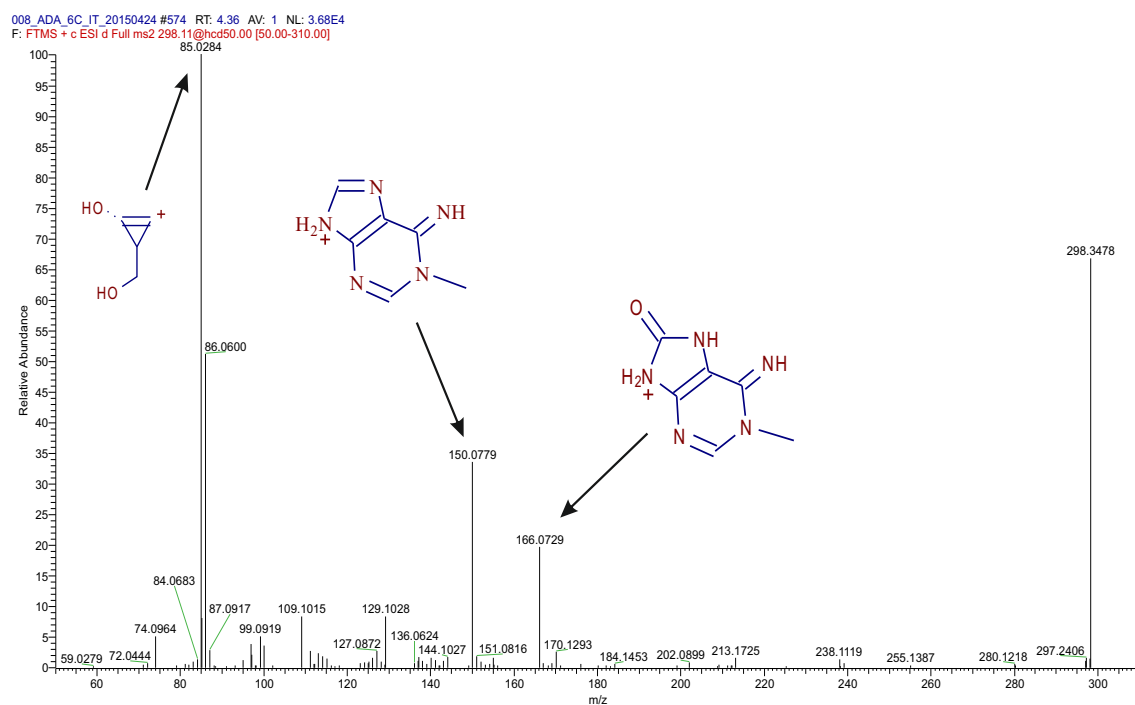


**Figure 42:** MS<sup>2</sup> fragmentation spectrum of 1-methyl-5-oxadenosine (exp. 298.1151 *m/z*; HCD; NCE 50).

As mentioned previously, 2'-deoxyadenosine is a general product of DNA degradation and it is behaving as a cytotoxic metabolite in place of intensive cell proliferation such as bone marrow or thymus.<sup>24,85</sup> The most severe alteration of ADA is accumulation of 2'-adenosinetriphosphate (inhibitor of ribonucleotide reductase) in the

erythrocytes and leukocytes.<sup>86,87</sup> These effects result in a high concentration of 2'-deoxyadenosine in peripheral body fluids. Several metabolites were reported to be found in the urine metabolome of ADA patients detectable mainly by GC/MS: 2'-deoxyadenosine, adenosine, 1-methyladenosine, N6-methyladenosine, 2'-O-methyladenosine and N6,2'-dimethyladenosine.<sup>87</sup> The summary of elucidated modified adenosine-like metabolites found in this study can be found in the Table 5. The origin of 1-methyladenosine (Figure 43) can be estimated as a degradation product of tRNA, rRNA, mRNA or snRNA from apoptotic lymphocytes.<sup>87,88</sup> 1-methyl-5-oxoadenosine (Figure 44) may be considered as an oxidative product of 1-methyladenosine, although 2'-O-methyladenosine can be found also as a degradation product of tRNA, rRNA, mRNA or snRNA.<sup>88</sup> The rest of compounds in Table 5 are result of malfunction of adenosine deaminase.

**Table 5:** Summary of adenosine-like metabolites in urine of patients suffering from adenosine deaminase deficiency.

<i>m/z</i> teor.	<i>m/z</i> exp.	error ppm	Name	MSI level of identification
252.1091	252.1096	2.78	2'-deoxyadenosine	1
268.104	268.1052	4.48	adenosine	1
282.1197	282.1188	-3.20	1-methyladenosine	1
298.1146	298.1151	1.68	1-methyl-5-oxoadenosine	3

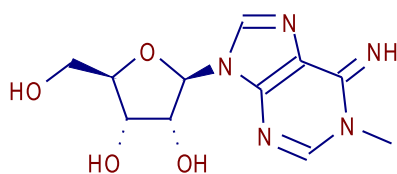


**Figure 43:** Structure of the 1-methyladenosine (MSI Level 1)

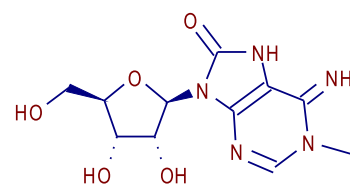


**Figure 44:** Structure of the 1-methyl-5-oxoadenosine (MSI Level 3)

### 4.3. Influence of a mass spectrometry resolution on metabolite detection in LC-MS untargeted metabolomics

This part of the thesis is focused on investigation of relationship between mass spectrometry resolution, scanning speed and feature detection capability in the field of metabolomics, both theoretical and experimental methods were used.

The effect of the separation cannot be included in the calculation due to the potentially unpredictable behaviour of the compounds during the separation (for example, lipids with very similar exact mass, but different formulas and chromatographic behaviour) and large variability chromatography methods. That means, the following calculations are only valid for flow injection analysis and metabolomics "worst case scenario" experiments in separation methods.

#### 4.3.1. *In silico* calculations

*In silico* calculations were performed in order to examine the distribution of overlapping  $m/z$  represent (622 110) metabolites, isotopes and adducts in the range of 50 to 2000  $m/z$ . The first step was to filter the combined list to identify unique metabolite  $m/z$  values. These unique  $m/z$  values are plotted on the X axis in Figure 45, while the Y axis shows the number of  $m/z$  values which lies in the interval  $[m/z - x; m/z + x]$ , as described in *Materials and Methods - Chapter 2.3.3*. The coordinates of each dot shown in Figure 45 represents a unique  $m/z$  value (X axis) and the number of functions that are apparently identical at a given resolution, and are not distinguishable within the curve of the mass spectrometry peak following a Gaussian profile (Y-axis). The scale variance (sigma squared) of the mass spectral peak was inversely proportional to the resolution. This means that the number of indistinguishable elements decreases with increasing resolution. The two main areas with the highest number of  $m/z$  overlap can be seen in Figure 45. The first important area is between 400  $m/z$  600 and  $m/z$ , corresponding to the short peptides (di-, tri-, tetra-) and partially secosteroids, lipids with a lower  $m/z$  (e.g. glycerophosphocholines, glycerophosphoethanolamines). A second area was 750  $m/z$  and 1050  $m/z$ , corresponding mainly to the lipid class. Three colour lines in Figure 45 representing percentiles (0.99; 0.75; 0.50) of the dot density distribution.

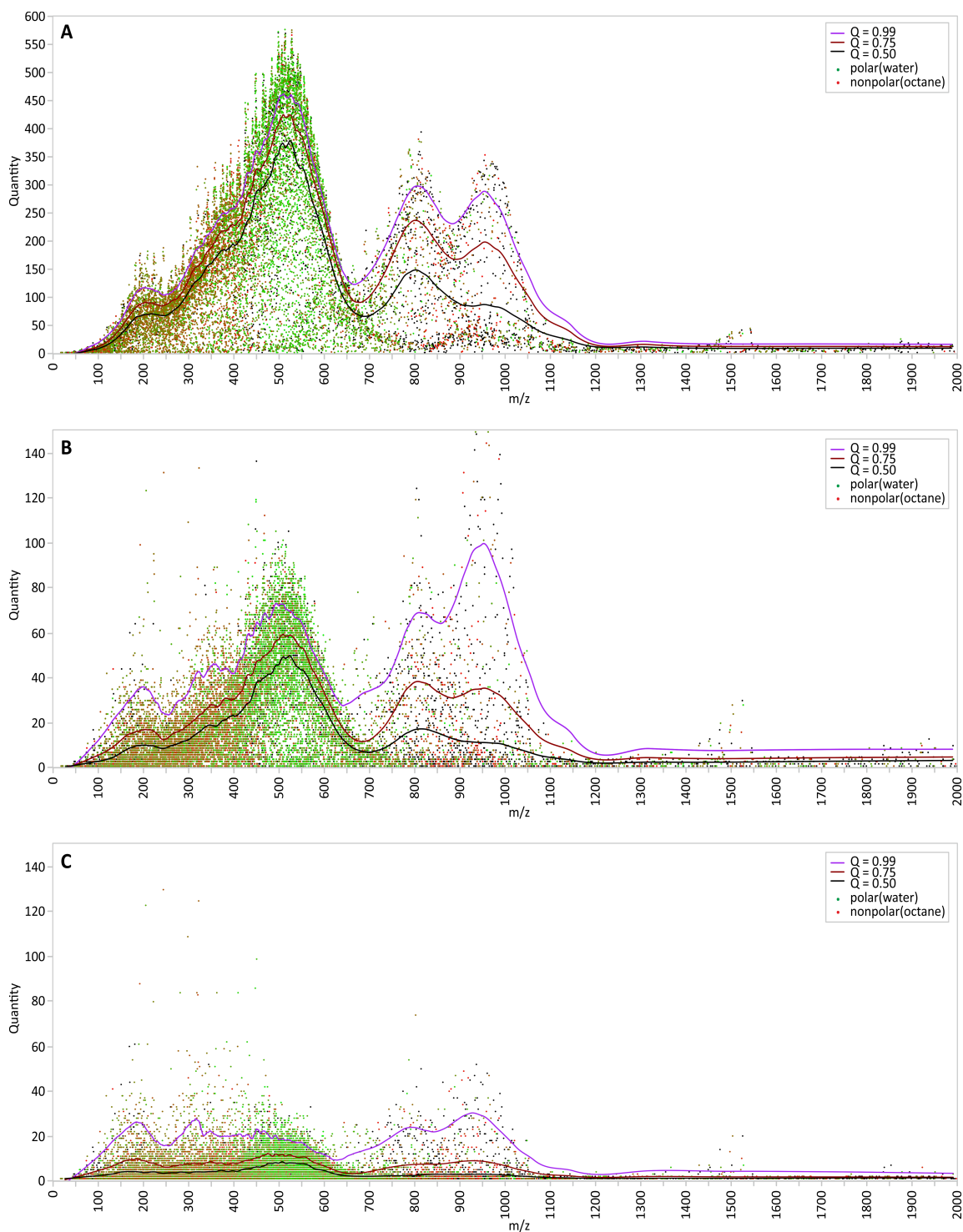


**Figure 45:** Mass distribution by *In silico* calculations at a resolution of 15 000 (A), 120 000 (B) and 960 000 (C) FWHM. X-axis shows the number of unique values of  $m/z$  within the filtered list of compiled metabolites, while the Y-axis indicates the number of values  $m/z$  which fits into the interval  $[m/z - x; m/z + x]$ , where  $x$  is based on the resolution. Lines indicate different percentiles (upper of 0.99, 0.75 and 0.50, respectively).

Independent colour dots indicate the polarity: green = polar, red = nonpolar (based on their logP values - octanol / water).

Figure 46 shows the maximum number and the median value of the calculated overlapping  $m/z$  at a particular resolution. Number of  $m/z$  masked by the isobaric matrix interference is decreased in conformity with the power function of limiting one. Above resolution 240 000 FWHM, the maximum number of indistinguishable functions did not fall. Evaluation of the data structure showed that it was caused by isobaric compounds with high structural diversity. For example, the  $m/z$  244.1549 corresponding to  $[M+K]^+$  ion mass 205.1951 ( $C_{15}H_{24}$ ), which refers to a group sesquiterpenes and prenols with 130 possible overlaps. Other most abundant overlaps ( $m/z$  205.1956, 298.2746, 322.2746, 450.3219) are generally attributed to various lipid adducts, which correspond to those lipids (see Figure 45). Mean values (dashed line) shows that, even at very high resolution, it is not possible to separate all the features completely. At a resolution of 3 840 000 FWHM a maximum of 35.2% of the features are represented by a particular  $m/z$  without overlaps, while for a typical resolution of 60 000 FWHM, only 3.63% of the features could be separated.<sup>56</sup>

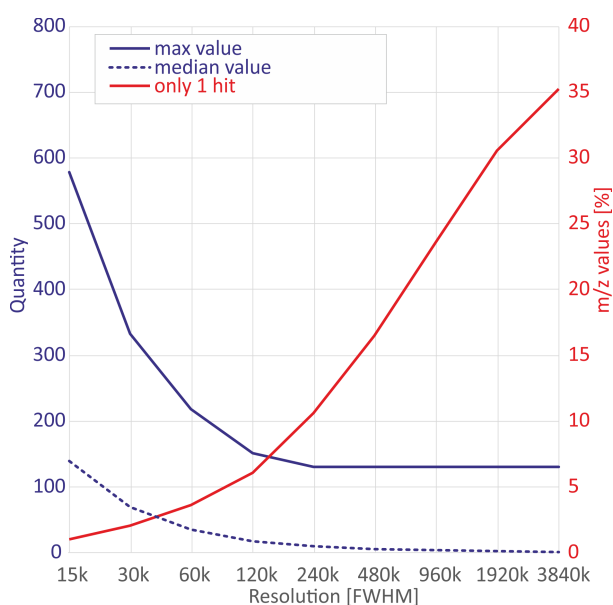


**Figure 46:** Regression of overlapping features based on the resolution (*in silico* calculation). The solid line represents the maximum value unrecognizable function by

resolution. Dashed line shows the mean indistinguishable functions in the list  $m/z$  for each resolution. Percentage of  $m/z$  values represented in the mass spectrum of a single value is shown by the red.

Comparison of influence on each individual 100bin- $m/z$ -region generated *in silico* was performed (Figure 47). In the range from 0 to 600  $m/z$  (Figure 47A), a big substantial increase of features from 1.47 ratio (0-100  $m/z$ ) to 23.11 ratio (501-600  $m/z$ ) was observed. In the range of 600-1400  $m/z$ , the opposite trend was observed from 14.43 ratio to 2.80 ratio (Figure 47B). The curves in Figure 47C show similar trends in the range of 1400 to 2000  $m/z$  (ratio of 2.85 to 3.67), but rather different trend than the previous dependence was observed because the data plateau at resolution higher than 960 000 FWHM. Therefore, these theoretical calculations in FWHM resolution of millions continue to have an impact on the calculated number of unique masses. Nevertheless, an extremely high resolution has a huge impact on distinguishing the isotopic patterns, which are helpful in structure elucidation.

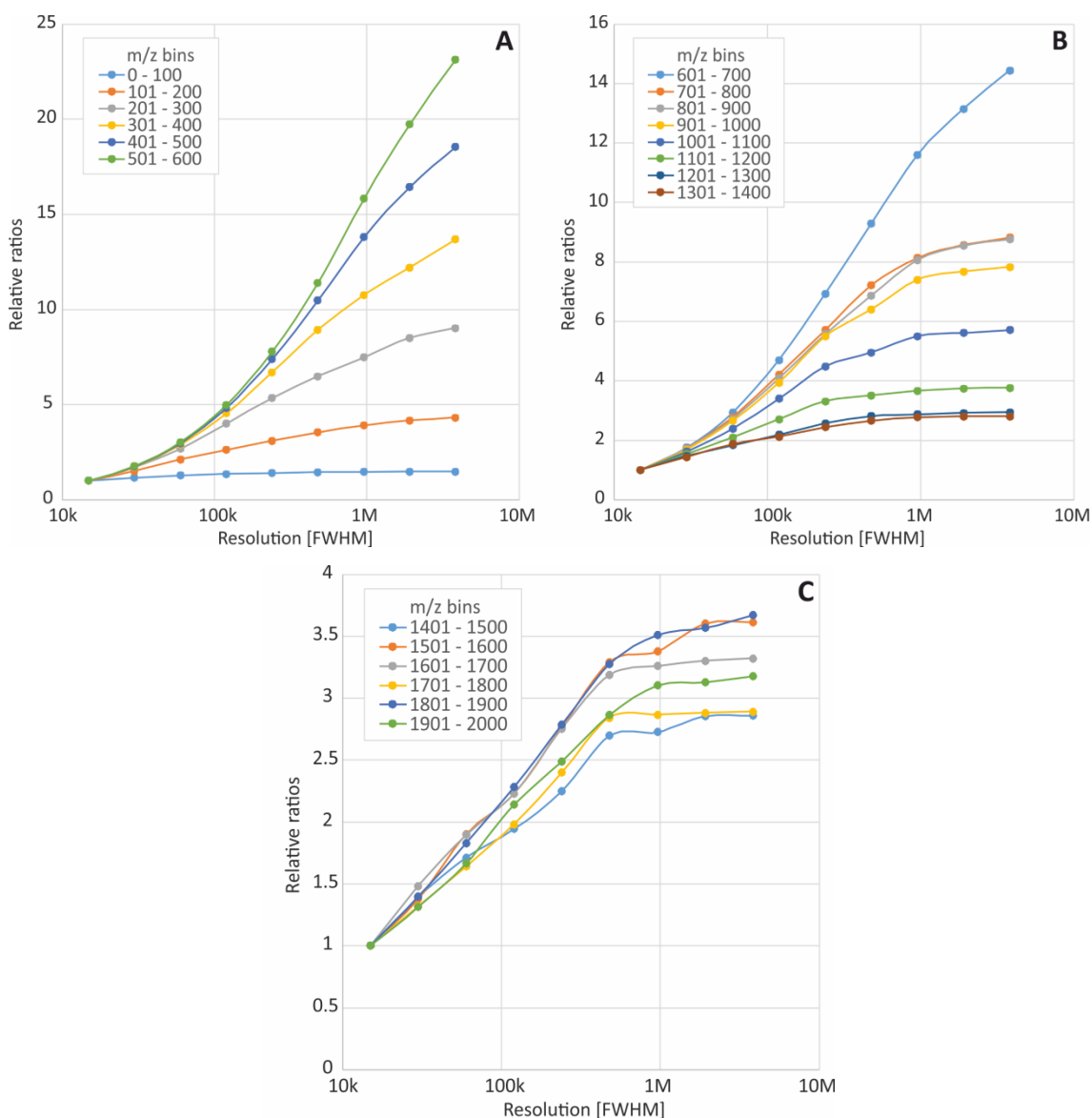


**Figure 47:** Relative increase in 100bin- $m/z$ -region detected features from the *in silico* calculations. The Y-axis represents the ratio of the detected features to a specific resolution value normalized to the 15 000 FWHM. X axis represents a resolution of 15 000 up to 3 840 000 FWHM.

#### 4.3.2. LC-MS data

The plasma sample were analysed at different mass spectrometry resolutions up to 480 000 FWHM resolution in order to investigate its influence on the number of detected features. Analysis time was 15 minutes with elution gradient and peak capacity  $P = 167$  ( $N = 90\ 000$  to  $576\ 000$  N/m). Total ion chromatogram and extracted ion chromatograms of selected isomeric compounds are shown in Figures 48 - 50.

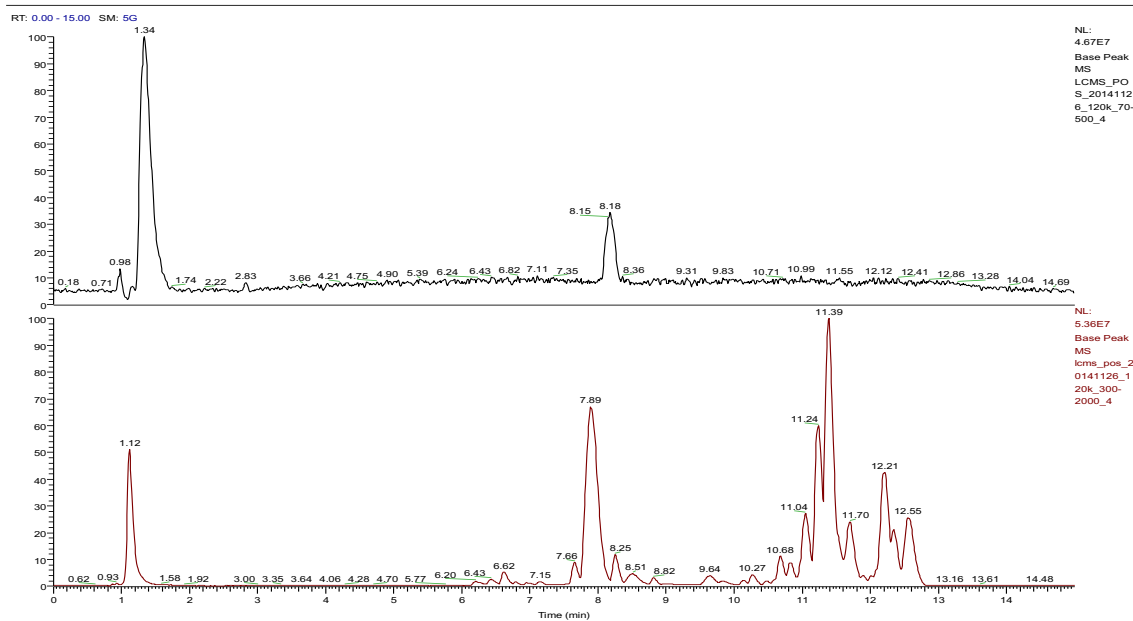


**Figure 48:** Total ion chromatogram in positive mode – Upper part of the figure is TIC for mass range 70 – 500  $m/z$  and part is TIC of a second mass range 350 – 2000  $m/z$ .

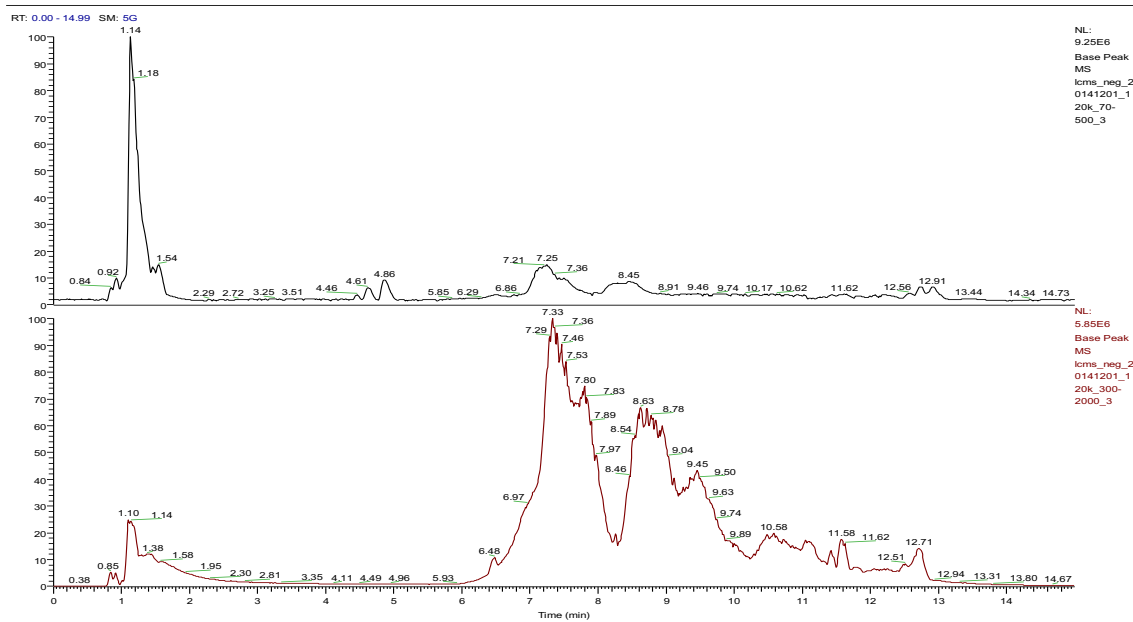


**Figure 49:** Total ion chromatogram in negative mode – Upper part of the figure is TIC for mass range 70 – 500  $m/z$  and part is TIC of a second mass range 350 – 2000  $m/z$ .

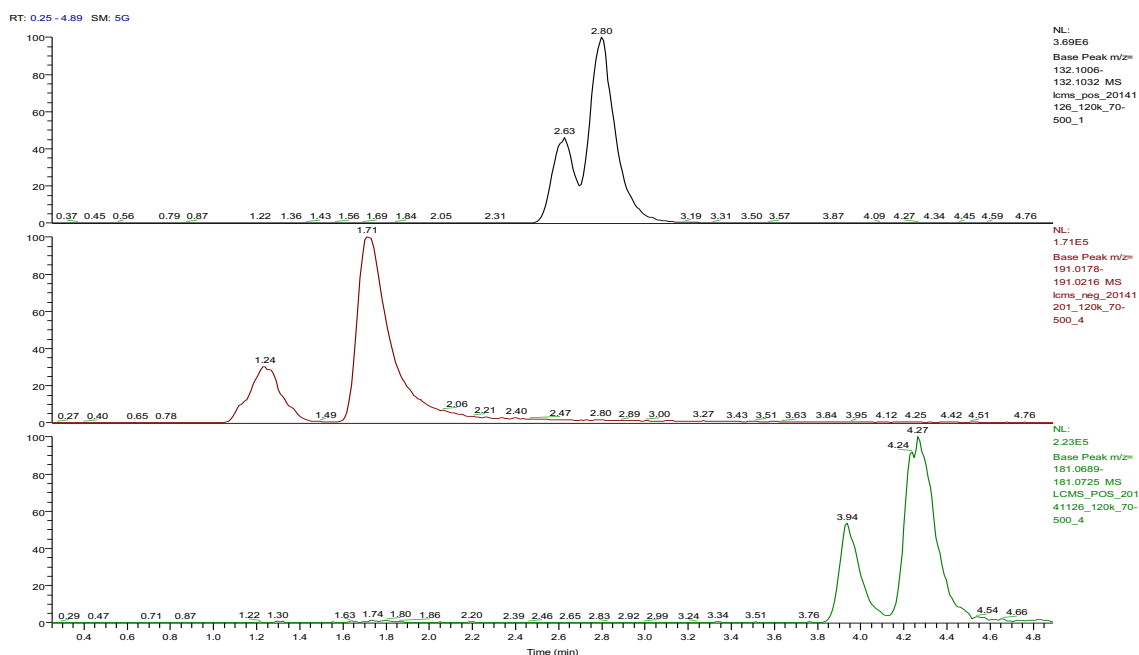


**Figure 50:** Separation of selected isomeric compounds on the column. Upper part of the figure is pair leucine/isoleucine; middle part is pair citrate/isocitrate; lower part of the figure is pair glucose/fructose (hexose)

Three different software were used for data processing LC-MS (data shown in Figure 51). Software XCMS, MZmine and Compound Discoverer yielded similar trends, i.e., sharp increase in the number of detected features with maximum at 60 000 FWHM in both positive and negative mode (120 000 FWHM for Compound Discoverer in positive mode). Each software is able to produce different types of lists features. XCMS detects all features without additional filtering, referred to as "raw" elements (for isotope and / or adduct grouping, additional software modules should be used). MZmine is able to identify "raw elements" or, if applied deisotoping module, "isotopic features". Thus, for ready comparison, XCMS raw functions and lists of functions raw MZmine were used to generate the graphs shown in Figure 51. The "Unknown Detector" module in the compound Discoverer is able to detect only functions with minimal set of isotopes at one or more, generating "isotopic features" list. Numbers obtained by Compound Discoverer software (Figure 51C) represent the sum of compounds present in the mass spectrum as several different ion species grouped as one (grouped isotopes and adducts). For the above reasons, the absolute numbers in Figure 51 are not strictly comparable and only trends should be considered. All software reported approximately

five times the number of elements on the positive mode as compared with negative mode. This observation may be originating from the fact that plasma metabolites are mainly ionized in the positive mode. The physico-chemical properties, and composition of the mobile phase may also contribute to the observed effects.<sup>89</sup> Considering a fewer features detected in the negative mode, the need for higher resolution is less important.

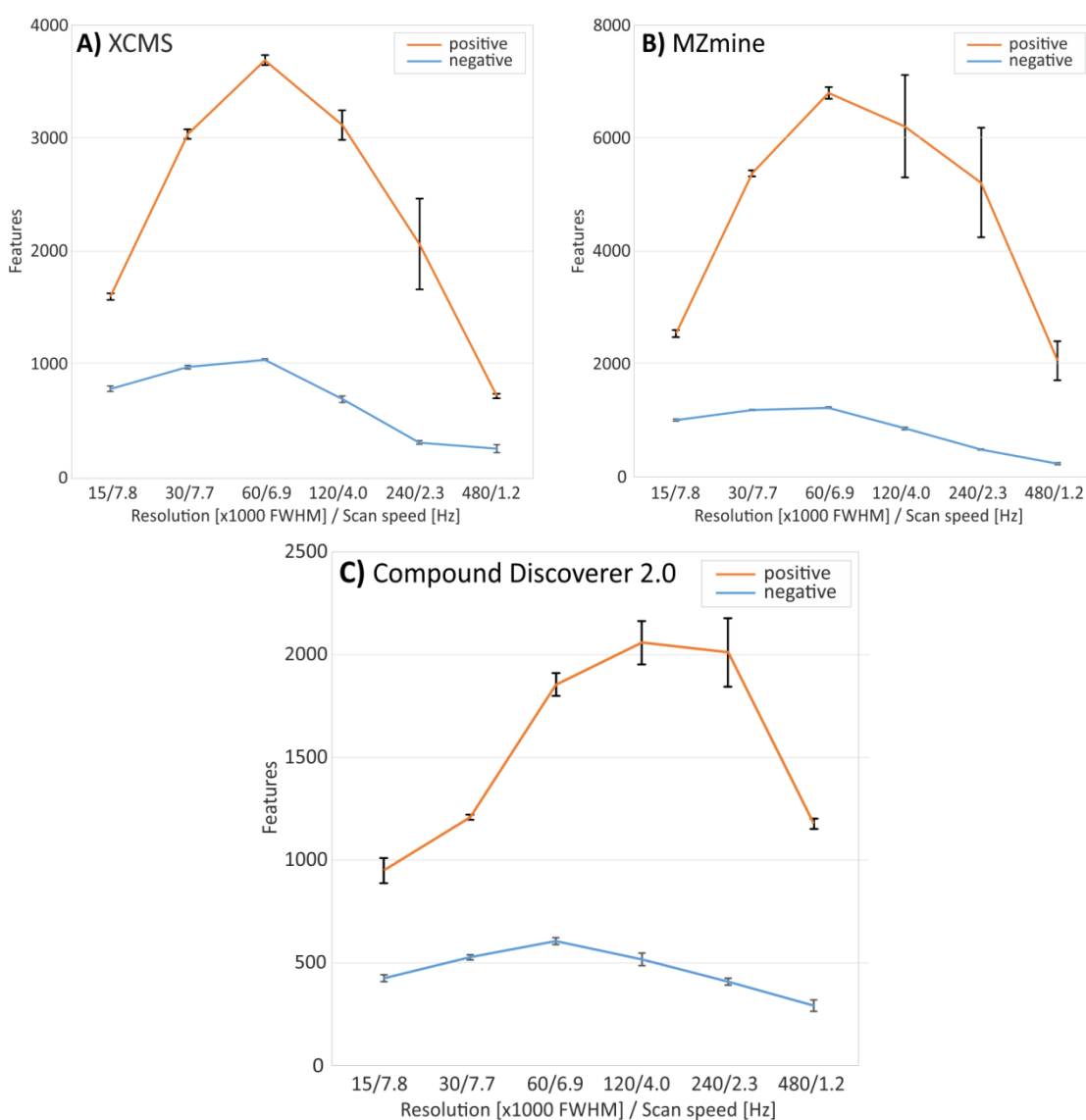


**Figure 51:** Number of detected features in plasma samples. Each part of the picture represents results from different software in both positive (yellow line) and negative mode (blue line): A) XCMS (raw features), B) MZmine (raw features), C) Compound list (grouped features as a compounds).

In plasma samples in the positive mode at 60 000 FWHM, 6778 features were detected (MZmine, Figure 51B). Error bars at higher resolutions will result in more individual ion signals, and therefore represents a challenge for detecting peak algorithms. In contrast, the number of features found in the *in silico* calculations at 60 000 FWHM was 49 529 (Figure 52). Although both analyses took into account metabolites, the most abundant isotopes and adducts, the number of features for the plasma samples should be theoretically higher because it includes fragments, noise features and other components, possibly generated by electrospray ionization. The discrepancy in the number of features can occur for various reasons. A large number of compounds listed in the databases are present in biological samples at concentrations below the detection limit of existing profiling methods (e.g., hormones, neurotransmitters). In addition, non-targeted metabolite extracts contain exogenous substances (pharmaceuticals, food metabolites, xenobiotics, etc.). Other features may be chemically and/or biologically unstable, and thus may be lost. Poor ionizability of certain compound classes may also reduce the number of the detected features. Another limitation is that some compounds are not retained (or captured) on the column, thus undetectable. Furthermore, isobars can exhibit unpredictable behaviour under given separation modes (for example, reverse phase, normal phase, aqueous, HILIC). In previously published works, it was demonstrated that right choice of separation method will also influence the number of detected features.<sup>90–92</sup> Together with high resolution, the yield of features from an untargeted metabolomic experiment may be significantly increased.

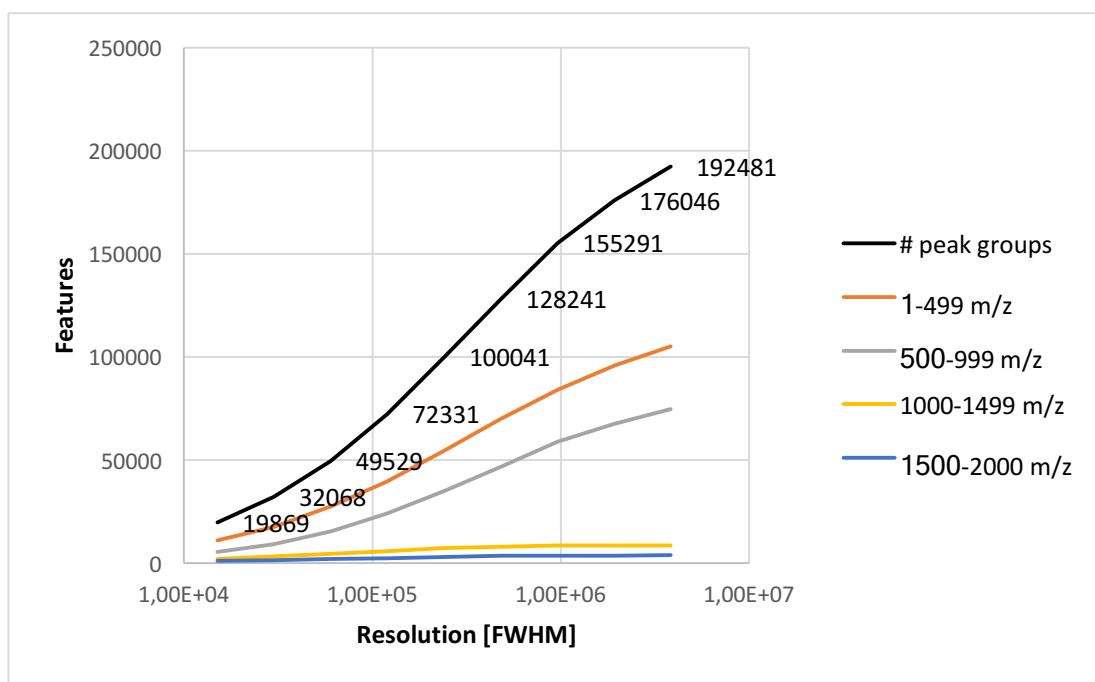


**Figure 52:** Number of detectable compounds based on the list of unique masses (227 060) by same calculation as Figure 47 in the thesis.

Figure 53 represent a histogram of  $m/z$  values (according XCMS) in plasma samples showing the distribution of the individual data points in Figure 51. The trend of the curves is generally almost the same as observed in the *in silico* calculations (Figure 45). Region 300-800  $m/z$  showed a strong dependency on resolution in positive mode (Figure 53A). In contrast, the area of 800-1400  $m/z$  showed almost the same number of functions for 60 000 and 120 000 FWHM (Figure 53A), suggesting less need for high resolution in the region. Resolution of the orbital ion trap detector is not linear with  $m/z$  (Figure 54). This effect results in lower resolution in the higher  $m/z$  values, and thus less number of detected features. In the negative ionization mode (Figure 53B), all curves in resolutions of from 15 000 to 120 000 FWHM showed similar profiles. The number of detected features with  $m/z$  of 400 with a resolution of 240 000 and 480 000 FWHM was significantly reduced due to the insufficient scanning frequency (data points). This problem can be overcome by using mass spectrometer with higher scanning speed.

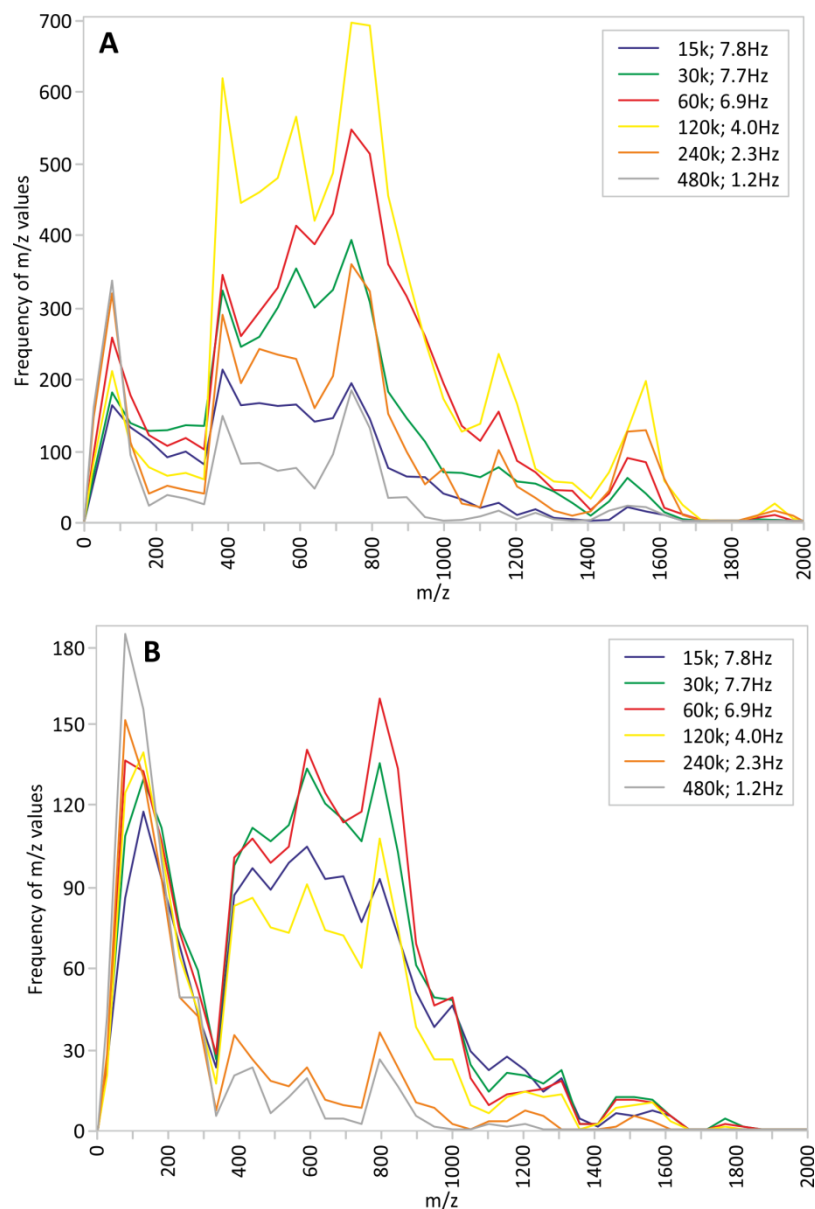


**Figure 53:** Histograms values  $m/z$  from plasma samples in the positive (A) and negative mode (B) (XCMS). Each point on the lines represents the frequency of  $m/z$  values in the window 50 Da. The numbers in the legend shows the resolution and scanning speed, respectively.

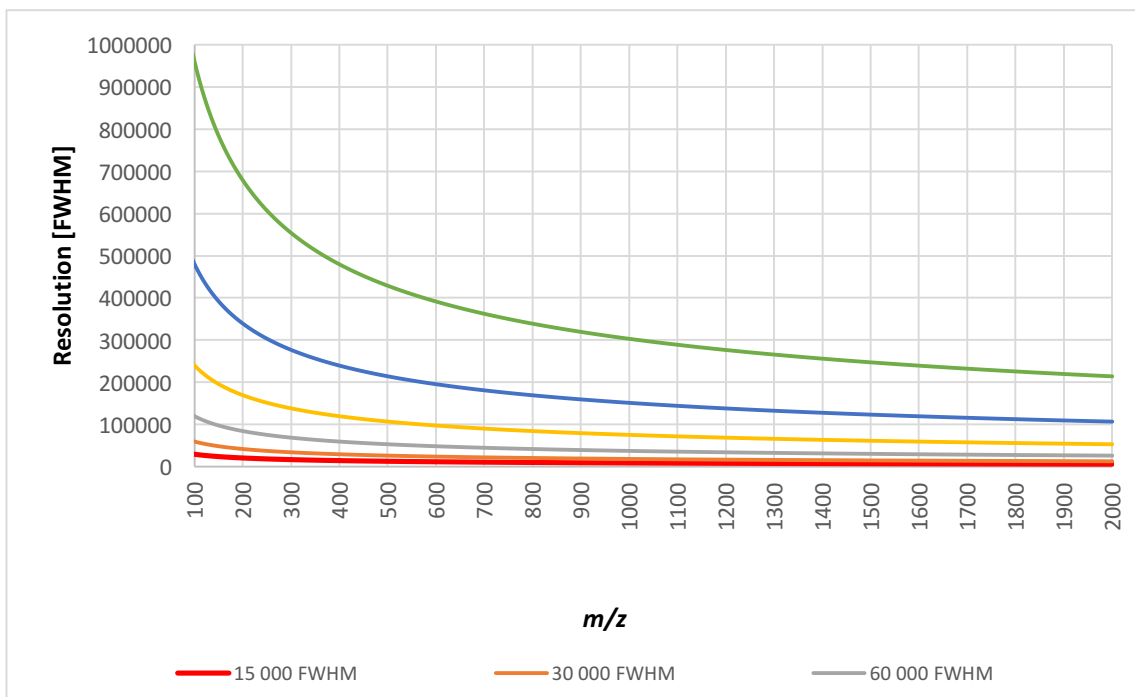


**Figure 54:** Dependency of  $m/z$  and resolution in Orbitrap based mass spectrometers

In the mass spectrometers based on orbital ion trap, the high resolution is achieved by longer acquisition of ions in the trap, and thereby the frequency of data points is reduced<sup>93</sup> (Figure 55). It is widely known that a minimum of four data points per peak should be present for the automatic detection algorithms function.<sup>61</sup> Thus, in order to minimize the impact of this parameter, the experiment was performed in which the minimum number of data points was set to 3 (centWave). Regardless of the resolution, higher number of functions was found (Figure 56). However, close inspection of the data revealed that most of the reported peaks were false positive hits. This may indicate that 60 000 to 120 000 FWHM is a good compromise in terms of resolution and scanning speed for metabolomics on the mass spectrometer used in this study.

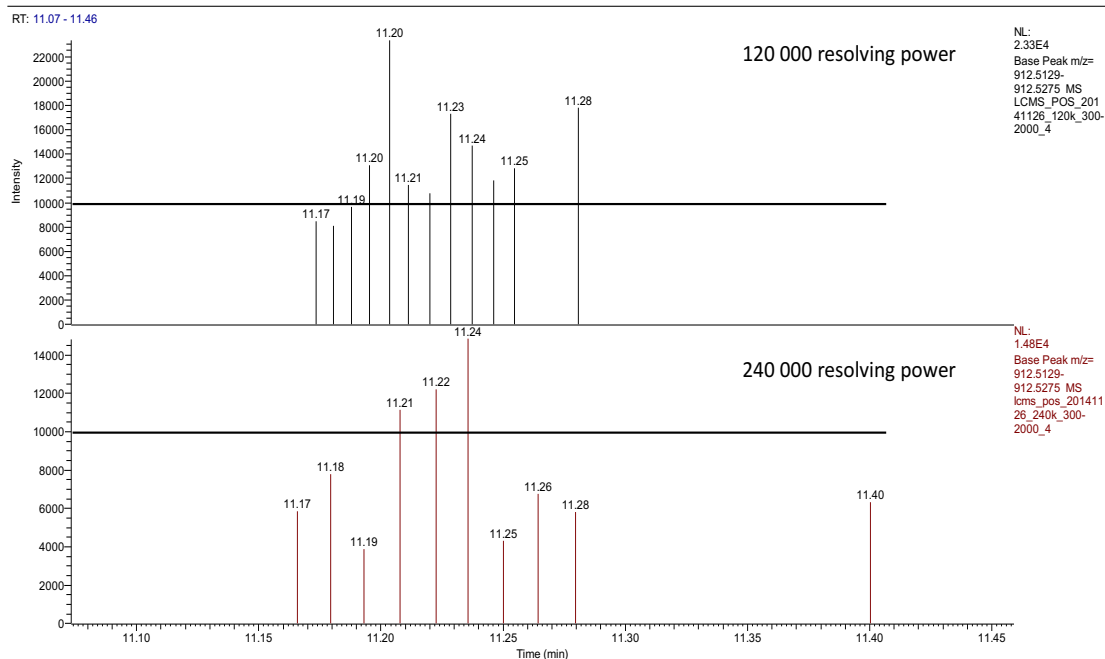
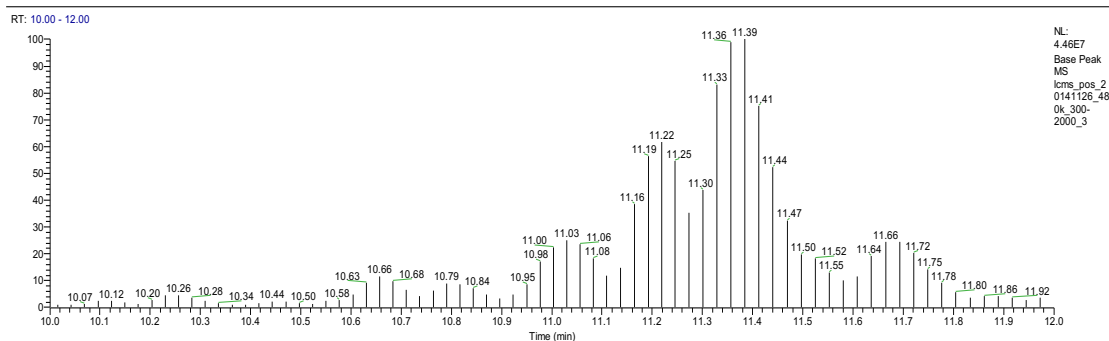
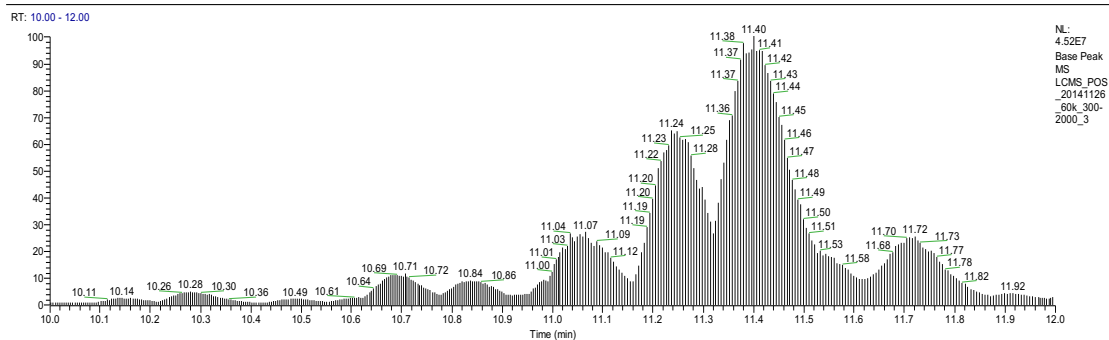


**Figure 55:** Lower number of data points (upper picture – 60 000 FWHM, lower picture 480 000 FWHM)

Our compiled list is covering metabolites present in the biological system, but it is not taking into account differences in tissue/bio-liquid distribution. It also contains exogenous compounds (drugs, xenobiotics, food and plant metabolites) that may be present to a varying extent in biological samples, depending on their nature. *In silico* calculations in this study were focused on human plasma and it would be interesting to see its application in plant metabolomics where many metabolites preferably ionized in the negative mode. A different scenario can also occur in lipidomics or glycomics, which are heavily influenced by the high number of structural isomers.<sup>56</sup>



**Figure 56:** CentWave algorithm in XCMS with minimum 3 points/peak for peak picking.

## 5. Conclusion

The aim of this work was focused on the development and the improvement of methods involved in the diagnosis of inherited metabolic diseases. Certain key aspects and bottlenecks in this field were suggested by several separated experiments.

The untargeted metabolomics approach applied on the dry blood spots (25 MCADD samples and 25 healthy controls) showed 14 significant metabolites discriminating those two groups from each other. Among them, already well known biomarkers of MCADD (C8, C10, C10:1) were correctly identified with MSI identification Level 1. Another eight compounds were identified as phosphatidylcholines. Some of them belong to a group of oxidized phosphatidylcholines (PAzPC - PC(16:0,9:0(COOH)); PC(16:0,8:0(COOH); PC (18:0,5:0(COOH))) associated with oxidative stress. These findings were also confirmed by FIA-TMS experiment (MCADD = 25, Controls = 250). These phosphatidylcholines correlated with disease markers mutually with  $R > 0.8$  pointing to a common mechanism of origin. Combination of untargeted metabolomics followed by targeted metabolomics in a wider patient cohort point out that patients suffering from MCADD experience oxidative stress.

In the second part a novel approach of “spectral trees” was tested in structure elucidation of metabolites in urine samples of adenosine deaminase deficiency. Four metabolites associated with ADA were successfully identified. Three of them (2'-deoxyadenosine, adenosine, 1-methyladenosine) were already found in the urine of patients suffering from ADA. Most of them are associated with degradation of tRNA, rRNA, mRNA or snRNA. Novel biomarker of ADA 1-methyl-5-oxoadenosine is probably an oxidation product of 1-methyladenosine.

The third part of the thesis was focused on influence of mass spectrometry resolution on number of detected features in untargeted metabolomics experiments. Theoretically and experimentally we addressed a relation between resolution and scan speed in orbital-ion-trap based mass spectrometers. *In silico* calculations showed that with increasing resolution more features can be detected (limited by the maximum number of features possible for the particular biological matrix). LCMS data showed that in the real assays the optimal resolution was 60 000 - 120 000 FWHM in positive ionization mode and 60 000 FWHM in negative ionization mode for ESI. In order to

retrieve the highest amount of information in current analytical assays, according to our findings, the resolution around 60 000 – 120 000 FWHM is necessary.

## 6. List of abbreviations

ACAD	acyl-CoA-dehydrogenase
ADA	adenosine deaminase (deficiency)
APCI	atmospheric pressure chemical ionization
ARG	argininemia
BTD	biotinidase deficiency
C10	decanoylcarnitine
C10:1	decenoylcarnitine
C12	dodecanoylcarnitine
C2	acetylcarnitine
C6	hexanoylcarnitine
C8	octanoylcarnitine
CACT	carnitine acyl-carnitine translocase deficiency
CAH	congenital adrenal hyperplasia
CBS	classical homocystinuria - cystathionine beta synthase deficiency
CE	capillary electrophoresis
CF	cystic fibrosis
CH	congenital hypothyroidism
CID	Collision-induced dissociation
CIT	citrulinemia type I.
clr	centered logratio transformation
CPT I	carnitine palmitoyltransferase I deficiency
CPT II	carnitine palmitoyltransferase II deficiency
CWT	Continuous Wavelet Transform
DDA	data dependent acquisition
DIA	data independent acquisition
DNA	deoxyribonucleic acid
ESI	electrospray ionization
FAD	flavin adenine dinucleotide
FAODs	Fatty acid oxidation disorders
FFT	Fast Fourier transformation

FIA	flow injection analysis
FIA-TMS	flow injection analysis-tandem mass spectrometry
FJHN	familial juvenile hyperuricaemic nephropathy
FT	Fourier transformation
FTICR	Fourier transform ion cyclotron resonance
FTMS	Fourier transform mass spectrometry
FTMS	Fourier Transform Mass Spectrometry
FWHM	Full-width-at-half-maximum
GA I	glutaric aciduria type I
GABA	<i>gamma</i> -Aminobutyric acid
GC	gas chromatography
GVHD	graft-versus-host disease
HCD	Higher-energy collisional dissociation
HILIC	hydrophilic interaction liquid chromatography
HLA	human leukocyte antigen
HMDB	Human Metabolome Database
HPA	hyperphenylalaninemia
HPLC	High performance liquid chromatography
HPRT	hypoxanthine-guanine phosphoribosyl transferase deficiency
HRAM	High resolution accurate mass
IEM	Inborn errors of metabolism
IMPDH1	inosine-5'-monophosphate dehydrogenase dehydrogenase 1
IVA	isovaleric aciduria
KEGG	Kyoto Encyclopedia of Genes and Genomes
LC	Liquid chromatography
LC-HRMS	Liquid chromatography-high resolution mass spectrometry
LC-MS	liquid chromatography-mass spectrometry
LCAD	long-chain acyl-CoA-dehydrogenase
LOESS	local regression
<i>m/z</i>	mass-to-charge ratio
MALDI	matrix assisted laser desorption/ionization
MCAD	medium chain acyl-CoA dehydrogenase enzyme

MCADD	Medium chain acyl-CoA dehydrogenase deficiency
MRM	multi-reaction-monitoring mode
MS	mass spectrometry
MS/MS	Tandem mass spectrometry
MSI	Metabolite Standards Initiative
MS <sup>n</sup>	Multistage fragmentation mass spectrometry spectrum/spectra
MSTFA	N-Methyltrimethylsilyltrifluoroacetamide; CAS: 24589-78-4
MSUD	maple syrup urine disease
MTHRF	homocystinuria based on deficiency of methylene tetrahydrofolate reductase
MUD	HLA-matched unrelated donor
NBS	newborn screening
NCE	normalized collision energy
NIST	National Institute of Standards and Technology ( <a href="http://www.nist.gov">www.nist.gov</a> )
NK	natural killers
NMR	nuclear magnetic resonance
OPLS-DA	orthogonal partial least squares discriminant analysis
PAPC	1-O-hexadecanoyl-2-O-(5Z,8Z,11Z,14Z)-5,8,11,14-eicosatetraenoyl-sn-glycerol-3-phosphocholine
PAzPC	1-O-hexadecanoyl-2-O-(9-carboxyoctanoyl)-sn-glycerol-3-phosphocholine
PC	phosphocholine
PCA	principal component analysis
PEG	polyethylene glycol
PGPC	1-O-hexadecanoyl-2-O-(9-carboxybutanoyl)-sn-glycerol-3-phosphocholine
PKU	phenylketonuria
PoxnoPC	1-O-hexadecanoyl-2-O-(9-oxononanoyl)-sn-glycerol-3-phosphocholine
PRPS	phosphoribosyl-pyrophosphate synthetase superactivity
PUFAs	polyunsaturated fatty acids
QC	Quality control
ROI	Regions of interest

ROS	reactive oxygen species
SCAD	short-chain acyl-CoA-dehydrogenase
SIDS	Sudden infant death syndrome
TIC	total ion chromatogram
TMS	Trimethylsilyl (C <sub>3</sub> H <sub>8</sub> Si)
TOF	Time-of-flight
UHPLC	ultra-high performance liquid chromatography
VLCAD	very long-chain acyl-CoA-dehydrogenase
WMA	World Medical Association

## 7. References

1. Nussban, R. L., McInnes, R. R. & Willard, H. F. *Genetics In Medicine*. (Elsevier, 2007).
2. Pampols, T. in *Advances in experimental medicine and biology* **686**, 397–431 (2010).
3. Fernandes, John, Saudubray, J. *Inborn Metabolic Disease*. (Springer Berlin Heidelberg, 2006). doi:10.1007/978-3-540-28785-8
4. Cox, D. W. Genes of the copper pathway. *Am. J. Hum. Genet.* **56**, 828–34 (1995).
5. Cao, L. C. *et al.* Mitochondrial dysfunction is a primary event in renal cell oxalate toxicity. *Kidney Int.* **66**, 1890–1900 (2004).
6. Lindner, M., Hoffmann, G. F. & Matern, D. Newborn screening for disorders of fatty-acid oxidation: Experience and recommendations from an expert meeting. *J. Inherit. Metab. Dis.* **33**, 521–526 (2010).
7. Gregersen, N. *et al.* Mitochondrial fatty acid oxidation defects--remaining challenges. *J. Inherit. Metab. Dis.* **31**, 643–57 (2008).
8. Gregersen, N., Lauritzen, R. & Rasmussen, K. Suberylglycine excretion in the urine from a patient with dicarboxylic aciduria. *Clin. Chim. Acta.* **70**, 417–25 (1976).
9. Kim, J. J. P. & Miura, R. Acyl-CoA dehydrogenases and acyl-CoA oxidases: Structural basis for mechanistic similarities and differences. *European Journal of Biochemistry* **271**, 483–493 (2004).
10. Aoyama, T. *et al.* Purification of human very-long-chain acyl-coenzyme A dehydrogenase and characterization of its deficiency in seven patients. *J. Clin. Invest.* **95**, 2465–2473 (1995).
11. Stierand, K. & Rarey, M. Drawing the PDB: Protein-ligand complexes in two dimensions. *ACS Med. Chem. Lett.* **1**, 540–545 (2010).
12. Satoh, A. *et al.* Structure of the transition state analog of medium-chain acyl-CoA dehydrogenase. Crystallographic and molecular orbital studies on the charge-transfer complex of medium-chain acyl-CoA dehydrogenase with 3-thiaoctanoyl-CoA. *J. Biochem.* **134**, 297–304 (2003).

13. Andresen, B. S. *et al.* MCAD deficiency in Denmark. *Mol. Genet. Metab.* **106**, 175–88 (2012).
14. Oerton, J. *et al.* Newborn screening for medium chain acyl-CoA dehydrogenase deficiency in England: prevalence, predictive value and test validity based on 1.5 million screened babies. *J. Med. Screen.* **18**, 173–81 (2011).
15. Derks, T. G. J. *et al.* The difference between observed and expected prevalence of MCAD deficiency in The Netherlands: a genetic epidemiological study. *Eur. J. Hum. Genet.* **13**, 947–52 (2005).
16. Rhead, W. J. Newborn screening for medium-chain acyl-CoA dehydrogenase deficiency: a global perspective. *J. Inherit. Metab. Dis.* **29**, 370–7 (2005).
17. Thodi, G. *et al.* Characterization of the molecular spectrum of Medium-Chain Acyl-CoA Dehydrogenase Deficiency in a Greek newborns cohort: identification of a novel variant. *Clin. Biochem.* **45**, 1167–72 (2012).
18. Gregersen, N. *et al.* Mutation analysis in mitochondrial fatty acid oxidation defects: Exemplified by acyl-CoA dehydrogenase deficiencies, with special focus on genotype-phenotype relationship. *Hum. Mutat.* **18**, 169–89 (2001).
19. Baumgartner, C. & Baumgartner, D. Biomarker discovery, disease classification, and similarity query processing on high-throughput MS/MS data of inborn errors of metabolism. *J. Biomol. Screen.* **11**, 90–9 (2006).
20. Gregersen, N. *et al.* General (medium-chain) acyl-CoA dehydrogenase deficiency (non-ketotic dicarboxylic aciduria): quantitative urinary excretion pattern of 23 biologically significant organic acids in three cases. *Clin. Chim. Acta* **132**, 181–191 (1983).
21. Rinaldo, P. *et al.* MCADD Diagnosis by Stable-isotope Dilution measurement of Urinary n=Hexanoylglycine and 3-Phenylpropionylglycine. *The New England journal of medicine* **319**, 1308–1313 (1988).
22. Chace, D. H. Mass spectrometry in newborn and metabolic screening: Historical perspective and future directions. *Journal of Mass Spectrometry* **44**, 163–170 (2009).

23. Maier, E. M. *et al.* Validation of MCADD newborn screening. *Clin. Genet.* **76**, 179–187 (2009).
24. Balasubramaniam, S., Duley, J. A. & Christodoulou, J. Inborn errors of purine metabolism: clinical update and therapies. *J. Inherit. Metab. Dis.* **37**, 669–86 (2014).
25. Cicalese, M. P. *et al.* Update on the safety and efficacy of retroviral gene therapy for immunodeficiency due to adenosine deaminase deficiency. *Blood* **128**, 45–54 (2016).
26. GIBLETT, E., ANDERSON, J., COHEN, F., POLLARA, B. & MEUWISSE.HJ. Adenosine Deaminase Deficiency in 2 Patients With Severely Impaired Cellular Immunity. *Lancet* **2**, 1067- (1972).
27. Hassan, A. *et al.* Outcome of hematopoietic stem cell transplantation for adenosine deaminase-deficient severe combined immunodeficiency. *Blood* **120**, 3615–3624 (2012).
28. Chan, B. *et al.* Long-term efficacy of enzyme replacement therapy for Adenosine deaminase (ADA)-deficient Severe Combined Immunodeficiency (SCID). *Clin. Immunol.* **117**, 133–143 (2005).
29. Baffelli, R. *et al.* Diagnosis, Treatment and Long-Term Follow Up of Patients with ADA Deficiency: a Single-Center Experience. *J. Clin. Immunol.* **35**, 624–637 (2015).
30. Blaese, R. M. *et al.* T Lymphocyte-Directed Gene Therapy for ADA- SCID: Initial Trial Results After 4 Years. *Science (80-. )*. **270**, 475–480 (1995).
31. Psychogios, N. *et al.* The human serum metabolome. *PLoS One* **6**, e16957 (2011).
32. Dunn, W. B., Broadhurst, D. I., Atherton, H. J., Goodacre, R. & Griffin, J. L. Systems level studies of mammalian metabolomes: the roles of mass spectrometry and nuclear magnetic resonance spectroscopy. *Chem. Soc. Rev.* **40**, 387–426 (2011).
33. Dunn, W. B. *et al.* Mass appeal: Metabolite identification in mass spectrometry-focused untargeted metabolomics. *Metabolomics* **9**, 44–66 (2013).
34. Fiehn, O. *et al.* The metabolomics standards initiative (MSI). *Metabolomics* **3**, 175–178 (2007).

35. Lu, W., Bennett, B. D. & Rabinowitz, J. D. Analytical strategies for LC-MS-based targeted metabolomics. *J. Chromatogr. B Anal. Technol. Biomed. Life Sci.* **871**, 236–242 (2008).
36. Rathahao-Paris, E., Alves, S., Junot, C. & Tabet, J.-C. High resolution mass spectrometry for structural identification of metabolites in metabolomics. *Metabolomics* **12**, 10 (2016).
37. Fiehn, O. Metabolomics - The link between genotypes and phenotypes. *Plant Mol. Biol.* **48**, 155–171 (2002).
38. Cajka, T. & Fiehn, O. Toward Merging Untargeted and Targeted Methods in Mass Spectrometry-Based Metabolomics and Lipidomics. *Analytical Chemistry* **88**, 524–545 (2016).
39. Griffiths, I. W. J. J. Thomson - The centenary of his discovery of the electron and of his invention of mass spectrometry. *Rapid Commun. Mass Spectrom.* **11**, 2–16 (1997).
40. Fenn, J., Mann, M., Meng, C., Wong, S. & Whitehouse, C. Electrospray ionization for mass spectrometry of large biomolecules. *Sci. (New York, NY)* **246**, 64–71 (1989).
41. Tsugawa, H. *et al.* MS-DIAL: data-independent MS/MS deconvolution for comprehensive metabolome analysis. *Nat. Methods* **12**, 523–526 (2015).
42. Scheidweiler, K. B., Jarvis, M. J. Y. & Huestis, M. A. Nontargeted SWATH acquisition for identifying 47 synthetic cannabinoid metabolites in human urine by liquid chromatography-high-resolution tandem mass spectrometry. *Anal. Bioanal. Chem.* **407**, 883–897 (2015).
43. Brown, M. *et al.* Mass spectrometry tools and metabolite-specific databases for molecular identification in metabolomics. *Analyst* **134**, 1322–32 (2009).
44. Chace, D. H., Kalas, T. A. & Naylor, E. W. Use of Tandem Mass Spectrometry for Multianalyte Screening of Dried Blood Specimens from Newborns. *Clinical Chemistry* **49**, 1797–1817 (2003).
45. Rashed, M. S. Clinical applications of tandem mass spectrometry: ten years of

- diagnosis and screening for inherited metabolic diseases. *J. Chromatogr. B. Biomed. Sci. Appl.* **758**, 27–48 (2001).
46. Zytковicz, T. H. *et al.* Tandem mass spectrometric analysis for amino, organic, and fatty acid disorders in newborn dried blood spots: A two-year summary from the New England newborn screening program. *Clin. Chem.* **47**, 1945–1955 (2001).
  47. Lisec, J., Schauer, N., Kopka, J., Willmitzer, L. & Fernie, A. R. Gas chromatography mass spectrometry–based metabolite profiling in plants. *Nat. Protoc.* **1**, 387–396 (2006).
  48. Rowena Monton, M. N. & Soga, T. Metabolome analysis by capillary electrophoresis–mass spectrometry. *J. Chromatogr. A* **1168**, 237–246 (2007).
  49. Bajad, S. U. *et al.* Separation and quantitation of water soluble cellular metabolites by hydrophilic interaction chromatography–tandem mass spectrometry. *J. Chromatogr. A* **1125**, 76–88 (2006).
  50. Sumner, L. W. *et al.* Proposed minimum reporting standards for chemical analysis: Chemical Analysis Working Group (CAWG) Metabolomics Standards Initiative (MSI). *Metabolomics* **3**, 211–221 (2007).
  51. Wishart, D. S. Computational strategies for metabolite identification in metabolomics. *Bioanalysis* **1**, 1579–1596 (2009).
  52. Kind, T. & Fiehn, O. Seven Golden Rules for heuristic filtering of molecular formulas obtained by accurate mass spectrometry. *BMC Bioinformatics* **8**, 105 (2007).
  53. Noury, S., Silvi, B. & Gillespie, R. J. Chemical bonding in hypervalent molecules: Is the octet rule relevant? *Inorg. Chem.* **41**, 2164–2172 (2002).
  54. Johnson, R. H. A new class of enumeration problems. *Czechoslov. Math. J.* **24**, 573–583 (1974).
  55. Wieser, M. E. & Coplen, T. B. Atomic weights of the elements 2009 (IUPAC Technical Report). *Pure Appl. Chem.* **83**, 2012 (2010).
  56. Najdekr, L. *et al.* Influence of mass resolving power in orbital ion-trap mass spectrometry-based metabolomics. *Anal. Chem.* **88**, acs.analchem.6b02319

(2016).

57. Kuehnbaum, N. L. & Britz-Mckibbin, P. New advances in separation science for metabolomics: Resolving chemical diversity in a post-genomic era. *Chem. Rev.* **113**, 2437–2468 (2013).
58. Dunn WB1, Broadhurst D, Begley P, Zelena E, Francis-McIntyre S, Anderson N, Brown M, Knowles JD, Halsall A, Haselden JN, Nicholls AW, Wilson ID, Kell DB, G. R. H. S. M. (HUSERMET) C. Procedures for large-scale metabolic profiling of serum and plasma using gas chromatography and liquid chromatography coupled to mass spectrometry. *Nat. Protoc.* **6**, 1060–83 (2011).
59. R Core Team. R: A Language and Environment for Statistical Computing. (2016).
60. Smith, C. A., Want, E. J., O’Maille, G., Abagyan, R. & Siuzdak, G. XCMS: Processing mass spectrometry data for metabolite profiling using nonlinear peak alignment, matching, and identification. *Anal. Chem.* **78**, 779–787 (2006).
61. Tautenhahn, R., Bottcher, C. & Neumann, S. Highly sensitive feature detection for high resolution LC/MS. *BMC Bioinformatics* **9**, 16 (2008).
62. Benton, H. P., Want, E. J. & Ebbels, T. M. D. Correction of mass calibration gaps in liquid chromatography-mass spectrometry metabolomics data. *Bioinformatics* **26**, 2488–2489 (2010).
63. Kuhl, C., Tautenhahn, R., Böttcher, C., Larson, T. R. & Neumann, S. CAMERA: An integrated strategy for compound spectra extraction and annotation of liquid chromatography/mass spectrometry data sets. *Anal. Chem.* **84**, 283–289 (2012).
64. Gaude, E. *et al.* muma , An R Package for Metabolomics Univariate and Multivariate Statistical Analysis. *Curr Metabolomics* **1**, 180–189 (2013).
65. Cleveland, W. S. Robust Locally Weighted Regression and Smoothing Scatterplots. *J. Am. Stat. Assoc.* **74**, 829–836 (1979).
66. Reyment, R. A. *Compositional Data Analysis. Terra review* **1**, (Wiley, 2011).
67. Yuan, M., Breitkopf, S. B., Yang, X. & Asara, J. M. A positive/negative ion-switching, targeted mass spectrometry-based metabolomics platform for bodily fluids, cells, and fresh and fixed tissue. *Nat. Protoc.* **7**, 872–81 (2012).

68. Wang, J. *et al.* Metabolomic Profiling of Anionic Metabolites in Head and Neck Cancer Cells by Capillary Ion Chromatography with Orbitrap Mass Spectrometry. *Anal. Chem.* **86**, 5116–5124 (2014).
69. Böcker, S., Letzel, M. C., Lipták, Z. & Pevukhin, A. SIRIUS: Decomposing isotope patterns for metabolite identification. *Bioinformatics* **25**, 218–224 (2009).
70. Böcker, S., Lipták, Z., Martin, M., Pevukhin, A. & Sudek, H. Decomp - From interpreting mass spectrometry peaks to solving the money changing problem. *Bioinformatics* **24**, 591–593 (2008).
71. Böcker, S. & Lipták, Z. A fast and simple algorithm for the money changing problem. *Algorithmica (New York)* **48**, 413–432 (2007).
72. Böcker, S., Letzel, M., Lipták, Z., Zsuzsanna & Pevukhin, A. Decomposing metabolomic isotope patterns. *Proc. Work. Algorithms Bioinforma. (WABI 2006)* **4175**, 12–23 (2006).
73. Sies, H. Oxidative stress: oxidants and antioxidants. *Exp. Physiol.* **82**, 291–5 (1997).
74. Valko, M., Izakovic, M., Mazur, M., Rhodes, C. J. & Telser, J. Role of oxygen radicals in DNA damage and cancer incidence. *Mol. Cell. Biochem.* **266**, 37–56 (2004).
75. Bochkov, V. N. & Leitinger, N. Anti-inflammatory properties of lipid oxidation products. *J. Mol. Med.* **81**, 613–626 (2003).
76. Khandelia, H. & Mouritsen, O. G. Lipid gymnastics: Evidence of complete acyl chain reversal in oxidized phospholipids from molecular simulations. *Biophys. J.* **96**, 2734–2743 (2009).
77. Latchoumycandane, C., Marathe, G. K., Zhang, R. & McIntyre, T. M. Oxidatively truncated phospholipids are required agents of tumor necrosis factor ?? (TNF??)-induced apoptosis. *J. Biol. Chem.* **287**, 17693–17705 (2012).
78. Sharma, V., Anderson, D. & Dhawan, A. Zinc oxide nanoparticles induce oxidative DNA damage and ROS-triggered mitochondria mediated apoptosis in human liver cells (HepG2). *Apoptosis* **17**, 852–870 (2012).
79. Wang, C. H., Wang, C. C., Huang, H. C. & Wei, Y. H. Mitochondrial dysfunction leads to impairment of insulin sensitivity and adiponectin secretion in adipocytes.

- FEBS J.* **280**, 1039–1050 (2013).
80. Schuck, P. F. *et al.* Medium-chain fatty acids accumulating in MCAD deficiency elicit lipid and protein oxidative damage and decrease non-enzymatic antioxidant defenses in rat brain. *Neurochem. Int.* **54**, 519–525 (2009).
  81. Schuck, P. F. *et al.* Oxidative stress induction by cis-4-decenoic acid: relevance for MCAD deficiency. *Free Radic. Res.* **41**, 1261–1272 (2007).
  82. Ashraf, M. Z. & Srivastava, S. in *Lipoproteins - Role in Health and Diseases* 409–430 (2012). doi:10.5772/2931
  83. Podrez, E. A. *et al.* Identification of a novel family of oxidized phospholipids that serve as ligands for the macrophage scavenger receptor CD36. *J. Biol. Chem.* **277**, 38503–38516 (2002).
  84. Najdekr, L. *et al.* Oxidized phosphatidylcholines suggest oxidative stress in patients with medium-chain acyl-CoA dehydrogenase deficiency. *Talanta* **139**, 62–66 (2015).
  85. Sauer, A., Brigida, I., Carriglio, N. & Aiuti, A. Autoimmune dysregulation and purine metabolism in adenosine deaminase deficiency. *Front. Immunol.* **3**, (2012).
  86. Hirschhorn, R., Nicknam, M. N., Eng, F., Yang, D. R. & Borkowsky, W. Novel deletion and a new missense mutation (Glu 217 Lys) at the catalytic site in two adenosine deaminase alleles of a patient with neonatal onset adenosine deaminase- severe combined immunodeficiency. *J. Immunol.* **149**, 3107–12 (1992).
  87. Schram, K. H. Urinary nucleosides. *Mass Spectrom. Rev.* **17**, 131–251 (1998).
  88. Limbach, P. A., Crain, P. F. & Mccloskey, J. A. Summary: The modified nucleosides of RNA. *Nucleic Acids Research* **22**, 2183–2196 (1994).
  89. Cech, N. B. & Enke, C. G. Practical implications of some recent studies in electrospray ionization fundamentals. *Mass Spectrom. Rev.* **20**, 362–87 (2002).
  90. Contrepois, K., Jiang, L. & Snyder, M. Optimized Analytical Procedures for the Untargeted Metabolomic Profiling of Human Urine and Plasma by Combining Hydrophilic Interaction (HILIC) and Reverse-Phase Liquid Chromatography

- (RPLC)–Mass Spectrometry. *Mol. Cell. Proteomics* **14**, 1684–1695 (2015).
91. Zhang, T., Creek, D. J., Barrett, M. P., Blackburn, G. & Watson, D. G. Evaluation of coupling reversed phase, aqueous normal phase, and hydrophilic interaction liquid chromatography with orbitrap mass spectrometry for metabolomic studies of human urine. *Anal. Chem.* **84**, 1994–2001 (2012).
  92. Zhang, R. *et al.* Evaluation of mobile phase characteristics on three zwitterionic columns in hydrophilic interaction liquid chromatography mode for liquid chromatography-high resolution mass spectrometry based untargeted metabolite profiling of *Leishmania* parasites. *J. Chromatogr. A* **1362**, 168–179 (2014).
  93. Zubarev, R. A. & Makarov, A. Orbitrap mass spectrometry. *Anal. Chem.* **85**, 5288–5296 (2013).

## 8. List of authors publications

### 8.1. Publication associated with the thesis

#### 8.1.1. Original research articles published in journals with IF

**Najdekr, L. et al.** Oxidized phosphatidylcholines suggest oxidative stress in patients with medium-chain acyl-CoA dehydrogenase deficiency. *Talanta* **139**, 62–66 (2015). IF (2015) = 4.035

**Najdekr, L. et al.** Influence of mass resolving power in orbital ion-trap mass spectrometry-based metabolomics. *Anal. Chem.* **88**, acs.analchem.6b02319 (2016). IF (2016) = 5.886

Janeckova, H. et al. Untargeted metabolomic analysis of urine samples in the diagnosis of some inherited metabolic disorders. *Biomed Pap Med Univ Palacky Olomouc Czech Repub.* **158**, 1–4 (2014). IF (2014) = 1.15

Kanagaratham, C. et al. Fenretinide prevents inflammation and airway hyperresponsiveness in a mouse model of allergic asthma. *Am. J. Respir. Cell Mol. Biol.* **51**, 783–792 (2014). IF (2015) = 4.082

#### 8.1.2. Published abstracts

**Najdekr, L. et al.** INFLUENCE OF MASS SPECTROMETRY RESOLUTION ON METABOLITE COVERAGE IN PLASMA. in *CECE 2014: 11TH INTERNATIONAL INTERDISCIPLINARY MEETING ON BIOANALYSIS* (ed. Foret, F and Krenkova, J and Drobnikova, I and Guttman, A and Kleparnik, K) 92–93 (INST ANALYTICAL CHEMISTRY ASCR, V V I-IAC, 2014).

#### 8.1.3. Poster presentations

**L. Najdekr, D. Friedecky, H. Podmore, G. Woffendin, T. Adam.** „Identification of new biomarkers of medium chain acyl-CoA dehydrogenase deficiency using Orbitrap and quadrupole mass spectrometry “, 27th International Symposium on MicroScale Bioseparations and Analyses, Genève (CH), 12<sup>th</sup> - 15<sup>th</sup> Feb 2012, Book of Abstracts p50, poster ID P502

**L. Najdekr, D. Friedecky, H. Podmore, G. Woffendin, T. Adam.** „New phospholipid biomarkers of medium chain acyl-CoA dehydrogenase deficiency identified by Orbitrap and quadrupole mass spectrometry”, 30th Informal Meeting on Mass Spectrometry, Olomouc (CZ), 29<sup>th</sup> April – 3<sup>th</sup> May 2012 , Book of Abstracts p91, posted ID P32

**L. Najdekr, D. Friedecky, H. Janečková, K. Mičová, I. Fikarová, H. Podmore, G. Woffendin, T. Adam.** „Identification of novel biomarkers of medium chain acyl-CoA dehydrogenase deficiency using untargeted metabolomics”, Chiranal 2012, Olomouc (CZ), 11<sup>th</sup> – 14<sup>th</sup> June 2012. Book of Abstracts

**Lukáš Najdekr, David Friedecký, Hana Janečková, Kateřina Mičová, Iveta Fikarová, Helene Podmore, Garry Woffendin, Tomáš Adam.** „Identification of novel biomarkers of medium chain acyl-CoA dehydrogenase deficiency using untargeted metabolomic approach”, 29th LC/MS Montreux Symposium, Montreux (CH), 7<sup>th</sup> – 9<sup>th</sup> November 2012, Book of abstracts, p. 69

**Najdekr L, Friedecký D, Janečková H, Mičová K, Kalivodová A, Župková M, Adam T.** “Identification of novel biomarkers of medium chain acyl-CoA dehydrogenase deficiency using untargeted metabolomic approach”, 28. pracovní dny Dědičné metabolické poruchy, Tábor (CZ), 15<sup>th</sup> – 17<sup>th</sup> May 2013. Book of abstracts, p25. ISBN 978-80-260-4295-2.

**Lukáš Najdekr, David Friedecky, Ralf Tautenhahn, Junhua Wang, Tomas Adam, Yingying Huang.** „Influence of mass spectrometry resolution on metabolite coverage in plasma”, Metabolomics 2014, Tsuruoce (J), 23<sup>th</sup> – 26<sup>th</sup> June 2014. Book of abstracts, p142, Poster ID P327

**Lukas Najdekr, David Friedecky, Ralf Tautenhahn, Junhua Wang, Tomas Adam, Yingying Huang.** „Influence of mass spectrometry resolution on metabolite coverage in plasma” na „20<sup>th</sup> International Mass Spectrometry Conference “, Genève (CH), 24<sup>th</sup> – 28<sup>th</sup> August 2014, Book of abstracts, p101, Poster ID WPS26-55

**Lukas Najdekr, Alžběta Kalivodová (Gardlo), Lucie Mádrová, David Friedecký, Hana Janečková, Jitka Šíroková, Elon S. Correa, Royston Goodacre, Tomáš Adam.** „Oxidized phosphocholines Suggest oxidative stress in patients with Medium-chain Acyl-CoA dehydrogenase deficiency”, Metabomeeting 2014, London (UK), 10<sup>th</sup> – 12<sup>th</sup> September 2014. Book of abstracts, p13, Poster ID 146

**Lukáš Najdekr, Kateřina Mičová, Lucie Mádrová, David Friedecký, Jitka Šíroká, Tomáš Adam.** „The use of spectral trees as a novel approach in identification of adenosine deaminase deficiency metabolites in human urine”, 4. konferenci české společnosti pro hmotnostní spektrometrii“, Hradec Králové (CZ), 15<sup>th</sup> – 17<sup>th</sup> April 2015, Book of abstracts, p62, Poster ID Wep-032

**Lukáš Najdekr, Kateřina Mičová, Lucie Mádrová, David Friedecký, Jitka Šíroká, Tomáš Adam** „The use of spectral trees as a novel approach in identification of adenosine deaminase deficiency metabolites in human urine”, Metabolomics 2015, San Francisco (CA, USA) 29<sup>th</sup> June – 2<sup>nd</sup> July 2015, Book of abstracts, p96, Poster ID P-436

**Lukas Najdekr, David Friedecky, Ralf Tautenhahn, Tomas Pluskal, Junhua Wang, Yingying Huang, Tomas Adam** “Influence of mass resolving power in high resolution mass spectrometry metabolomics”, Metabolomics 2016, Dublin (IRE), 27<sup>th</sup> – 30<sup>th</sup> June 2016, Book of abstracts, abstract number 2528, Poster ID P423

**Lukas Najdekr, David Friedecky, Ralf Tautenhahn, Tomas Pluskal, Junhua Wang, Yingying Huang, Tomas Adam** “Influence of mass resolving power in high resolution mass spectrometry metabolomics”, Microscale separation and bioanalyses 2016, Niagara-on-the-lake (CA) 3<sup>rd</sup> – 7<sup>th</sup> April 2016, Book of abstracts, Poster ID W1

#### **8.1.4. Oral presentations**

**Lukas Najdekr, David Friedecky, Ralf Tautenhahn, Junhua Wang, Tomas Adam, Yingying Huang** „Influence of mass spectrometry resolution on metabolite coverage in plasma” na “CECE 2014”, Brno (CZ), 20<sup>th</sup> – 22<sup>nd</sup> October 2014, Book of abstracts, p11

**Lukas Najdekr, David Friedecky, Ralf Tautenhahn, Junhua Wang, Tomas Adam, Yingying Huang** „Influence of mass spectrometry resolution on metabolite coverage in plasma” 29. Pracovních dny Dědičných metabolických poruch, Donovaly (SK), 21<sup>st</sup> – 23<sup>rd</sup> May 2014, Book of abstracts, p29-30

**Lukáš Najdekr, Kateřina Mičová, Lucie Mádrová, David Friedecký, Jitka Šíroká, Tomáš Adam,** „The use of spectral trees as a novel approach in identification of adenosine deaminase deficiency metabolites in human urine”, 30. pracovní dny Dědičné metabolické poruchy“, Dolní Morava (CZ), 20<sup>th</sup> – 22<sup>nd</sup> May 2015, Book of abstracts, Varia10 p5

**Lukáš Najdekr, Lucie Mádrová, Kateřina Mičová, David Friedecký, Tomáš Adam.** “Využití spektrálních stromů jako nový přístup v identifikaci metabolitů deficitu adenosindeaminasy v moči”, 16. Škola hmotnostní spektrometrie, Frymburk (CZ), 13<sup>th</sup> – 18<sup>th</sup> September 2015, Book of abstracts, Section N

**Lukas Najdekr, David Friedecky, Ralf Tautenhahn, Tomas Pluskal, Junhua Wang, Yingying Huang, Tomas Adam** “Influence of mass resolving power in high resolution mass spectrometry metabolomics”, Chiranal 2016, Olomouc (CZ), 6<sup>th</sup> – 9<sup>th</sup> June 2016, Book of abstracts, p9 & p54

**Lukas Najdekr, David Friedecky, Ralf Tautenhahn, Tomas Pluskal, Junhua Wang, Yingying Huang, Tomas Adam** “Influence of mass resolving power in high resolution mass spectrometry metabolomics”, Microscale separation and bioanalyses 2016, Niagara-on-the-lake (CA), 3<sup>rd</sup> – 7<sup>th</sup> April 2016, Book of abstracts, 3MT p16

## **8.2. Other publications**

### **8.2.1. Original research articles published in journals with IF**

Kalivodova, A. *et al.* PLS-DA for compositional data with application to metabolomics. *J. Chemom.* **29**, 21–28 (2015). IF (2015) = 1.873